Palaeoecology and palaeoenvironment of Mississippian coastal lakes and marshes during the early terrestrialisation of tetrapods

Bennett, C.E.[1*], Kearsey, T.I.[2], Davies, S.J.[1], Leng, M.J.[3], Millward, D.[2], Smithson, T.R.[4], Brand, P.J.[2], Browne, M.A.E.[2], Carpenter, D.K.[5], Marshall, J.E.A.[5], Dulson, H.[1], Curry, L.[1]

[1] *School of Geography, Geology and Environment, University of Leicester, Leicester, LE1 7RH*

[2]*British Geological Survey, The Lyell Centre, Research Avenue South, Edinburgh EH14 4AP*

[3]*National Environmental Isotope Facility, British Geological Survey, Keyworth, Nottingham, NG12 5GG and School of Biosciences, Centre for Environmental Geochemistry, University of Nottingham, Loughborough, LE12 5RD*

[4]*Department of Zoology, University of Cambridge, Cambridge,* CB2 3EJ

[5] *School of Earth Science, University of Southampton, National Oceanography Centre, European Way, Southampton, SO14 3ZH, UK*

Email addresses: Carys E. Bennett, ceb28@le.ac.uk (corresponding author); Timothy I. Kearsey, timk1@bgs.ac.uk; Sarah J. Davies, Sjd27@le.ac.uk; Melanie J. Leng, mjl@bgs.ac.uk; David Millward, dmill@bgs.ac.uk; Timothy R. Smithson, ts556@cam.ac.uk; Peter J. Brand, peter@pjbrand.plus.com; Michael A.E. Browne, maeb@bgs.ac.uk; David K. Carpenter, dkcarpenter97@gmail.com; John E.A. Marshall, jeam@soton.ac.uk; Hattie Dulson, hattie_d@hotmail.co.uk; Levi Curry, Lc345@live.co.uk.

Abstract

The Ballagan Formation of northern Britain provides an exceptional record of Early Mississippian ecosystems that developed as tetrapods emerged onto land. In this paper, we study two 500-metre sections of the formation near Berwick-upon-Tweed, which are characterised by abundant ferroan dolostone beds. Five lithofacies are identified: cemented siltstone and sandstone, homogeneous dolomicrite, mixed dolomite and siltstone, mixed calcite and dolomite, and dolomite with evaporite minerals. Cemented sediments have non-

planar to planar subhedral dolomite crystals, up to 40 μm in size, whereas other facies predominantly comprise dolomicrite or planar euhedral dolomite rhombs 15 μm in size, with patches of larger rhombs indicating partial recrystallisation. The macro- and microfossil content of the dolostones is dominated by sarcopterygian (rhizodont) and actinopterygian fish, bivalves, *Serpula*, ostracods and *Chondrites* trace fossils; with rarer *Spirorbis*, chondrichthyans (*Ageleodus*, hybodonts and ?ctenacanths, xenacanths), non-gyracanth acanthodians, gastropods, eurypterids, brachiopods, plant debris, wood, lycopsid roots, charcoal, megaspores, phycosiphoniform burrows, *Zoophycos*? and *Rhizocorallium*. The oxygen and carbon isotope composition of dolomites range from –3.6‰ to –1.7‰ (for $\delta^{18}O$) and –2.6‰ to +1.6‰ (for $\delta^{13}C$) respectively indicating dolomite growth in mixed salinity waters. Frequent marine storm-surge events transported marine waters and animals into floodplain lakes, where evaporation, interstitial sulphate-reducing bacteria, iron reduction and methanogenesis allowed dolomite growth in the shallow sub-surface. Secondary pedogenic modification (by roots, brecciation, desiccation, and soil forming processes) is common and represents lake evaporation with, in some cases, saline marsh development. The dolostone facies are part of a complex environmental mosaic of sub-aerial dry floodplain, wet marshy floodplains, rivers, and lakes ranging in salinity from freshwater to hypersaline. Marine influence is strongest at the base of the formation and decreases over time, as the floodplain became drier, and forested areas became more established. Coastal lakes were an important habitat for animals recovering from the end-Devonian Hangenberg Crisis and may have acted as a pathway for euryhaline fishes, molluscs and arthropods to access freshwater environments.

Keywords: Carboniferous; dolostone; lake; hypersaline; floodplain; tetrapods

1. Introduction

Following the end-Devonian mass extinction (the Hangenberg Crisis), new terrestrial habitats developed related to changes in plant cover and river morphology (Davies and Gibling, 2013; Kaiser et al., 2016). The extinction resulted in changes in body size of fishes (Challands et al., 2019; Sallan and Galimberti, 2015), while tetrapods evolved pentadactyl limbs for terrestrial locomotion (Smithson et al., 2012). In continental brackish to freshwater environments dipnoans and gyracanthid fish occupied the niches left vacant by extinct placoderms and porolepiformes (Friedman and Sallan 2012). The late Devonian to early Carboniferous was a time of marine to freshwater radiation for many animal groups, including elasmobranch chondrichthyans (Cressler et al., 2010), xiphosurans (Bicknell and Pates, 2019; Lamsdell, 2016), eumalacostracans and branchiopods (Gueriau et al., 2014a,b, 2018), ostracods (Bennett, 2008), gastropods (Yen, 1949) and bivalves (Ballèvre and Lardeux, 2005; Bridge et al., 1986).

The Tournaisian Ballagan Formation of the Scottish Borders preserves some of the most continuous and important records of the evolution of early terrestrial ecosystems during recovery from the Hangenberg Crisis. The formation hosts rare terrestrial tetrapods (Clack, 2002; Clack et al., 2016, 2018, 2019; Otoo et al., 2019), fishes (Carpenter et al., 2014; Challands et al., 2019; Richards et al., 2018; Sallan and Coates 2013; Smithson et al., 2012, 2016), shrimps (Cater et al., 1989), xiphosurans (Bicknell and Pates, 2019), millipedes (Ross et al., 2018), ostracods (Williams et al., 2005, 2006), plants (Bateman and Scott, 1990; Scott et al., 1984) and palynomorphs (Stephenson et al., 2004a, b; Marshall et al., 2019). Dolostone and evaporite beds are common in the formation and comprise 17% of the total thickness (Bennett et al., 2016). Primary micritic dolomite formation at the present day is fairly rare and occurs in sabkhas (Bontognali et al., 2010), hypersaline lakes (Wright, 1999) or lagoons (Vasconcelos and McKenzie, 1997), deposited from groundwater (Mather et al., 2019), and in peritidal or deep marine environments (Warren, 2000). Micritic dolomite in the geological record has been associated with these environments, as well as with palaeosols

(Kearsey et al., 2012) and marshes (Barnett et al., 2012). The Mississippian was an interval of globally low levels of dolomite abundance, especially compared with very high dolomite abundance episodes in the Ordovician, Silurian and Cretaceous (Given and Wilkinson, 1987). Yet dolostones are a key component of the Ballagan Formation and part of the story of the diverse environments that existed when tetrapods first evolved to walk on land.

Until recently, the fossil record in dolostones has not been examined in detail, and both Belt et al. (1967) and Ghummed (1982) noted the paucity of fossils within the dolostones. New work is challenging the previous conception of dolostones as rather barren rocks: a mesofossil study on two dolostone beds from the Isle of Bute identified a diverse fish fauna (Carpenter et al., 2014), and common *Chondrites* burrows were found in dolostones from the Norham Core (Bennett et al., 2017). Our study continues the palaeontological analysis of the dolostones and is the first to integrate palaeontology with detailed sedimentological and geochemical analysis. The aim of this study is to interpret the palaeoenvironment of these dolostone-bearing successions, using an extensive dataset of more than 500 dolostone samples from the Ballagan Formation. The study interprets a mosaic of coastal lake environments, which may have been influential in the radiation of fish and aquatic invertebrates from marine to freshwater environments as new ecosystems developed.

2. Geological background

The Ballagan Formation crops out across the Midland Valley of Scotland and in the Borders region between Scotland and England (Figure 1A), and spans most of the Tournaisian stage and early Visean (Marshall et al., 2019). Formerly placed within the Dolostone Group in the Scottish Borders (Greig, 1988), the Calciferous Sandstone Measures in Midland Valley of Scotland (MacGregor, 1960), and the Lower Border Group in the Langholm area (Lumsden et al., 1967), the Ballagan Formation is now part of the Inverclyde Group (Browne et al., 1999). The entire formation is exposed in a 513-metre-thick, vertically-dipping coastal section at Burnmouth, bound by sandstone units of the upper Devonian Kinnesswood Formation at the base and the Visean Fell Sandstone Formation at the top (Kearsey et al., 2016; Marshall et

al., 2019). A new palynological analysis at Burnmouth revealed that the section does not span just the CM spore zone as previously thought, but it encompasses the VI, HD, Cl 1 and CM spore zones, spanning the early Tournaisian to early Visean (Marshall et al., 2019).

The Ballagan Formation comprises ten facies and three facies associations, each of which occurs throughout the formation: 1) fluvial facies association (sandstones, deposited in meandering to anastomosing fluvial channels); 2) overbank facies association (fine-grained siliciclastic sediments and conglomerate lenses, deposited in temporary floodplain lakes, streams and sub-aerial vegetated land surfaces); and 3) saline-hypersaline lake facies association (dolostones and evaporites, the focus of this study) (Bennett et al., 2016). Dolostones (locally referred to as 'cementstones'; Bennett et al., 2016) are present only in the saline-hypersaline lake facies association, together with evaporites. They occur interbedded within the siltstones, palaeosols and sandstones of the overbank facies association, and represent time periods when the coastal floodplain was covered in extensive lakes.

Ballagan Formation dolostones from Scotland have been studied from the East Lothian Cockburnspath Outlier, including Cove and Pease Bay (Andrews et al., 1991; Andrews and Nabi, 1994, 1998), the western Midland Valley of Scotland (Freshney, 1961; Ghummed, 1982), the River Tweed area at Burnmouth (Scott, 1971, 1986), Foulden (Anderton, 1985), the Firth of Tay boreholes (Browne, 1980), Ballagan Burn, Gairney Burn field sections, and the Glenrothes, Little Freuchie and Knowehead boreholes (Turner, 1991). Tournaisian dolostones of Scotland and Canada have a composition of ferroan dolomite with minor calcite and a siliciclastic component (clays and silts) of 6 to 30% (Belt et al., 1967). In the Midland Valley of Scotland, Tweed Basin and Northumberland-Solway Basin, dolostones can be associated with evaporites (Armstrong et al., 1985; Millward et al., 2018, 2019; Scott, 1986). Dolostones have been interpreted to represent deposition in floodplain lakes (Anderton, 1985; Andrews et al., 1991; Andrews and Nabi, 1994, 1998; Scott, 1971), and as marginal marine deposits (Belt et al., 1967), or continental sabkha (Scott, 1986). Ferroan dolostones from the Tournaisian of New Brunswick, Newfoundland, Northumberland and Scotland have similar characteristics, including homogeneous, layered, hummocky, nodular and brecciated or pedogenic (rooted) forms (Belt et al., 1967; Andrews, 1991; Freshney, 1961; Leeder, 1974; Scott, 1971,

1986). Dolostones from eastern Canada are primarily associated with alluvial successions with fewer marine indicators than British examples (Belt et al., 1967), with the Maritimes Basin isolated from marine influence for much of the Carboniferous (Falcon-Lang et al., 2015a).

In the Tournaisian, Scotland and Northern England were situated 4ºS of the palaeo-equator (Scotese and McKerrow, 1990). The climate was tropical and evidence from sandy siltstones, palaeosols and tree rings indicates seasonal flooding or monsoon-like heavy rainfall (Bennett et al., 2016; Falcon-Lang, 1999, Kearsey et al., 2016). Mississippian deposition took place in a number of NE-trending transtensional basins along the southern margin of Laurussia which formed as a consequence of oblique dextral collision between Laurussia and Gondwana (Figure 1B; Coward, 1993; Waters and Davies, 2006). The hypothesis of a marine influence from the east (Cope et al., 1992) is confirmed by a detailed analysis of the occurrence of evaporites, marine fossils, and other indicators, in boreholes across the Midland Valley of Scotland, Tweed Basin and Northumberland-Solway Basin (Millward et al., 2019).

3. Materials and methods

Dolostones were studied from a coastal field site at Burnmouth (British National Grid NT 95797 60944) and a fully cored borehole drilled at Norham West Mains Farm, known as the Norham Core, (British National Grid NT 91589 48135), near Berwick-upon-Tweed (Millward et al., 2013). The entire Ballagan Formation (513 m thick) is exposed at Burnmouth, and the 490 m thick Norham Core fully cores the Ballagan Formation, but did not penetrate the base, suggesting the total thickness of the formation is variable. The two sections complement each other: the field exposure at Burnmouth reveals the extensive lateral continuity of the dolostone beds and the Norham Core provides fine detail of the internal structures of the dolostones and their relationship with underlying and overlying beds. The Norham Core palynostratigraphy has not been published yet, and whilst it isn't possible to correlate the two sections based on individual beds, they host the same facies and facies associations (Bennett et al., 2016). Core and field sections were recorded by sedimentary logging, and samples were taken approximately every 1 metre.

Dolostones are described from hand specimens, field exposures, core photographs and thin sections: 278 dolostone beds are recorded in the Norham Core and 267 at Burnmouth. Beds at Burnmouth were not identified to facies level unless they were sampled (166/267 beds), because weathering obscures the detail at outcrop. Standard-sized polished thin sections, 30 μm thick, were made from 70 Burnmouth and 52 Norham Core samples. Thin sections were examined using a Leica petrographic microscope to identify dolostone facies and mineralogy. The Hitachi S-3600N SEM at the University of Leicester was used to determine between calcite and dolomite using the Back Scattered Electron detector and identify ferroan dolomite and zoned crystal compositions using energy dispersive X-ray (EDX) spot analysis. X-ray Diffraction (XRD) geochemistry of 49 dolostone powder samples were analysed using a Bruker D8 Advance with DaVinci and DIFFRACplus data analysis software at the University of Leicester.

Fossil material was identified from surface-sampling and micropalaeontological residues. Five samples from the Burnmouth section, one from each facies, of weights varying from 390-500 g per sample, were processed for micropalaeontology. Each sample was broken into centimetre size pieces and placed in a plastic sieve in a bucket to aid breakdown. The samples were repeatedly immersed in a 5% solution of acetic acid, buffered using tricalcium diorthophosphate and spent acid from each cycle. Each processing cycle comprised a one week immersion in the acid solution, followed by an hour long rinse in water. Then disaggregated sediment residue was wet sieved at 1000, 425, 250, 125, 65 μm fractions and oven dried at 40^{o}C. The cycle was repeated until all the rock had broken down. The 1000, 425, and 250 μm fractions were fully picked, and total fossil counts recorded. Microfossil components were identified from literature records, or through direct comparison with macrofossil specimens from the Ballagan Formation.

A representative set of eleven samples were analysed for carbon and oxygen isotopes. Dolomite samples were ground to a fine powder in agate, and an aliquot of the powder (c. 20 mg) was reacted with anhydrous phosphoric acid *in vacuo* at 25.2°C for 72 hours. The CO_2 liberated was cryogenically separated from water vapour and collected for analysis. Measurements were made on a VG Optima mass spectrometer. Isotope values ($\delta^{13}C$, $\delta^{18}O$) are reported as per mille (‰) deviations of the isotopic ratios ($^{13}C/^{12}C$, $^{18}O/^{16}O$) calculated to the VPDB scale using a within-run laboratory dolomite standard calibrated against NBS-19.

The dolomite-acid fractionation factor applied to the gas values is 1.01109. The Craig (1957) correction is also applied to account for ^{17}O. Overall analytical reproducibility for these samples is on average better than 0.1‰ for $\delta^{13}C$ and $\delta^{18}O$ (1σ).

4. Results

4.1. Dolostone characteristics and distribution

Dolostones comprise 14% of the total sedimentary rock thickness in the Norham Core and 8% at Burnmouth. Typically, pale grey internally, with a pale yellow weathered surface at outcrop, dolostones are present within repeating successions that include siltstones, thin sandstone beds and palaeosols. Dolostone beds are distributed fairly evenly throughout both successions (Figures 2-3) and it is not possible to correlate individual beds between the two. At Burnmouth dolostones are generally parallel-bedded and can be traced the entire length of the foreshore at low tide (~500 m), without any significant changes in thickness or structure. We estimate that the true lateral extent of individual beds is of the order of 1 km or more based on the common occurrence of dolostones across the region (Millward et al., 2019).

Dolostones are categorised into five facies. Facies 1: Cemented siltstone and sandstone; Facies 2: Homogeneous dolomicrite; Facies 3: Mixed dolomite and siltstone; Facies 4: Mixed calcite and dolomite; Facies 5: Dolomite with evaporite minerals. Facies 2 and 3 represent approximately 60% of the dolostone beds. For each facies bed thickness is highly variable (Table S1), with average (mean) bed thickness of 14 cm (Burnmouth) to 26 cm (Norham Core) for Facies 1-4. Facies 5 comprises thicker beds in the Norham Core (mean thickness 37 cm), but is poorly represented at Burnmouth due to the effects of weathering.

Dolostones are thickest and most common in the lowermost 200 m of the Burnmouth section, and the lowest 80 m of the Norham Core (Figures 2-3). There are high abundance peaks, and thick dolostone beds in the Norham section at 320 m and 220-230 m depth. High-abundance peaks at 60 and 100 m depth

correspond to a section with closely-spaced but thin dolostone beds. Dolostone bed abundance variations in both sections are primarily controlled by the occurrence of sandstone beds of the fluvial facies association. Where thick fluvial sandstone units are present dolostones are absent or very rare. Removing the sandstone bodies from the sequence shows a trend of a reduction in the number of dolostone beds over time in both sections. Dolostone facies 5 is most common at the base of the Norham Core, but there are no other apparent trends in facies variation in progressively younger rocks.

At Burnmouth 77% of dolostone beds are laterally continuous over hundreds of metres. Of the discontinuous beds studied (n = 40), many are nodular (n = 23), or have a lateral extent of a few metres to tens of metres. Each dolostone facies contains some discontinuous beds, with Facies 1 the greatest (35% of beds are discontinuous). Nodule associations are varied: some occur within organic-rich black siltstones and preserve dolomitised anatomically-preserved plant fossils, whereas others comprise homogeneous dolomicrite or are associated with palaeosols or evaporites. Nodules composed of calcite and calcite-cemented sandstone beds are observed more rarely.

4.2. *Sedimentology of dolostone facies*

Dolostone photographs, outcrop profiles, microfacies and microtextures are shown in Figures 4-6 and Table S2.

4.2.1. Facies 1: Cemented siltstone and sandstone

The facies comprises siliciclastic sediments that have been cemented by dolomite. At outcrop and in core they are typically nodular and interbedded with sandstone or siltstone (Figure 3, Section A; Figure 4A). Bed boundaries between dolostone and surrounding rocks are sharp. Original sedimentary structures such as laminae, cross-lamination and clasts remain visible. The siliciclastic component dominates (approximately 90% sediment volume), with dolomite typically cementing quartz, feldspars and clays (Figure 5; Figure 6A). Dolomite crystal textures are non-planar anhedral to planar, interlocking subhedral, with crystal size ranging

from 5-40 μm. Crystals can be zoned, with calcium-rich cores, and zoned and unzoned crystals can occur in the same sample. Fossil voids can be filled with dolomite or calcite spar. One facies 1 sample is cemented by calcite instead of dolomite, and in another sample, burrows and plant material are pyritised.

4.2.2. Facies 2: Homogeneous dolomicrite

The facies comprises dolomite, clays (20-50% volume) and silt. Facies 2 units have a homogeneous structure, bedding is usually absent, though thin clay-rich partings are rarely present (Figure 5). Diffuse bed boundaries that are transitional into siltstone at the top and base of dolostones are recorded in 11% of facies 2 beds in the core (Figure 4B), but are not observed in field exposure. *In situ* brecciation structures and desiccation cracks are common and mudstone occurs within the cracks (see section 4.3). Dolomicrite patches or evenly distributed dolomite rhombs occur within a matrix of clays (Figure 6B). Rhombs are usually planar euhedral, have a unimodal size distribution (Sibley and Gregg, 1987), and size range of 2-15 μm. No dolomite overgrowth fabrics or cements are present. In samples where a brecciation crack is filled with silt-rich mudstone, the dolomite rhombs are larger within the silt matrix than in the underlying clay matrix. Dolomite rhombs can be zoned, with calcium-rich centres (Figure 6B). Dolomicrite (<4 μm size dolomite crystals) content of samples is variable, from none, to comprising significant proportions of a sample. Sparse euhedral pyrite crystals and rare pyrite framboids are present in some samples (Figure 6B).

4.2.3. Facies 3: Mixed dolomite and siltstone

The facies comprises laminated or bedded alternations of dolostone and siltstone, with a minor component of sandstone. In the Norham Core 34% of facies 3 beds comprise thick composite units of interbedded dolostone and siltstone, bioturbated by *Chondrites* (Bennett et al., 2017). Diffuse bed boundaries into siltstone are present in 12% of facies 3 beds in the core, and it is likely that bioturbation obscures in others. Soft-sediment deformation structures (Figure 4C), brecciation (Figure 4D) and desiccation cracks are

recorded in some samples. Siltstone laminae or beds are cemented by large dolomite rhombs, whereas the dolostone layers comprise micritic dolomite or planar euhedral rhombs of 5-20 μm size (Figure 6C), some of which are zoned with calcium-rich centres. In three samples laminated dolostone resembles the structure of microbial laminites, due to the millimetre-scale spacing of the planar and wavy laminae (cf. Narkiewicz et al., 2015), but no organic structures are preserved. One of these putative microbial samples has a lamina that is pyritised, but in general the occurrence of pyrite is rare in samples of this facies.

4.2.4. Facies 4: Mixed calcite and dolomite

The facies is characterised by pale yellow calcite-rich beds interbedded with pale grey dolomite and clastic components. Beds can contain an abundant shelly fauna (Figure 4E). Soft-sediment deformation structures such as convolute lamination (cf. Törö and Pratt, 2015) are present within 7 out of 14 beds of this facies at Burnmouth (Figure 3) and there are rip-up clasts in one bed. Diffuse bed boundaries have not been observed in this facies and the bases of the beds sometimes exhibit load structures into underlying siltstones. The calcite component has mostly been replaced by dolomite and is absent in some samples. Where present, micritic calcite occurs as patches, surrounded by a matrix of dolomicrite (Figure 6D) or patches of dolomite rhombs (Figure 6E) or dolomite spar. Calcite crystals form inter-crystalline textures or the cores of larger dolomite crystals. Dolomite textures range from non-planar anhedral to planar euhedral or subhedral, crystals are 5-50 μm in size. Rhombs can be zoned and some have magnesium-rich centres and micropores. One sample contains calcitic ooids that are partially replaced by dolomite, and some ooids have a rim of euhedral pyrite crystals (Figure 6F). The matrix between the ooids comprises patches of micritic calcite and dolomite spar. Pyrite is rare, occurring as sparse euhedral crystals in the matrix. In two fossil-rich samples it occurs in greater abundance, as discrete euhedral crystals, small framboid clusters, fine crystal drapes over quartz grains, or along the rim of fossils (Figure 6E).

4.2.5. Facies 5: Dolomite with evaporite minerals

Millward et al. (2018) detailed the complex variety of evaporite-bearing rocks in the Norham Core, comprising 12 gypsum-anhydrite forms and seven facies, some of which are also associated with dolostone. Herein, facies 5 is identified as dolostone units containing any type of evaporite form. Rarely seen in surface exposures, where gypsum is replaced by calcite or dolomite, six beds are identified at Burnmouth. They are either localised or nodular, and one evaporite bed changes laterally into a facies 2 dolostone. Facies 5 beds in the Norham Core (n = 38) are well preserved (Figure 4F), have sharp bed boundaries, and are commonest in the lowest 80 m of the core (Figure 2). Some of the evaporite occurrences are within composite successions of dolostone and siltstone with nodular (Figure 5; Figure 6G), chicken-wire and massive evaporite (Millward et al., 2018). Uncommon units of thinly laminated siltstone and dolostone with small evaporite nodules were interpreted by Millward et al. (2018) as preserved microbial mats. Micron-sized pyrite crystals and larger pyrite framboids were observed in evaporite-bearing dolostones by Millward et al. (2018). The dolostone is usually homogeneous, comprising planar euhedral rhombs of 40-140 μm, or in some rocks 12-15 μm size (Figure 6H), evenly distributed within a clay matrix, similar to facies 2; a few examples comprise rhombohedral grains <5 μm. Evidence for the synsedimentary growth of dolomite and evaporite minerals include prismatic aggregates of aphanitic anhydrite inferred as pseudomorphs after primary gypsum, soft-sediment deformation and de-watering structures, diffuse small (<1 cm size) irregularly shaped gypsum nodules within dolomicrite, and the compaction of siltstone lamination associated with nodule growth.

4.3. *Post-depositional features*

Previously, similar dolostones have been categorised using the presence of brecciation or pedogenic alteration as defining features (Barnett et al., 2012; Turner, 1991). While not reflecting original deposition, brecciation and pedogenic alteration have been identified in all facies in this study, and are important in understanding post-depositional environmental conditions.

Brecciation, desiccation cracks and pedogenic modification of dolostone beds are common throughout both sections. Brecciation is the most common, observed in 47% of dolostones in the core and 36% at Burnmouth. Brecciation is usually *in situ*, occurring internally within a bed, without a connection to the top surface. Facies 2 and 4 have the highest percentage of brecciation, whereas facies 5 has the least (Figure 7A). In the core, brecciated dolostones are more common towards the top of the borehole, but this trend is not seen in Burnmouth. Brecciation and pedogenic modification are not mutually exclusive, brecciation associated with roots or pedogenic modification occurs in both the core (8% of dolostones) and Burnmouth (9% of dolostones sampled).

Desiccation cracks and internal brecciation (synaeresis cracks cf. Plummer and Gostin, 1981) are quite difficult to distinguish, due to erosion of the top of the bed in the field, and the small volume exposed in the borehole. Approximately 20% brecciation observed in dolostone beds is at the top of the bed, but verifiable desiccation cracks with polygonal structures are only observed in much lower numbers (Figure 7A; Table S1), and are not recorded in facies 5. Stylolites are also occasionally present and are most common within thick facies 2 beds.

Pedogenic modification features include roots, red-staining, mottling, iron-oxide or carbonate nodules (Table S1). Overall, 11% of dolostones in the Norham Core and 18% of dolostones at Burnmouth are pedogenically altered. In both sections, facies 1, 2 and 4 exhibit the highest percentage of pedogenic modification, and facies 5 has none (Figure 7A). Despite the presence of these features, none of the pedogenically altered dolostones show the development of sub-soil horizons, such as a clay-rich B horizon (cf. Kearsey et al., 2016). Developed palaeosol levels within the Ballagan Formation are not associated with dolostones (Kearsey et al., 2016). The palaeosols of the overbank facies association are siltstones and only rarely contain small carbonate nodules (Kearsey et al., 2016). They represent a range of floodplain environments including woodland (Vertisols), scrubby vegetation (Entisols, Inceptisols) and saline marshes (gleyed Inceptisols) (Kearsey et al., 2016). The pedogenic modification of the dolostones can be considered as minor because it does not completely destroy primary lamination, where present. In addition, rooting is sparse and often forms vertical root cavities indicative of single-colonization events.

4.4. Plant fossils

Twelve dolostones at Burnmouth have a bulbous basal or top surface and are rooted (Figure 7B-D). The facies of these bulbous beds is variable; 8/12 beds are facies 2, the others are facies 1 and 3. Four of these bulbous beds preserve ~10 cm diameter circular depressions (Figure 7C) similar to vertical arborescent trunk traces (Rygel et al., 2004). One Burnmouth facies 2 bed with a bulbous top contains an *in situ* lycopsid root impression on the top surface (Figure 7D). Lycopsid rhizomorph impressions are also recorded from one facies 1 sample each at Burnmouth and in the core. The specimens have spirally arranged roots and closely resemble *Protostigmaria* as described (Rygel et al., 2006) from the correlative Blue Beach Member of the Horton Bluff Formation in Nova Scotia and in the Albert Formation of New Brunswick (Falcon-Lang, 2004). Significantly these rhizome systems supported trees attributed to *Lepidodendropsis* which formed substantive *in situ* forests at Blue Beach. Similar large lycopods are not uncommon (Long, 1959) in the Tournaisian of the Borders implying the presence of analogous forests. However, further work is needed on better preserved specimens to confirm these identifications as they are quite rare at the Burnmouth section. Internal brecciation, sparse fish and plant fragments are observed. Dolostones with a hummocky or bulbous base are described from boreholes in the Gargunnock area of Scotland (Belt et al., 1967; Francis et al., 1970). Anatomically preserved plant fossils occur within dolostones in two horizons at Burnmouth (facies 1 nodules) and one in the Norham Core (facies 2 dolostone). In these nodules dolomite permineralises plant structures in three dimensions, but plant identification has not been accomplished in this study. Anatomically preserved fossils are identified by Scott et al. (1984) and the extensive work of Albert Long (first published in Long 1960, and in ten subsequent papers, see Scott et al., 1984 for full details). Long's specimens were largely recovered from loose blocks or recorded *in situ* at Partanhall, which is a locality 500 m along-strike, but at the same stratigraphic position, as the Burnmouth specimens reported herein. They identified ferns, lycopods, pteridosperms, and gymnosperms. Small plant fragments comprising fibrous, elongate, broken pieces, probably originating from plant stems, are present in 111 hand specimen samples, encompassing all dolostone facies. Rarer wood fragments (10 samples), charcoal (3 samples) and

indeterminate megaspores (5 samples) are present. Charcoal specimens are identified by their brittle texture, fibrous external structure, and hollow internal structure of preserved cellular tissue. The specimens herein have not been identified, but charcoal from a conglomerate bed at Burnmouth was identified as arborescent pteridosperm wood (Clack et al., 2019).

4.5. *Vertebrate Palaeontology*

The fossil content of each dolostone bed observed from hand specimens is reported in Table S1 and is presented by facies in Figure 8 in order to assess ecological differences. The macrofossil vertebrate content of the dolostone hand specimen samples is dominated by indeterminate fish fragments (present in 79 samples), actinopterygian scales, teeth and bones (36 samples) and rhizodont scales and teeth (12 samples). Rarer fossils include two *Ageleodus* teeth and two samples with dipnoan bones and scales. Additional vertebrate groups are recorded in microfossil samples. Tetrapods have not been reported or identified in dolostones from Burnmouth or the Norham Core.

4.6. *Invertebrate Palaeontology*

An assemblage of fish, ostracods, bivalves and *Serpula* are present within most dolostone facies. Ostracods are most common, identified in 112 hand specimen samples. *Shemonaella*, *Paraparchites* and a putative *Cavellina* are recorded, but most are poorly preserved (recrystallised to dolomite) and cannot be identified. The three identified ostracod genera have a benthic mode of life (Crasquin-Soleau et al., 2006). Indeterminate, thin-shelled bivalves are present in 37 samples. Small *Modiolus* (18 samples) and *Naiadites* (14 samples) bivalves are recorded, with one thick-shelled ?*Schizodus* and two unidentified large bivalves (referred to herein as robust bivalves). Both *Modiolus* and *Naiadites* are thought to have a semi-infaunal to benthic mode of life (Owada, 2007; Vasey, 1984).

Serpula is common, recorded from 39 hand specimen samples. It comprises calcified polychaete worm tubes, loosely coiled helical cylinders that are 1-2 mm in diameter (Figure 9). In the Ballagan Formation these fossils are exclusively present in dolostones. The spiral tubes have a similar morphology and size to those described from peritidal carbonates of the late Tournaisian of Northern England, the Scottish Borders and Wales (Burchette and Riding, 1977; Leeder, 1973). Burchette and Riding (1977) interpreted these as gastropod in origin, but the absence of internal septa and a planispiral-shaped basal part of the tube (cf. Vinn and Mutvei, 2009) precludes a gastropod affinity. *Serpula* sometimes co-occurs with, but are distinct from, the microconchid '*Spirorbis'*, which is less abundant (11 samples). *'Spiroribis'* has a lamellar skeletal microstructure, micropores and bulb like (rather than open) tube origin (Wilson et al., 2011; Taylor and Vinn, 2006).

Fragments of arthropod cuticle (7 samples) and gastropods (6 samples) occur in almost all facies in very low numbers. Cuticle is not complete enough to identify, but is likely to be eurypterid in origin as these are the most common arthropods in the Ballagan Formation (Ross et al., 2018; Smithson et al., 2012). Gastropod identification is limited by poor preservation but may belong to *Naticopsis scotoburdigalensis* which has been recorded in the Ballagan Formation (Brand, 2018). Small brachiopods putatively identified as rhynchonellids occur in three beds.

Fossil content is not evenly distributed between facies, with facies 2 and 5 having the lowest content (Figure 8A). The distribution of each fossil group is illustrated in Figure 8B. Key points include: 1) thick-shelled robust bivalves are most common in facies 4 in the Norham Core; 2) *Spirorbis* and *Serpula* are most common in facies 4, then facies 3; 3) while lower in abundance, the faunal composition of facies 5 is no different from that from other facies. To further examine the differences between each facies, one sample of each was processed for micropalaeontology.

4.7. *Ichnology*

Bioturbation is observed in 191 samples, in all dolostone facies, and is most common in facies 3 where more than 75% of samples are bioturbated (Figure 8C). Within Burnmouth and the Norham core there are 71 intervals of *Chondrites* bioturbation within dolostones (Table S1). A detailed ichnofauna study by Bennett et al. (2017) described *Chondrites* traces as sub-vertical, branching with a dendritic pattern and have a burrow diameter range of 0.5–3 mm (Figure 4A). *Chondrites* is horizons are usually monospecific, but are associated with phycosiphoniform burrows (13 horizons), *Zoophycos*? (5 horizons) and *Rhizocorallium* (1 horizon). Bennett et al. (2017) reported that *Chondrites* horizons range in thickness from 1 to 37 cm, with a mean of 10 cm, and are mostly single-colonisation, simple-tier, with a high bioturbation intensity (bioturbation index of 5 or 6). Phycosiphoniform burrows are oblique to sub-horizontal, sinuous, of 2 mm burrow diameter, and have a bioturbation index of 4. Some *Chondrites* occurrences in siltstone rocks were reported in Bennett (et al., 2017) to be associated with orthocone fragments and scolecodonts.

4.8. *Micropalaeontology*

The microfossil composition of a representative sample from each facies (total present in all size fractions) is shown in Figure 10. The majority of specimens picked are below 1 mm in size and comprise small fragments of bones, scales, teeth, plant material or ostracod shells, which have the greatest occurrence in the 250 µm size fraction (Table S3). Examples of more complete specimens of the most abundant microfossils are illustrated in Figure 11. The amount of unidentified vertebrate bone and scale material strongly varies per sample (Facies 1: 64%; Facies 2: 18%; Facies 3: 87%; Facies 4: 17%; Facies 5: 1%). In all facies microfossils are well-preserved with no wear or abrasion identified. The microfossil results reveal the following groups that are not identified in hand specimen: chondrichthyan denticles and elasmobranch teeth (hybodonts and ?ctenacanths, xenacanths) and non-gyracanth acanthodian scales.

Facies 1 – This sample has by far the highest fossil concentration of the five samples analysed, at 16.6 fossils/g, but no fossils are present within the 1 mm size fraction (Table S3). The assemblage is dominated by indeterminate fish fragments, but also includes actinopterygian, rhizodont and rarer

chondrichthyan microfossils. Indeterminate fragments have a range of textures and colours, but are generally thin plates resembling fragments of fish scales, or chunky bone fragments. Actinopterygian components comprise scales, dermal bones, lepidotrichia bones and teeth. Actinopterygian scales have a rhombic shape with a smooth interior surface with keel, and a shiny exterior outer surface layer (ganoine mineralised tissue). The external ornament is typically transverse ridges and grooves of various heights, with small pores. Straight and recurved conical actinopterygian teeth occur in both size fractions and are identified by their transparent apical caps and cross-hatched ornament on the shaft (Carpenter et al., 2011). Only a few specimens are broken with a missing cap. Eleven of the 66 actinopterygian teeth identified are pharyngeal – rows of small, unornamented, curved, blunt teeth. Actinopterygian dermal bone has a pustulate ornament on one side, and a shiny, ganoine surface texture (cf. Clack et al., 2019). The lepidotrichia bones are most common in the 250 μm size fraction and are small, so are more likely to be actinopterygian than rhizodont. They have a range of surface textures ranging from smooth to longitudinal striations or ridges.

Rhizodont scale fragments and teeth are present. The exterior surface of rhizodont scales is cream coloured, with a fibrous structure, whereas the interior layers of broken scales have a range of structural elements characteristic of rhizodonts, including sheets of tubercules, pits or interlocking ridges and grooves. Curved rhizodont teeth fragments have ornament of well-defined striae similar to that of *Archichthys* (Jeffery, 2006). Eight dipnoan scales are identified by their cream coloured exterior surface with regularly spaced pits, a characteristic of macrofossil specimens from the Ballagan Formation. One putative dipnoan toothplate fragment has three aligned rounded teeth.

Chondrichthyan material comprises 10 *Ageleodus* teeth, one small xenacanth tooth and 90 chondrichthyan denticles. The *Ageleodus* teeth have a flat root with 4-8 tooth cusps, which is within the mean cusp count range of the genus (Downs and Daeschler, 2001). Some of the tooth cusps are broken off, and all specimens are small (less than 1 mm in length), likely to be from juvenile animals. One chondrichthyan tooth of the order Xenacanthiformes is identified by two principal cusps, with a smaller intermediate cusp in the centre (Johnson and Thayer, 2009). Chondrichthyan denticles are identified as hybodont (n = 36), ?ctenacanth (n = 7), and indeterminate elasmobranch specimens (n = 47). Hybodont

scales have a concave base, spinose top and distinctive grouping of spines which form a single flat star-shape, or multiple star-shaped clusters in dorsal view (Garvey and Turner, 2006; Yazdi and Turner, 2000). Putative ctenacanth scales have a flat base, spinose top, with numerous strongly curved spines of irregular height (Ivanov, 1996; Yazdi and Turner, 2000). Indeterminate elasmobranch scales have a flat or concave base and a top of curved spines which in dorsal view form clusters of irregular height, or individual spines (Burrow et al., 2009; Carpenter et al., 2011).

Facies 2 – The sample has the lowest fossil concentration of the five samples, at 1.9 fossils/g, but the assemblage is not notably different from facies 1. It is dominated by actinopterygians and indeterminate fish fragments, with chondrichthyans and rhizodonts a minor component. Actinopterygian scales are most numerous in the 250 μm size fraction. 25 actinopterygian teeth of various sizes are present, of which three are pharyngeal. One actinopterygian lepidotrichia bone has a smooth surface ornament (Figure 11A). Indeterminate fragments mostly comprise scale fragments of various textures and colours. One large *Ageleodus* tooth (3 mm in length) has a large flat root and nine tooth cusps. Chondrichthyan denticles are assigned to hybodont (n = 5, see Figure 11B), ?ctenacanth (n = 1), and indeterminate elasmobranch specimens (n = 11). Rarer rhizodont material comprises scale and teeth fragments.

Facies 3 – Indeterminate fish fragments dominate the assemblage. They are dark brown, chunky, with small pores, and some specimens have internal layers. There is a minor component of actinopterygian scales, lepidotrichia bone and small teeth. One rhizodont tooth fragment is identified by its well-defined striae (Figure 11C). Four acanthodian scales are diamond shaped, with a flat base and convex, asymmetrical top. Rare plant fragments and charcoal are present. One indeterminate megaspore and three ostracod moulds (podocopid in shape, two are tentatively assigned to *Cavellina*) are present.

Facies 4 – Actinopterygian fragments comprise two-thirds of the microfossils present and indeterminate fish fragments one quarter. Actinopterygian scales are abundant, most common in the 250 μm size fraction, and many specimens have transverse grooves (Figure 11D), and a shiny exterior surface. Small numbers of actinopterygian lepidotrichia bone occur in the 250 μm size fraction. Also present are 12

actinopterygian teeth (Figure 11E), four of which are pharyngeal. Indeterminate fish material comprises mostly scales but some bone material with a layered, porous internal structure (Figure 11F). Lower numbers of rhizodont scales are present (Figure 11G), and rhizodont teeth fragments. Moulds of 61 adult and large juvenile ostracods were recorded, most of which are carapaces. The following were identified: *Acutiangulata, Carbonita?, Cavellina* (Figure 11H), *Geisina, Sansabella* and palaeocopid ostracods, but most are too poorly preserved to identify. Low numbers of hybodont, ?ctenacanth and indeterminate elasmobranch scales are present, along with plant fragments.

Facies 5 – The assemblage is dominated by plant stem fragments with a fibrous structure, comprising 96% of the microfossils present (Figure 11I). Seven charcoal fragments are identified. Light brown actinopterygians scales and indeterminate fish scales of varying colour are present. Moulds of 32 adult and juvenile ostracod carapaces, and some single valves composed of sparry dolomite are recorded, including *Shemonaella, Sansabella* and palaeocopids. Rare broken fragments of the internal moulds of *Serpula* tubes are preserved.

4.9. *Taphonomy*

Taphonomic data are important for an assessment of which animals were living in the environment (autochthonous assemblages), or those that have been transported from other environments (allochthonous assemblages). There are no major differences identified in fossil presence/absence between the processed microfossil samples of different facies, but there are large differences in abundance. These could be attributed to local effects, for example an abundance of actinopterygian scales may mean that an actinopterygian macrofossil occurs within the same sample. Sample size can, of course, bias faunal diversity. For example, *Megalichthys* and Climatiiformes acanthodians occur in dolostones of the Isle of Bute (Carpenter et al., 2014), but are absent here, perhaps due to the smaller sample sizes analysed (500g versus 15 kg sample size). The larger hand specimen samples from Burnmouth (approximately double the

493 size of samples from the Norham Core) mean that there is a higher fossil presence per facies recognised at
494 Burnmouth (Figure 8A).

495 Facies 1 contains an abundant fossil assemblage, but an absence of fossils in the 1 mm fraction, indicates
496 size-sorting during deposition. The sample is a sandy siltstone that has been dolomitised. This is the most
497 fossil-rich facies of the Ballagan Formation, it commonly contains clasts of millimetre size or less, and it
498 formed as a cohesive debris flow due to meteoric flooding over a vegetated, often dry floodplain (Bennett et
499 al., 2016). As is characteristic for the sandy siltstone facies, the fossils are well-preserved and bones are
500 often still articulated (Otoo et al., 2019). Here, most actinopterygian teeth are intact, indicating only local
501 transportation. Facies 2-5 dolostones also contain microfossils that are well-preserved with no abrasion
502 observed. The only broken microfossils present are *Serpula* tubes within facies 5. Ostracod assemblages
503 comprise a range of adults and juveniles, and significant numbers of carapaces to single valves, indicative of
504 autochthonous assemblages (Boomer et al., 2003).

505 The analysis of over 400 dolostone hand specimen samples from Burnmouth and the core provides a
506 more comprehensive overview of fossil taphonomy. Table 1 summaries the taphonomy of each fossil group,
507 where known. No complete vertebrates are identified within the dolostones, so fossil fish taphonomy is
508 difficult to assess, although other studies of dolostones interpret that they were living in this environment
509 (Carpenter et al., 2014). *Naiadites* and *Modiolus* bivalves are usually sparsely distributed on bedding planes,
510 represent juvenile and adult stages and are un-broken, indicating minimal transport. In contrast, robust
511 bivalves (*Schizodus*) and brachiopods are concentrated, with stacked broken valves indicative of
512 transportation. All occurrences of the microconchid *Spirorbis* are as broken, isolated and often juvenile
513 forms, with no colonial or accumulation structures.

514 The taphonomy of *Serpula* occurrences in the Norham Core is recorded in Table S4. Autochthonous
515 *Serpula* colonies are present within the centre of dolostone beds (Figure 9A-B) and comprise orientated
516 tubes of varying size. Facies 3 contains the highest proportion of samples with *Serpula* colonies. But in total,
517 70% of all *Serpula* assemblages are allochthonous, forming centimetre thick horizons of broken tube
518 fragments that are at random orientations (Figure 9C). The taphonomy of chondrichthyans, acanthodians,

519 eurypterids, and gastropods has not been assessed, because of low specimen numbers. Future work to
520 enhance the taphonomy interpretation could be to analyse freshly exposed dolostone bedding surfaces at
521 Burnmouth and identify either trackways, or trace fossil evidence of transport or hostile environmental
522 conditions, such as eccentric xiphosuran trails (Falcon-Lang et al., 2015b).

523

524 ***4.10.*** *Geochemical and isotope composition*

525 EDX and XRD analysis reveal a ferroan dolomite composition for all facies. The XRD spectra
526 differentiated ordered dolomite from high-magnesium calcite (cf. Gregg et al., 2015). Facies 1 and 4 also
527 contain calcite and all samples contain minor amounts of mixed clays, quartz and feldspar (most common in
528 facies 1). Facies 5 samples contain gypsum, anhydrite, and in some samples calcite as a secondary
529 replacement of gypsum. Clay mineralogy is not examined in detail here, but Wilson et al. (1972) identified
530 illite within homogeneous type dolostones. An extensive carbonate geochemical analysis has not been
531 undertaken here, but previous studies report an average 10 wt% Mg and 2-3 wt% Fe for homogeneous
532 dolostones from the Cockburnspath area, analysed by electron microprobe (Andrews et al., 1991). XRD
533 analysis identified the presence of pyrite in one sample each of facies 1, 3 and 5.

534 Facies 2-5 dolostones examined in this study have a range of $\delta^{18}O$ and $\delta^{13}C$ from –8.5‰ to –0.2‰ (for
535 $\delta^{18}O$, mean –3.0‰) and –5.4‰ to 1.6‰ (for $\delta^{13}C$, mean –1.2‰) (Figure 12, Table S5). There is a large
536 degree of overlap between the different facies, and the isotope ranges fall within the results of a more
537 extensive isotope study into the Ballagan Formation dolostones by Turner (1991), also shown on Figure 12.

538

539 **5. Interpretation**

540 ***5.1.*** *Mechanism of dolomite formation*

541 The presence of marine fauna and ichnofauna in each dolostone facies indicate that dolomite formation
542 is likely to have originated from a marine water source. Previous studies interpreted that dolomite formed

543 from the alteration of primary calcite or aragonite (Belt et al., 1967; Leeder, 1974). The dolostones in this
544 study have no features typically associated with dolomitised limestones such as relict bioclastic fabric
545 (Searl, 1988), loss of internal structures (Muchez and Viaene, 1987), large crystal size (Gregg et al., 2001),
546 or a red rusty colour (McHargue et al., 1982). Storm surges were proposed as the mechanism to explain how
547 marine waters were transported into floodplain lakes (Bennett et al., 2017), yet did not form established
548 marine incursions across the floodplain. Modern storm surges can transport sand, mud and marine fauna
549 many river kilometres upstream and deposit across floodplain lakes (Donnelly et al., 2004; Goodbred and
550 Hine, 1995; Liu et al., 2014; Pilarczyk et al., 2016; Park et al., 2009; Williams, 2009). The taphonomic
551 evidence of disarticulated marine fauna and presence of a restricted marine ichnofauna (Bennett et al., 2017)
552 are also consistent with the storm surge model.

553 Facies 1 beds were deposited as fluvial to floodplain sediments that are interpreted to have been
554 cemented during early diagenesis, where eogenetic dolomite precipitated from solution within sediment pore
555 spaces, after the lithification of the sediment. The cementation of these deposits likely occurred at relatively
556 shallow burial depths, prior to significant sediment compaction, due to the presence of 3D plant remains and
557 sedimentary structures such as cross-lamination.

558 Facies 2, 3 and 5 dolostones are interpreted as synsedimentary dolomite, where dolomite crystals
559 precipitated from solution within the pore spaces of soft sediment, before lithification. Evidence for this
560 includes: 1) the preservation of 3D plants within nodules; 2) the presence of dolostone clasts within
561 conglomerate lags of the fluvial sandstone units in the Ballagan Formation (Bennett et al., 2016); 3) the even
562 distribution and abundance of dolomite crystals within a clay matrix indicates that dolomite grew when there
563 was a high sediment porosity; 4) some dolomite bed boundaries are gradational into siltstone, indicating a
564 transitional micro-environment zone of dolomite formation in the subsurface: 5) beds and laminae of
565 rhombohedral dolomite grains <5 μm, interpreted as either primary precipitates, or more probably, early
566 replacement of high-Mg calcite (Millward et al., 2018; Vasconcelos and McKenzie, 1997). In experimental
567 studies of microbially mediated (Petrash et al., 2017) and abiotic dolomite formation (Liu et al., 2019),
568 proto-dolomite (or disordered dolomite) first forms as micron or sub-micron sized spherulitic, cauliflower-

shaped crystals or aggregates, which then transforms to ordered euhedral dolomite rhombs with burial. Wanas and Sallam (2016) described 20–30 μm size euhedral dolomite rhombs within a clay matrix in Eocene saline lake sediments, interpreted as primary dolomite. This is similar to the microtextures observed in the facies 2 Ballagan Formation dolostones. Zoned euhedral dolomite rhombs are common in dolomitised limestones (Olanipekun and Azmy, 2017; Rameil, 2008), but can also occur due to a change in the composition of the dolomitising fluid rather than due to diagenesis (Jones, 2013).

Some facies 2-5 samples also host eogenetic dolomite, evidenced by the presence of some planar subhedral dolomite crystals 30 μm in size (facies 2), larger size dolomite rhombs within siltstone interbeds (facies 3), or in some homogeneous dolomite associated with evaporites (facies 5). In facies 2, 3 and 5 eogenetic microcrystalline dolomite may have formed due to the neomorphic replacement of original dolomicrite, as suggested by Ghummed (1982). The timing of this recrystallisation is difficult to ascertain. Primary dolomite precipitation likely occurred below the sediment surface, within the top metre of sediment, as has been proposed for nodular dolostones (Andrews et al., 1991). In addition, sub-surface synaeresis cracks in clay-rich sediments have been interpreted as forming due to de-watering or salinity changes (Plummer and Gostin, 1981), and internal brecciation is a common feature of the dolostones. Dolostone recrystallisation may have occurred in the near sub-surface prior to burial compaction. Eocene dolomitised limestones of the Kachchh Basin, western India, with planar euhedral, 40–100 μm size zoned rhombs are interpreted to have formed by diagenesis in a shallow marine environment in low temperature and salinity conditions (Singh et al., 2018).

In facies 4 samples, dolomite forms as a replacive secondary stage to calcite, indicated by the non-planar to planar-subhedral crystal textures, rhombs with micropores, patches of large sized dolomite rhombs or spar. The loading structures, rip-up clasts and soft-sediment deformation present in some facies 4 beds indicates the transport of carbonate into the lakes from a marine source. The facies 5 mineralogy of dolomite, gypsum and anhydrite along with trace amounts of celestine and barite is more commonly recorded in marginal marine settings rather than continental deposits (Millward et al., 2018; Warren, 2006; Chagas et al., 2016).

595 The dolomite-precipitating fluid may have derived from the evaporative enrichment of marine brines, a
596 common mechanism in modern day lagoons (Bahniuk et al., 2015). Why was dolomite precipitated instead
597 of calcite? Dolomite precipitation requires a concentration of calcium and magnesium ions, with low
598 concentrations of dissolved-sulphate (Baker and Kastner, 1981). Calcium and magnesium originated from
599 seawater, and the minor presence of pyrite within the dolostones indicates that some sulphate input.
600 Sulphate-reducing bacteria mediate the formation of ferroan dolomite in modern lakes in both oxic
601 (Sánchez-Román et al., 2009; Shinn et al., 1969) and anoxic (Vasconcelos and McKenzie, 1997; Wright,
602 1999; Wright and Wacey, 2004) conditions. The Ballagan Formation evidences semi-infaunal bivalves and
603 benthic ostracods living on the lake bottom, so conditions were likely to be oxic. Organic matter decay
604 would produce favourable conditions for dolomite formation by sulphate-reducing bacteria by reducing the
605 alkalinity and pH of pore waters (Slaughter and Hill, 1991). These reducing conditions would also allow the
606 incorporation of ferrous iron into the dolomite lattice (Barnett et al., 2012; Wright et al., 1997).

607 An abiotic primary dolomite formation model involving smectite is proposed by Wanas and Sallam
608 (2016). Eocene saline lake sediments comprised of clays with a gel-like highly viscous smectitic medium,
609 low sedimentation rate, high evaporation rate, and an alkaline solution, allowed for dolomite precipitation in
610 the absence of microbes. Due to diagenesis the original amount of smectite in the Ballagan Formation is
611 unknown (Kearsey et al., 2016), but illite has been identified in dolostones (Wilson et al., 1972) and
612 palaeosols (Kearsey et el., 2016). In addition, an experimental study demonstrated that illite can aid the
613 precipitation of abiotic dolomite under ambient conditions (Liu et al., 2019). However, the presence of
614 microbial mats, and pyrite hints that some biotic mediation was involved in forming the dolostones. An
615 alternative mechanism to explain the low pyrite levels in the dolostones was put forward by Andrews et al.
616 (1991). Organic matter decay and anaerobic oxidation via iron reduction and methanogenesis would have
617 created suitable alkaline conditions for ferroan dolomite growth.

618

619 ***5.2.*** *Palaeosalinity interpretation - fauna*

620 The fauna, microfauna and ichnofauna in the dolostones indicate a range of palaeosalinities were
621 encountered during the development of these intervals, summarised in Table 1. Each dolostone facies
622 contains fauna which can be interpreted as living in marine to freshwater environments.

623

624 5.2.1. Fossils with a marine origin

625 Rhynchonellid brachiopods are interpreted as stenohaline (Kammer and Lake, 2001). *Naticopsis*
626 *scotoburdigalensis* is described from a non-marine assemblage of *Modiolus, Curvirimula, Spirorbis,*
627 *Promytilus?, 'Estheria'* and ostracods from the Visean of Edinburgh (Chisholm and Brand, 1994). However,
628 *Naticopsis* is usually associated with marine conditions, for example in reef limestones of the Frasnian to
629 Tournaisian of Australia (Cook et al., 2003; Yoo, 1988). Palaeozoic *Spirorbis* has been interpreted as
630 tolerant of a wide salinity range (Zatoń et al., 2012); however, an extensive review by Gierlowski-Kordesch
631 and Cassle (2015) provided good evidence to suggest a marine origin, with larval spirorbids readily
632 transported into non-marine environments by tidal currents or storm deposits. Modern *Serpula* encrusts
633 bivalves, stones and substrates or forms colonial reefs along the sub-littoral zone of the British coast (Moore
634 et al., 1998). One record of a brackish-water serpulid colony occurs in the Holocene (Ferrero et al., 2005),
635 although most evidence points to a marine origin: In the geological record, *Serpula* forms in colonial
636 bioherm structures within shallow marine carbonates (Beus, 1980; Braga and López-López, 1989; Suttner
637 and Lukeneder, 2003) and Cretaceous serpulid bioherms are recorded from carbonate ramps (Palma and
638 Angeleri, 1992). The salinity tolerance of *Serpula* in the Palaeozoic has not been rigorously examined,
639 although most serpulid occurrences in the Ballagan Formation indicate significant transport and thus implies
640 they were washed-in from a marine environment. Despite this, some of them (30%) were able to survive and
641 colonise the sediment within the coastal lakes. The marine faunal diversity is low compared with other
642 Mississippian ferroan dolostones which host echinoderms, brachiopods and bryozoans (Barnett et al., 2012)
643 and conodonts (Somerville et al., 2001).

644 The ichnofacies that would be expected in the Ballagan Formation based on palaeoenvironment of
645 *Scoyenia* (floodplains), *Skolithos* (river channels), and *Mermia* (coastal lakes) are absent. There are no
646 arthropod, annelid, mollusc, fish or tetrapod traces or trackways, as reported from the Lower Pennsylvanian
647 Tynemouth Creek Formation (Falcon-Lang et al., 2015b). Bennett et al. (2017) discussed that the absence
648 could be due to a combination of few freshly exposed bedding-plane surfaces in the field succession, poor
649 preservation, overprinting of these traces by *Chondrites*, or true absence. The ichnotaxa present within
650 dolostones (*Chondrites*, phycosiphoniform, *Zoophycos*? and *Rhizocorallium*) are all indicator species of
651 normal marine salinities (Bhattacharya and Bhattacharya, 2007; Buatois et al., 2005; Knaust, 2013). But
652 because the ichnoassemblages are usually monospecific or of low diversity, they do not represent normal
653 marine assemblages. Low diversity assemblages can be recorded in brackish settings (Mángano and Buatois,
654 2004), or deep marine turbidites (Carvalho et al., 2005). The Ballagan Formation ichnoassemblages indicate
655 unusual environmental conditions. The high-bioturbation intensity but shallow burrowing depth of
656 *Chondrites* represents rapid but short-lived colonisation of the sediment. Either normal marine conditions
657 were never sustained in the lakes, or it was too hostile for most marine burrowing organisms to exploit
658 successfully.

659

660 5.2.2. Euryhaline

661 Based on their facies distribution during the Mississippian, Carpenter et al. (2014) interpreted the
662 following taxa as euryhaline: ctenacanths, acanthodians and *Ageleodus;* while rhizodonts and dipnoans
663 favoured brackish to freshwater conditions. Xenacanths are more commonly associated with freshwater
664 sedimentary deposits than contemporaneous holocephalan chondrichthyans (Friedman and Sallan, 2012).
665 Xenacanths, rhizodonts, *Ageleodus*, actinopterygians and dipnoans have all been recorded in fluvial (oxbow
666 lake) facies in the Late Mississippian (Greb et al., 2016). A study of fish palaeoecology from Pennsylvanian
667 rocks deposited across a marine-brackish salinity gradient demonstrated that out of all these groups,
668 chondrichthyans (xenacanths and *Ageleodus*) were able to live in the widest range of salinity (Ó Gogáin et
669 al., 2016). Holocephalan teeth are numerically dominant over elasmobranch teeth in lagoonal dolostones

from Whitrope Burn (Richards et al., 2018). This site, in the Northumberland-Solway Basin, had a stronger marine connection than the Tweed Basin (Millward et al., 2019). Carboniferous hybodonts occur in non-marine to marginal marine assemblages (Garvey and Turner, 2006). Xenacanths, hybodonts and cteanacanths are reported from a shallow marine environment at Late Mississippian age localities in Arizona (Hodnett and Elliott, 2018). *Shemonaella*, *Paraparchites* and *Cavellina* are common euryhaline Mississippian ostracods (Bennett, 2008; Bennett et al., 2012) that are typical of the Ballagan Formation ostracod assemblage (Williams et al., 2005). The thicker-shelled *Schizodus* bivalves are likely euryhaline (Kammer and Lake, 2001).

5.2.3. Brackish to freshwater

The most common fish in the Ballagan Formation (actinopterygians, rhizodonts and dipnoans) are interpreted as euryhaline, or brackish-freshwater tolerant (Carpenter et al., 2014). Actinopterygians, rhizodonts and dipnoans have occupied freshwaters for the entire Devonian period (Friedman and Sallan, 2012). But there may be differences within groups. In a study of vertebrate fossil distribution in the Pennsylvanian Minto Formation of New Brunswick, Canada, Ó Gogáin et al. (2016) found that certain rhizodont genera were more common in marine facies (*Archichthys, Strepsodus*) while others (*Rhizodus*) were more numerous in brackish tidal estuary facies. This is supported by the presence of *Rhizodus in* Late Mississippian oxbow lake facies (Greb et al., 2015). Actinopterygian fish were the most common freshwater fish in the Carboniferous and Permian (Gray, 1988). Late Devonian-Early Carboniferous eurypterids are mostly restricted to brackish or freshwater environments (Braddy, 2001; Lamsdell and Braddy, 2010; Lamsdell et al., 2019) and were not tolerant of hypersalinity (Vrazo et al., 2016). *Modiolus* and *Naiadites* bivalves are typical of brackish to freshwater deposits in the Mississippian (Ballèvre and Lardeux, 2005; Bennison, 1960; Trueman and Weir, 1946), and of freshwater-brackish deposits in the Pennsylvanian (Eagar and Weir, 1971; Rogers, 1965). Restricted faunas, assemblages of *Serpula*, *Modiolus* and ostracods, are typical of Mississippian dolostones (Ramsbottom, 1973).

695

696 5.2.4. Hypersaline

697 A hypersaline-tolerant fauna has not been recognised from facies 5 dolostones. Today, however,
698 ostracods live in the dolomitic hypersaline lakes of the Coorong region, Western Australia, in salinities
699 ranging from 1 to 195‰ (De Deckker, 1983; De Deckker and Geddes, 1980). Some species are adapted to
700 hypersaline conditions, for example *Australocypris rectangularis* only occurs in salinities over 50‰. Further
701 analysis of ostracod-bearing facies 5 dolostones is required to determine if a salinity-tolerant fauna is
702 present.

703 In summary, the fauna and ichnofauna of the Ballagan Formation dolostones represent a mixture of
704 autochthonous fauna living within brackish lakes (fish, ostracods, bivalves) and allochthonous fauna derived
705 from marine incursions (*Spirorbis*, *Serpula,* gastropods, brachiopods, robust bivalves, ichnofossil trace-
706 makers). Plant material and eurypterid cuticle were derived from the nearby floodplain environment. The
707 taphonomy of the Ballagan Formation dolostones indicates that, apart from ichnofossil trace-makers, most
708 of the marine animals, with the exception of some serpulids, did not survive in the lacustrine environment.

709

710 ***5.3.*** *Palaeosalinity interpretation - isotopes*

711 The $\delta^{18}O$ of the dolostones will have been primarily controlled by palaeosalinity, waxing and waning
712 between fresh, brackish and marine environments. The presence of eogenetic dolomite in facies 1 and some
713 other samples shows that diagenetic fluids may have also had an influence on dolostone $\delta^{18}O$ composition.
714 We do not have data on the stable isotopic composition of a freshwater dolomite as an end member to
715 compare. However, comparisons can be made to other Mississippian datasets (Figure 12). The $\delta^{18}O$ data
716 from facies 2-5 dolostones are within the same range as data from Mississippian ferroan dolomites
717 associated with palaeosols (Barnett et al., 2012). Some facies 1 samples plot towards the range of calcite

cements (although there will be a fractionation difference of several per mil) analysed by Kearsey et al. (2016) and calcretes (Barnett et al., 2012), perhaps indicating a different formation mechanism.

Typical marine Mississippian dolomite will have $\delta^{18}O$ of around +4‰ (based on the difference in fractionation compared to marine calcite, Barnett et al., 2012) while freshwater dolomite will have lower $\delta^{18}O$. All the dolostones here have lower $\delta^{18}O$ than the marine dolomite value of Barnett et al. (2012), which may indicate a mixed input from marine, brackish, or fresher water. Evidence from palaeosols and overlying sandy siltstone cohesive debris flow deposits show that seasonal flooding events with high rainfall were common, adding freshwater to floodplain lakes (Bennett et al., 2016; Kearsey et al., 2016). An increase in the temperature of the dolomite-precipitating solution produces dolomite with lower $\delta^{18}O$ (Vasconcelos et al., 2005). Given the palaeoequatorial position temperature was likely elevated in shallow floodplain lakes, but evaporation is also important and this would result in higher $\delta^{18}O$ values. The analysis of only one facies 5 sample precludes further interpretation.

The dolostones from this study have $\delta^{13}C$ values lower than Mississippian marine dolomite with $\delta^{13}C$ of +2‰ (Barnett et al., 2012). The $\delta^{13}C$ data sit within the range of those recorded from dolomitic lake sediments of the Coorong, Australia (Wacey et al., 2007) where there has been degradation of terrestrial (and possibly some marine) organic matter by sulphate-reducing bacteria suggesting a marginal environment with freshwater incursion bringing terrestrial material. Andrews et al. (1991) proposed that dolostone $\delta^{13}C$ values are principally a combined result of bicarbonate ions originating from iron reduction and the methanogenesis of organic matter. Iron reduction would produce bicarbonate ions that were isotopically light ($\delta^{13}C$ of −23‰), while methanogenesis produced bicarbonate that was isotopically heavy ($\delta^{13}C$ of 0‰). Andrews et al. (1991) also discussed the role of methane oxidation, but typical very light signatures ($\delta^{13}C$ of −60‰) means that this was likely minimal. The equilibration of floodplain lakes with atmospheric CO_2 would also have changed the carbon isotope value of dissolved inorganic carbon in surface waters. Experimental models show that evaporation results in dissolved inorganic carbon with higher $\delta^{13}C$ values (Abongwa and Atekwana, 2013).

6. Discussion

6.1. *Palaeoenvironments*

Extensive planar dolostone beds represent formation in large coastal lakes, whereas nodular and discontinuous beds are interpreted to represent variations in topography at the edge of lakes, lateral changes in dolostone morphology, or cementation around fossils in the near sub-surface. The lateral extent of the lakes is a few kilometres in size at maximum, as individual dolostone beds do not correlate between the Norham Core and Burnmouth which are 13 km apart. There was a high degree of environmental complexity, with coastal lakes occurring at the same time as rivers, swamps and vegetated floodplains. The depositional environment of each dolostone facies and their main fossil assemblages is detailed in Figure 13.

6.1.1. Closed saline lake

Facies 2 dolostones developed with the growth of dolomite crystals in mud-rich lake sediments below wave base. The presence of zoned dolomite crystals, with increasing Mg towards the rim shows that salinity increased over time, probably due to evaporation. Rare detrital quartz grains and silt in these dolostones were probably derived from runoff flood-waters generated across the floodplain during times of heavy rainfall. The homogeneous character of many of these beds indicates hydrologically closed lakes with a minimal clastic input from rivers. This facies does contain some marine fossils, but relatively low percentage of samples with bioturbation shows that the water conditions were inhospitable to marine life, and were perhaps too saline. The high incidence of brecciation indicates water bodies that were subject to evaporation and the substrate starting to dry out.

6.1.2. Closed and hypersaline lake

Some closed lakes became highly evaporitic and hypersaline, precipitating gypsum, with a continuum from facies 2 to 5. Facies 5 dolostones primarily represent formation in closed saline lakes that became increasingly hypersaline over time. Though a continental sabkha model was proposed by Scott (1986) to explain the formation of evaporites in the Ballagan Formation, Millward et al (2018) argued that most of the evaporites formed in coastal floodplain sabkhas, ephemeral brine pans and semi-permanent hypersaline lakes or salinas. Though most modern coastal evaporite deposits occur in arid or semi-arid climate zones, they can form in seasonally wet tropical biomes, for example in the Bahamas and Florida (Ziegler et al., 2003) and coastal lagoons in Belize (Rejmankova et al., 1996).

6.1.3. Open saline lake

Facies 3 has the highest number of samples that exhibit bioturbation, but the lowest incidence of brecciation. These characteristics, in combination with alternations of clastic and carbonate material, suggest a hydrologically open saline lake with a fluvial connection. Marine waters would have inundated the lakes at times of storm surge, bringing small animals such as polychaete worms and microconchid larvae. Conditions remained stable enough for *Serpula* colonies to form and *Chondrites* and phycosiphoniform trace-makers to establish themselves. In modern dolomite-precipitating saline lakes 'soupy' soft substrates are typical (De Deckker and Last, 1988). *Chondrites* and *Phycosiphon* have been reported from soft, clay-rich substrates (Taylor et al., 2003) where *Chondrites* is one of the first colonisers (Ming, 2004). Facies 3 and facies 4 form a continuum in terms of proximal to marine (facies 4) and distal (facies 3) lake environments (Figure 13).

Why are limestone beds missing in these successions? In a depositional model for the Famennian of Belgium, dolomite was inferred to have formed closest to land, in evaporitic lagoons or marshes, and ooidal limestones formed in tidal flats and skeletal limestones in the inner shelf (Thorez et al., 2006). In the Mississippian Slade Formation of Kentucky, ferroan dolomites are laterally associated with peritidal limestones (Barnett et al., 2012). Rare ooids and microbial mats are identified within the Ballagan Formation (in facies 4, and associated with evaporites; Millward et al., 2018, 2019), and in Tournaisian dolostones of

Eastern Canada (Belt et al., 1967). Whereas ooids do not always form under marine conditions, limestones are a characteristic of the partially contemporaneous Lyne Formation in the Northumberland Basin (Leeder, 1975a, b), implying that marine deposition was taking place to the south and west (Millward et al., 2019). The 'missing' marine limestones in the Tweed Basin indicate that most dolomite formed in floodplain lakes that did not have an open marine connection. Instead these lakes were inundated by marine waters by storm surges which may have travelled a long distance inland across a very low-lying floodplain.

6.1.4. Coastal marsh

While fully developed palaeosol horizons did not form within the dolostones, the presence of brecciation, roots, mottling and other post-depositional modifications requires an assessment of their potential to be palustrine carbonates: sediments deposited in freshwater lakes or marshes then subjected to sub-aerial processes. Most modern and Palaeozoic palustrine carbonates are composed of micritic calcite and contain an assemblage of charophytes, ostracods and molluscs (usually gastropods), with rare fish material (Alonso-Zarza, 2003; Freytet and Verrecchia, 2002; Montañez and Cecil, 2013; Platt and Wright, 1992; Tandon and Andrews, 2001). Palustrine ferroan dolostones associated with roots or palaeosols, have been identified from South Wales (Searl, 1988; Wright and Robinson, 1988), South West England (Wright et al., 1977; Vanstone, 1991), Belgium (Muchez and Viaene, 1987), Tennessee (Caudill et al., 1996) and Kentucky (Barnett et al., 2012). In Tennessee ferroan dolomicrite overlies a Vertisol and is thought to have formed by the sporadic inundation of the coastal plain by storm tides (Caudill et al., 1996). In the Upper Mississippian of Kentucky, the dolostones are interpreted to have formed in a brackish to schizohaline coastal marsh (Barnett et al., 2012). These deposits are similar to the dolostones of the Ballagan Formation because they: 1) occur in between palaeosol or fluvial facies; 2) form continuous sheets extending several hundred meters; 3) have a micritic or microspar texture, with zoned rhombs; 4) commonly exhibit a homogeneous structure, with *in situ* brecciation; 5) have $\delta^{13}C$ and $\delta^{18}O$ compositions that are within the same range as dolostones. Also similar are Mississippian dolostones of South-West England, which occur overlying palaeosols or limestones (they do not replace either), and comprise dolomicrite with an average

817 crystal size of 4 μm (Wright et al., 1997; Vanstone, 1991). These deposits are interpreted to have formed in
818 brackish to schizohaline coastal marshes or swamps, with iron sourced from soil horizons and provide a
819 good analogue for the rooted bulbous bedded dolostones of the Ballagan Formation. Clay-rich
820 microcrystalline dolostones, some containing roots and tree casts, also occur in the Tournaisian Horton Bluff
821 Formation of Nova Scotia, interpreted as lacustrine marshes (Martel and Gibling, 1991).

822 The observation that secondary pedogenic alteration affects facies 1-4 dolostones may indicate that
823 some of the lakes evolved to become vegetated marshes. However, only 8-9% of the Ballagan Formation
824 dolostones are secondarily altered by brecciation and pedogenesis. While the evidence of tree rooting
825 structures within the dolostones (Figure 7) may indicate salt-tolerant vegetation, further studies are needed
826 to elucidate if there is a link between Mississippian dolostones and emerging new plant communities such as
827 *Rhizophora mangle-like* wetlands or mangroves (Greb et al., 2006).

828 The common desiccation cracks in all facies in the Norham Core (including siltstone, sandstone,
829 dolostone, palaeosol) indicate that very dry conditions alternated with wetter periods characterised by likely
830 seasonally heavy rains (Bennett et al., 2016; Kearsey et al., 2016). The presence of roots, root disturbance
831 and rarer desiccation cracks indicate that fluctuations in water level briefly exposed the top of the
832 dolostones, which sometimes became vegetated. The mottling indicates re-mobilisation of iron which is
833 thought to be due to changes in Eh of groundwater caused by oscillation in the water table (Alonso-Zarza,
834 2003). While evaporation would have led to the development of brecciation, desiccation and evaporites
835 within the dolostones, there is no evidence for long-lived arid conditions. The Ballagan Formation does not
836 contain calcrete-bearing palaeosols such as those seen in the Tournaisian of Southern England (Wright,
837 1990) and the older latest Devonian Kinnesswood Formation of Scotland (Wright et al., 1993).

838 A good analogue from the geological record that contains the variation in carbonate lakes seen in the
839 Ballagan Formation is the Early Cretaceous, Leza Formation of the Cameros Basin, Northern Spain (Suarez-
840 Gonzalez et al., 2015). The formation contains a mosaic of carbonate and clastic coastal wetland
841 depositional environments, including freshwater, brackish, marginal-marine, evaporitic and tidal carbonate
842 water bodies. Tidal water bodies were near the shoreline and contained ooidal sediment, while all lakes had

variable clastic input due to their connection with alluvial fans. In the Leza Formation carbonate rocks dominate over clastic rocks in terms of total thickness, but the mosaic of different water bodies provides a useful conceptual analogue to the range of dolostone facies in the Ballagan Formation. Although there are examples of tropical, coastal wetlands with highly saline conditions today, for example in the Salum, Gambia and Casamance river estuaries of Senegal and The Gambia, in West Africa (Barusseau et al., 1985) they do not form significant evaporite deposits.

Iron was essential to the formation of the dolostones, but synsedimentary ferroan dolostones are relatively rare in the geological record. The Ballagan Formation dolostones and evaporites formed at a time when crustal extension opened-up the southern margin of Laurussia to marine waters from the Palaeotethys and Panthalassa oceans (Millward et al., 2018, 2019). Basaltic volcanism preceded deposition of Ballagan Formation sediments and relicts of the volcanic fields may well have been exposed during at least some of the Tournaisian. This is evidenced by the intercalation of beds of volcaniclastic sedimentary rocks within the Ballagan succession in the Spilmersford and East Linton boreholes (Davies et al., 1986), and at Oxroad Bay (Bateman and Scott, 1990). Remnants of Devonian andesite volcanoes (Browne et al., 2002) from the Ochil Volcanic Formation and several other units (that formed the Cheviot, Pentland, Ochil and Sidlaw hills) may also have stood above the coastal plain and supplied sediment to the system. Newly rifted basins at sites of crustal extension in the Mississippian host ferroan dolostones (Figure 1A). At these locations, the enhanced weathering of volcanic bed-rock due to the wet tropical climate may have provided the right conditions for ferroan dolomite formation within coastal lakes.

6.2. Temporal trends

The tropical climate of the Ballagan Formation is thought to have been fairly constant throughout the formation, with seasonal wet-dry cycles, and no periods of aridity (Bennett et al., 2016; Kearsey et al., 2016; Millward et al., 2018). Long-term changes in sedimentology over time represent changing palaeoenvironments on the coastal floodplain. In both sections studied, thicker dolostones at the base of the

succession (the lowest 80 m at Norham, and the lowest 200 m at Burnmouth), indicate that hypersaline lakes were long-lived. Abundant dolostone beds can be interpreted as a product of more intense strong storm surges, or a more proximal marine shoreline. Thick and more common facies 5 dolostones and evaporites in the lowermost 80 m of the Norham Core (Millward et al., 2018) indicate that hypersaline lakes, ephemeral brine pans or salinas were common in the early Tournaisian at this location. Dolostone abundance patterns correspond to the abundance of bioturbated horizons, especially those colonised by *Chondrites*, and to occurrences of beds containing marine fauna (Bennett et al., 2017). These horizons are of the highest concentration at the base of the Norham Core, but also occur at other intervals throughout both successions.

Where dolostones are uncommon and thinner in the middle and top of both sections, the thickness of palaeosol horizons increases, interpreted as a lowering of the floodplain water table over time (Kearsey et al., 2016). Vertisols show the strongest trend and show the greatest development at times of low dolostone deposition, with units over one metre thick forming in the top part of both sections. There is a strong association between Vertisols and overlying sandy siltstone beds (Kearsey et al., 2016), which overlie palaeosols and form as cohesive debris flows in seasonal meteoric flooding events (Bennett et al., 2016). In the Norham Core where the abundance of sandy siltstone beds is low there is a corresponding increase in dolostone abundance, for example in the lowest 80 metres of the section. Although there are these larger scale associations, there is also much small-scale variability; sandy siltstones, desiccation cracks, *in situ* brecciation of dolostones, gleyed Inceptisols, Inceptisols and Entisols are all fairly well distributed throughout the Norham Core.

In summary, there is a large-scale pattern of waning marine influence and drying of the floodplain over the Tournaisian. At the base of the formation, marine fauna and infauna are washed into the lakes during storms, but fully marine conditions never develop, instead evaporation produced thick dolostones and in some cases a range of evaporite forms. In the middle to top of the formation, a drier, forested floodplain emerges, with shorter-lived saline-hypersaline lakes. Despite this long-term trend, there are smaller-scale peaks in dolostone abundance, and marine fauna do appear in the upper parts of the Tournaisian too. A long-term drying of the environment is not evident at Tournaisian sites in the Midland Valley of Scotland or in

894 the Northumberland – Solway Basin, where dolostones and evaporites are present throughout the formation
895 (Millward et al., 2018, 2019). The range of dolostone facies, and palaeosol types observed, and the changing
896 deposition of the sandstones of fluvial facies association all contribute to the complex picture. These thick
897 fluvial sandstone units and their interactions with the overbank facies association is the subject of a future
898 study. This study provides more evidence to confirm the long-lived existence of a mosaic of coastal
899 floodplain palaeoenvironments in the Tournaisian of the Scottish Borders.

900

901 **6.3. Importance to terrestrialisation**

902 Were coastal lakes and marshes important to the terrestrialisation of tetrapods? The *Pederpes* specimen
903 from Dumbarton was discovered between two dolostone beds within a nodule described as a *'clayey*
904 *limestone nodule typical of a cementstone facies*' (Clack, 2002). Further examination of the sample by CEB
905 reveals its composition to be a cemented siltstone, categorised as a facies 1 dolostone nodule. But there is no
906 evidence of tetrapods having lived within dolostone-forming environments in the Ballagan Formation, or in
907 the contemporaneous Horton Bluff Formation of Nova Scotia (Anderson et al., 2015). It is surprising that
908 tetrapods are absent from dolostones given that many Carboniferous groups appear to have been euryhaline
909 (Ó Gogáin et al., 2016). Numerous new tetrapod species have been reported from siltstones, sandy siltstones
910 overlain by palaeosols, or conglomerate lags within the Ballagan Formation, indicating that they inhabited
911 vegetated floodplain land surfaces, lakes and rivers (Bennett et al., 2016; Clack et al., 2016). Perhaps the
912 dolomite-forming coastal lakes were too hostile an environment, with water that was too saline for these
913 Tournaisian tetrapods. While there is no direct link between tetrapod terrestrialisation and these coastal lakes
914 and marshes; these environments may have been vital for numerous groups of euryhaline animals.
915 Coastal lakes precipitating dolomite were extensive across the region (Millward et al., 2019), had a wide
916 salinity range, and were a repeated feature of the coastal plain environment. The fauna autochthonous to the
917 dolostone-forming lakes (fish, ostracods and bivalves) appear to have thrived after the Hangenberg Crisis.
918 Dipnoans, actinopterygians and chondrichthyans recovered and diversified quickly (Challands et al. 2019;
919 Friedman, 2015; Richards et al., 2018; Sallan and Coates 2010; Smithson et al., 2016), whereas ostracods

and bivalves radiated into first brackish (Williams et al., 2006), then freshwater far later in the Mississippian (Bennett, 2008; Gray, 1988). Many fish groups (Ó Gogáin et al., 2016) and invertebrates such as *Naiadites* (Falcon-Lang et al., 2006) found in the dolostones maintained a euryhaline capacity into the Pennsylvanian. The coastal lakes may have acted both as a habitat for euryhaline animals, and as a place for them to breed. Carpenter et al. (2014) suggested that the Ballagan Formation lakes acted as nurseries for juvenile fishes and sharks. The lakes could also have been a pathway into freshwater rivers or pools for anadromous fishes. There is no evidence of a permanent marine connection, like the lagoon, brackish embayments, or tidal estuary environments euryhaline fish inhabited in the Pennsylvanian Minto Formation (Ó Gogáin et al., 2016). Yet the presence of allochthonous marine faunas and dolostone ichnoassemblages demonstrate marine input, so how did vertebrates access these coastal lakes? None of the vertebrates are stenohaline, and similar vertebrate assemblages have been documented from Ballagan Formation floodplain temporary lakes (Otoo et al., 2019) and rivers (Clack et al., 2019). We speculate that when these environments were flooded by marine storm surges the osmoregulatory capacity of the fishes enabled them to thrive in the new lakes which became increasingly saline over time. While there are no major marine transgression surfaces, the presence of rare scolecodonts and orthocones in overbank facies indicates a low-lying coastal floodplain with an intermittent marine influence (Bennett et al., 2016, 2017). There may have been a connection to the more marine Northumberland-Solway Basin (Millward et al., 2019) or a nearby lagoon environment which is unclear at this time.

The association of bivalves, ostracods, rhizodonts and actinopterygians is common in dolostones, but also in overbank sandy siltstones of the Ballagan Formation (Bennett et al., 2016), pointing towards both a euryhaline salinity adaptation, and feeding behaviours. The rich detrital plant matter in freshwater-brackish floodplain lakes (Bennett et al., 2016) would have provided a food source for invertebrates at the base of the food chain. Freshwater ostracods that inhabit lakes are usually detritivores (De Deckker, 2002; Rennie and Jackson, 2005), and Mississippian non-marine ostracods are thought to have consumed detrital plant material (Bennett et al., 2012). Modern freshwater bivalves are both suspension and filter feeders that consume bacteria, algae, detrital plant matter, dissolved organic matter and zooplankton (Coma et al., 2001; Vaughn et al., 2008). Bivalves from the Ballagan Formation may have consumed particulate or detrital plant

947 and algal material. It is likely that actinopterygians consumed ostracods and juvenile bivalves, as has been
948 recorded in modern environments (Masdeu et al., 2011; Victor et al., 1979). The diet of rhizodonts is
949 unknown, but their large size and predatory-type dentition (Jeffery, 2006) means that actinopterygians may
950 have been a part of their diet. The coastal lake environment played a major role in the radiation of life from
951 marine to freshwaters, by forming large, long-lived floodplain lake and marsh habitats, with an intermittent
952 marine connection.

953

954 **7. Conclusions**

955 • Synsedimentary ferroan dolostones occur in Mississippian successions deposited within newly rifting
956 basins along the southern margin of Laurussia. The Tournaisian Ballagan Formation of the Scottish
957 Borders provides an exceptional record enabling a comprehensive study of ferroan dolostones
958 through most of the Tournaisian, at a time when new terrestrial environments and ecosystems were
959 established after an extinction event.
960 • From this record, five ferroan dolostone facies are identified in core and field section: cemented
961 siltstone and sandstone; homogeneous dolomicrite; mixed dolomite and siltstone; mixed calcite and
962 dolomite; dolomite with evaporite minerals. Facies 1 formed by the diagenetic cementation of
963 alluvial and floodplain siliciclastic sediments, whereas facies 2-5 represent synsedimentary dolomite
964 formation, or the eogenetic replacement of calcite by dolomite. There is a continuum between
965 homogeneous dolostones and those containing evaporite minerals.
966 • The temporal and spatial occurrence of Mississippian dolostones is related to their palaeogeographic
967 position along the southern rift basins of Laurussia with a connection to marine water, and also to the
968 equatorial seasonal climate. The marine water crucial to initiate dolomite formation resulted from
969 storm surges, which also transported marine fossils across the floodplain.
970 • Dolomite and evaporite-forming environments include closed saline lakes, many becoming
971 hypersaline, brine pans, sabkhas, and open saline lakes connected to fluvial systems. The distribution
972 of these dolostones throughout the Ballagan Formation indicates a more established marine

connection at the base of the formation, then a gradual drying of the floodplain through time. There was a mosaic of co-existing floodplain, alluvial and saline-hypersaline lake environments with frequent periods of pedogenesis and desiccation.

- The palaeontology (macrofauna, microfauna, ichnofauna) and isotope geochemistry of the dolostones reveal variable salinity from brackish to hypersaline conditions. The lakes were a habitat for dipnoans, rhizodonts, actinopterygians, acanthodians, several types of chondrichthyans, bivalves and ostracods. Most marine animals washed-into the lakes appear not to have survived, with the exception of some *Serpula* colonies and *Chondrites*-producing polychaetes.
- Although tetrapods did not appear to inhabit these saline lakes, their variable salinity and habitat they represent may have been an important factor in the radiation of aquatic animals (chondrichthyans, actinopterygians, sarcopterygians, bivalves, ostracods and gastropods) from marine to freshwater at this time.

Acknowledgments

This study is a contribution to the TW:eed Project (Tetrapod World: early evolution and diversification), a major research programme investigating the rebuilding of Carboniferous ecosystems following a mass extinction at the end of the Devonian. This study was funded by NERC Consortium Grant '*The Mid-Palaeozoic biotic crisis: setting the trajectory of tetrapod evolution*', led by the late Prof. Jenny Clack (University Museum of Zoology, Cambridge) and involving the universities of Leicester (NE/J020729/1) and Southampton (NE/J021091/1), the British Geological Survey (NE/J021067/1) and the National Museum of Scotland. Jenny Clack took a great interest in all aspects of the TW:eed Project and is thanked for comments on a draft of the manuscript. We thank Anne Brown and Colin MacFadyan at NatureScot and Paul Bancks from Crown Estate Scotland for permission to collect from the foreshore at Burnmouth. The Norham cores are archived in the National Geological Repository at BGS, Keyworth. The support of staff in curation and facilitating access is acknowledged. The following TW:eed Project volunteers are thanks for their assistance with fossil identification from dolostone beds: Catherine Caseman, Rachel Curtis, Daniel

999 Downs, Graham Liddiard, Jessica Mason, James Mawson and Kirsty Summers. We thank Mike Turner for
1000 allowing the use of dolostone isotope data from his PhD thesis. TIK, DM, MAEB, PJB and MJL publish
1001 with the permission of the Executive Director, British Geological Survey. Julian Andrews, Paul Wright and
1002 an anonymous reviewer are thanked for their insightful comments on this manuscript.

1003

1004 **References**

1005 Abongwa, P.T. and Atekwana, E.A. 2013. Assessing the temporal evolution of dissolved inorganic carbon in
1006 waters exposed to atmospheric CO2 (g): A laboratory approach. Journal of hydrology, 505, 250-265.

1007 Alonso-Zarza, A.M. 2003. Palaeoenvironmental significance of palustrine carbonates and calcretes in the
1008 geological record. Earth-Science Reviews, 60, 261-298.

1009 Anderson, J.S., Smithson, T., Mansky, C.F., Meyer, T. and Clack, J. 2015. A diverse tetrapod fauna at the
1010 base of 'Romer's Gap'. PLoS ONE, 10, 1-27, doi:10.1371/journal.pone.0125446.

1011 Anderton, R. 1985. Sedimentology of the Dinantian of Foulden, Berwickshire, Scotland. Transactions of the
1012 Royal Society of Edinburgh: Earth Sciences, 76, 7-12.

1013 Andrews, J.E. and Nabi, G. 1994. Lithostratigraphy of the Dinantian Inverclyde and Strathclyde Groups,
1014 Cockburnspath Outlier, East Lothian-North Berwickshire. Scottish Journal of Geology, 30, 105-119.

1015 Andrews, J.E. and Nabi, G. 1998. Palaeoclimatic significance of calcretes in the Dinantian of the
1016 Cockburnspath Outlier (East Lothian-North Berwickshire). Scottish Journal of Geology, 34, 153-164.

1017 Andrews, J.E., Turner, M.S., Nabi, G. and Spiro, B. 1991. The anatomy of an early Dinantian terraced
1018 floodplain: palaeo-environment and early diagenesis. Sedimentology, 38, 271-287.

1019 Armstrong, M., Paterson, I.B. and Browne, M.A. 1985. Geology of the Perth and Dundee district. Memoir
1020 of the British Geological Survey, Sheets 48W, 48E and 49, Scotland.

1021 Bahniuk, A., McKenzie, J.A., Perri, E., Bontognali, T.R., Vögeli, N., Rezende, C.E., Rangel, T.P. and
1022 Vasconcelos, C. 2015. Characterization of environmental conditions during microbial Mg-carbonate

precipitation and early diagenetic dolomite crust formation: Brejo do Espinho, Rio de Janeiro, Brazil, in: Bosence, D.W.J., Gibbons, K.A., Le Heron, D.P., Morgan, W.A., Pritchard, T. and Vining, B.A., eds., Microbial Carbonates in Space and Time: Implications for Global Exploration and Production. Geological Society, London, Special Publications, 418, 243-259.

Baker, P.A. and Kastner, M. 1981. Constraints on the formation of sedimentary dolomite. Science, 213, 214-216.

Ballèvre, M. and Lardeux, H. 2005. Signification paléoécologique et paléogéographique des bivalves du Carbonifère inférieur du bassin d'Ancenis (Massif armoricain). Comptes Rendues Paleovol, 4, 109-121.

Barnett, A.J., Wright, V.P. and Crowley, S.F. 2012. Recognition and significance of paludal dolomites: Late Mississippian, Kentucky, USA. International Association of Sedimentology Special Publications, 45, 477-500.

Barusseau, J.P., Diop, E.H.S. and Saos, J.L. 1985. Evidence of dynamics reversal in tropical estuaries, geomorphological and sedimentological consequences (Salum and Casamance Rivers, Senegal). Sedimentology, 32, 543-552.

Bateman, R.M. and Scott, A.C. 1990. A reappraisal of the Dinantian floras at Oxroad Bay, East Lothian, Scotland. 2. Volcanicity, palaeoenvironments and palaeoecology. Transactions of the Royal Society of Edinburgh: Earth Sciences, 81, 161-194.

Belt, E.S., Freshney, E.C. and Read, W.A. 1967. Sedimentology of Carboniferous dolostone facies, British Isles and Eastern Canada. The Journal of Geology, 75, 711-721.

Bennett, C. 2008. A review of the Carboniferous colonisation of non-marine environments by ostracods. Senckenbergiana Lethaea, 88, 37-46.

Bennett, C.E., Howard, A.S.H., Davies, S.J., Kearsey, T.I., Millward, D., Brand, P.J., Browne, M.A.E., Reeves, E.J. and Marshall, J.E.A. 2017. Ichnofauna record cryptic marine incursions onto a coastal

floodplain at a key early Mississippian tetrapod site. Palaeogeography, Palaeoclimatology, Palaeoecology, 468, 287-300.

Bennett, C.E., Kearsey, T.I., Davies, S.J., Millward, D. Clack, J.A., Smithson, T.R. and Marshall, J.E.A. 2016. Early Mississippian sandy siltstones preserve rare vertebrate fossils in seasonal flooding episodes. Sedimentology, 63, 1677-1700.

Bennett, C.E., Siveter, D.J., Davies, S.J., Williams, M., Wilkinson, I.P., Browne, M. and Miller, C.G. 2012. Ostracods from freshwater and brackish environments of the Carboniferous of the Midland Valley of Scotland: the early colonisation of terrestrial water bodies. Geological Magazine, 149, 366-396.

Bennison, G.M. 1960. Lower Carboniferous non-marine lamellibranchs from East Fife, Scotland. Palaeontology, 3, 137-152.

Beus, S.S. 1980. Devonian serpulid bioherms of Arizona. Journal of Paleontology, 54, 1125-1128.

Bhattacharya, B. and Bhattacharya, H.N. 2007. Implications of trace fossil assemblages from late Paleozoic glaciomarine Talchir Formation, Raniganj basin, India. Gondwana Research, 12, 509-524.

Bicknell, R.D. and Pates, S. 2019. Xiphosurid from the Tournaisian (Carboniferous) of Scotland confirms deep origin of Limuloidea. Scientific reports, 9, 1-13.

Bontognali, T.R.R., Vasconcerlos, C., Warthmann, R.J., Bernasconi, S.M., Dupraz, C., Strohmenger, C.J. and McKenzie, J.A. 2010. Dolomite formation within microbial mats in the coastal sabkha of Abu Dhabi (United Arab Emirates). Sedimentology, 57, 824-844.

Boomer, I., Horne, D.J. and Slipper, I.J. 2003. The use of ostracods in palaeoenvironmental studies, or what can you do with an ostracod shell. Paleontological Society Papers, 9, 153-179.

Braddy, S. J. 2001. Eurypterid palaeoecology: palaeobiological, ichnological and comparative evidence for a ‘mass-moult-mate’hypothesis.". Palaeogeography, Palaeoclimatology, Palaeoecology, 172, 115-132.

Braga, J.C. and López-López, J.R. 1989. Serpulid bioconstructions at the Triassic-Liassic boundary in southern Spain. Facies, 21, 1-10.

1071 Brand, P.J. 2018. A list of fossil specimens in the BGS biostratigraphy collections from the Ballagan
1072 Formation in Scotland and from the former Lower Border Group of the Northumberland-Solway
1073 Basin. British Geological Survey Internal Report IR/18/03.

1074 Bridge, J.S., Gordon, E.A. and Titus, R.C. 1986. Non-marine bivalves and associated burrows in the Catskill
1075 Magnafacies (Upper Devonian) of New York State. Palaeogeography, Palaeoclimatology,
1076 Palaeoecology, 55, 65-77.

1077 Browne, M.A.E. 1980. The Upper Devonian and Lower Carboniferous (Dinantian) of the Firth of Tay,
1078 Scotland. Institute of Geological Sciences Report, 80/9.

1079 Browne, M.A.E., Dean, M.T., Hall, I.H.S., McAdam, A.D., Monro, S.K. and Chisholm, J.I. 1999. A
1080 lithostratigraphical framework for the Carboniferous rocks of the Midland Valley of Scotland. British
1081 Geological Survey Research Report, RR/99/07.

1082 Browne, M.A.E., Smith, R.A. and Aitken, A.M. 2002. Stratigraphical framework for the Devonian (Old Red
1083 Sandstone) rocks of Scotland south of a line from Fort William to Aberdeen. British Geological
1084 Survey Research Report, RR/01/04.

1085 Buatois, L.A., Gingras, M.K., Maceachern, J., Mángano, M.G., Zonneveld, J.P., Pemberton, S.G., Netto,
1086 R.G. and Martin, A. 2005. Colonization of brackish-water systems through time: evidence from the
1087 trace-fossil record. Palaios, 20, 321-347.

1088 Burchette, T.P. and Riding, R. 1977. Attached vermiform gastropods in Carboniferous marginal marine
1089 stromatolites and biostromes. Lethaia, 10, 17-28.

1090 Burrow, C.J., Long, J.A. and Trinajstic, K. 2009. Disarticulated acanthodian and chondrichthyan remains
1091 from the upper Middle Devonian Aztec Siltstone, southern Victoria Land, Antarctica. Antarctic
1092 Science 21, 71-88.

1093 Carpenter, D.K., Falcon-Lang, H.J., Benton, M.J. and Nelson, W.J. 2011. Fishes and tetrapods in the Upper
1094 Pennsylvanian (Kasimovian) Cohn coal member of the Mattoon formation of Illinois, United States:
1095 systematics, paleoecology, and paleoenvironments. Palaios 26, 639-657.

Carpenter, D.K., Falcon-Lang, H.J., Benton, M.J, and Henderson, E. 2014. Carboniferous (Tournaisian) fish assemblages from the Isle of Bute, Scotland: systematics and palaeoecology. Palaeontology, 57, 1215-1240.

Carvalho, I.D.S., Fernandes, A.C.S., Andreis, R.R., Paciullo, F.V.P., Ribeiro, A. and Trouw, R.A., 2005. The ichnofossils of the Triassic Hope Bay Formation, Trinity Peninsula Group, Antarctic Peninsula. Ichnos, 12, 191-200.

Cater, J.M.L., Briggs, D.E.G. and Clarkson, E.N.K. 1989. Shrimp-bearing sedimentary successions in the Lower Carboniferous (Dinantian) Dolostone and Oil Shale groups of northern Britain. Transactions of the Royal Society of Edinburgh: Earth Sciences, 80, 5-15.

Caudill, M.R., Driese, S.G. and Mora, C.I. 1996. Preservation of a palaeovertisol and an estimate of late Mississippian palaeoprecipitation. Journal of Sedimentary Research, 66, 58-70.

Chagas, A.A.P., Webb, G.E., Burne, R.V. and Southam, G. 2016. Modern lacustrine microbialites: towards a synthesis of aqueous and carbonate geochemistry and mineralogy. Earth Science Reviews, 162, 338-363.

Challands, T.J., Smithson, T.R., Clack, J.A., Bennett, C.E., Marshall, J.E.A., Wallace-Johnson, S.M. and Hill, H. 2019. A lungfish survivor of the end-Devonian extinction and an Early Carboniferous dipnoan radiation. Journal of Systematic Palaeontology, 17, 1825-1846.

Chisholm, J.I. and Brand, P.J. 1994. Revision of the late Dinantian sequence in Edinburgh and West Lothian. Scottish Journal of Geology, 30, 97-104.

Clack, J.A. 2002. An early tetrapod from 'Romer's Gap'. Nature, 418, 72-76.

Clack, J.A., Porro, L.B. and Bennett, C.E. 2018. A *Crassigyrinus*-like jaw from the Tournaisian (Early Mississippian) of Scotland. Earth and Environmental Science Transactions of the Royal Society of Edinburgh, 108, 37-46.

Clack, J.A., Bennett, C.E., Carpenter, D., Davies, S.J., Fraser, N.C., Kearsey, T.I., Marshall, J.E.A., Millward, D., Otoo, B.K.A., Reeves, E.J., Ross, A.J., Ruta, M., Smithson, K.Z., Smithson, T.R. and

121 Walsh, S. 2016. Phylogenetic and environmental diversity revealed for Tournaisian tetrapods. Nature
122 Ecology and Evolution, 1, 1-11, doi:10.1038/s41559-016-0002.

123 Clack, J.A., Bennett, C.E., Davies, S.J., Scott, A.C., Sherwin, J.E. and Smithson, T.R. 2019. A Tournaisian
124 (earliest Carboniferous) conglomerate-preserved non-marine faunal assemblage and its environmental
125 and sedimentological context. PeerJ, 6, p.e5972.

126 Clayton, G. 1986. Late Tournaisian miospores from the Ballycultra Formation at Cultra, County Down,
127 Northern Ireland. Irish Journal of Earth Sciences, 8, 73-79.

128 Coma, R., Ribes, M., Gili, J.M. and Hughes, R.N. 2001. The ultimate opportunists: consumers of seston.
129 Marine Ecology Progress Series, 219, 305-308.

130 Cook, A.G., Blodgett, R.B. and Becker, R.T. 2003. Late Devonian gastropods from the Canning Basin,
131 Western Australia. Alcheringa, 27, 181-207.

132 Cope, J.C.W., Guion, P.D., Sevastopulo, G. D, and Swan, A.R.H. 1992. Carboniferous, in Cope, J.C.W.,
133 Ingham, J.K. and Rawson, P.F. eds, Atlas of palaeogeography and lithofacies. Geological Society of
134 London Memoir, 13, 67-86.

135 Coward, M.P. 1993. The effect of Late Caledonian and Variscan continental escape tectonics on basement
136 structure, Paleozoic basin kinematics and subsequent Mesozoic basin development in NW Europe.
137 Geological Society, London, Petroleum Geology Conference series, 4, 1095-1108.

138 Craig, H. 1957. Isotopic standards for carbon and oxygen & correction factors for mass spectrometric
139 analysis. Geochemica et Cocmochemica Acta, 12, 133-149.

140 Crasquin-Soleau, S., Vaslet, D. and Le Nindre, Y. 2006. Ostracods of the Permian-Triassic Khuff
141 Formation, Saudi Arabia: palaeoecology and palaeobiogeography. GeoArabia, 11, 55-76.

142 Cressler, W.L., Daeschler, E.B., Slingerland, R. and Peterson, D.A. 2010. Terrestrialization in the Late
143 Devonian: a palaeoecological overview of the Red Hill site, Pennsylvania, USA. Geological Society,
144 London, Special Publications, 339, 111-128.

Davies, A., McAdam, A.D. and Cameron, I.B. 1986. Geology of the Dunbar district: Memoir of the British Geological Survey, Sheet 33E and part of 41(Scotland).

Davies, N.S. and Gibling, M.R. 2013. The sedimentary record of Carboniferous rivers: Continuing influence of land plant evolution on alluvial processes and Palaeozoic ecosystems. Earth-Science Reviews, 120, 40-79.

De Deckker P. 2002. Ostracoda Paleoecology, The Ostracoda: Applications in Quaternary Research Geophysical Monograph 131. American Geophysical Union.

De Deckker, P. 1983, Notes on the ecology and distribution of non-marine ostracods in Australia. Hydrobiologia, 106, 223-234.

De Deckker, P. and Geddes, M.C. 1980. Seasonal fauna of ephemeral saline lakes near the Coorong Lagoon, South Australia. Australian Journal of Marine and Freshwater Research, 31, 677-699.

De Deckker, P. and Last, W.M. 1988. Modern dolomite deposition in continental, saline lakes, western Victoria, Australia. Geology, 16, 29-32.

Donnelly, J.P., Butler, J., Roll, S., Wengren, M. and Webb, T. 2004. A backbarrier overwash record of intense storms from Brigantine, New Jersey. Marine Geology, 210, 107-121.

Downs, J.P. and Daeschler, E.B. 2001. Variation within a large sample of *Ageleodus pectinatus* teeth (Chondrichthyes) from the Late Devonian of Pennsylvania, U.S.A. Journal of Vertebrate Paleontology, 21, 811–814.

Eagar, H.M.C. and Weir, J. 1971. Some Spanish Upper Carboniferous non-marine bivalve faunas: A preliminary statement with emphasis on facies in north-west Spain and in Britain. Trabajos de geología, 3, 87-101.

Falcon-Lang, H.J. 1999. The early Carboniferous (Courceyan-Arundian) monsoonal climate of the British Isles: evidence from growth rings in fossil woods. Geological Magazine, 136, 177-187.

Falcon-Lang, H.J. 2004. Early Mississippian lycopsid forests in a delta-plain setting at Norton, near Sussex, New Brunswick, Canada. Journal of the Geological Society, 161, 969-981.

Falcon-Lang, H.J., Benton, M.J., Braddy, S.J. and Davies, S.J. 2006. The Pennsylvanian tropical biome reconstructed from the Joggins Formation of nova Scotia, Canada. Journal of the Geological Society, 163, 561-576.

Falcon-Lang, H.J., Pufahl, P.K., Bashforth, A.R., Gibling, M.R., Miller, R.F. and Minter, N.J. 2015a. A marine incursion in the Lower Pennsylvanian Tynemouth Creek Formation, Canada: implications for paleogeography, stratigraphy and paleoecology. Palaios, 30, 779-791.

Falcon-Lang, H.J., Minter, N.J., Bashforth, A.R., Gibling, M.R. and Miller, R.F. 2015b. Mid-Carboniferous diversification of continental ecosystems inferred from trace fossil suites in the Tynemouth Creek Formation of New Brunswick, Canada. Palaeogeography, Palaeoclimatology, Palaeoecology, 440, 142-160.

Ferrero, L., Obenat, S. and Zárate, Z. 2005. Mid-Holocene serpulid build-ups in an estuarine environment (Buenos Aires Province, Argentina). Palaeogeography, Palaeoclimatology, Palaeoecology, 222, 259-271.

Francis, E.H., Forsythe, I.H., Read, W.A. and Armstrong, M. 1970. The geology of the Stirling district. Memoir of the British Geological Survey, Sheet 39.

Freshney, E.C. 1961. The Dolostone Group of the west Midland Valley of Scotland. Ph.D. thesis, Glasgow University.

Freytet, P. and Verrecchia, E.P. 2002. Lacustrine and palustrine carbonate petrography: an overview. Journal of Paleolimnology, 27, 221-237.

Friedman, M. 2015. The early evolution of ray- finned fishes. Palaeontology, 58, 213-228.

Friedman, M. and Sallan, L.C. 2012. Five hundred million years of extinction and recovery: a Phanerozoic survey of large- scale diversity patterns in fishes. Palaeontology, 55, 707-742.

Garvey, J.M. and Turner, S. 2006. Vertebrate microremains from the presumed earliest Carboniferous of the Mansfield Basin, Victoria. Alcheringa, 30, 43-62.

194 Ghummed, M.A. 1982. Petrology and geochemistry of the carbonates, Ballagan Formation, N.W. Midland
195 Valley, Scotland. Ph.D. thesis, University of Glasgow.

196 Gierlowski-Kordesch, E.H. and Cassle, C.F. 2015. The 'Spirorbis' Problem Revisited: Sedimentology and
197 Biology of Microconchids in Marine-Nonmarine Transitions. Earth-Science Reviews, 148, 209-227.

198 Given, R.K. and Wilkinson, B.H. 1987. Dolomite abundance and stratigraphic age: constraints on rates and
199 mechanisms of Phanerozoic dolostone formation. Journal of Sedimentary Petrology, 57, 1068-1078.

200 Goodbred, S.L. and Hine, A.C. 1995. Coastal storm deposition: Salt-marsh response to a severe extratropical
201 storm, March 1993, west-central Florida. Geology, 23, 679-682.

202 Gray, J. 1988. Evolution of the freshwater ecosystem: the fossil record. Palaeogeography,
203 Palaeoclimatology, Palaeoecology, 62, 1-214.

204 Greb, S.F., DiMichele, W.A. and Gastaldo, R.A. 2006. Evolution and importance of wetlands in earth
205 history, in Greb, S.F. and DiMichele, W.A. eds. Wetlands through time. Geological Society of
206 America Special Paper, 399, 1-40.

207 Greb, S.F., Storrs, G.W., Garcia, W.J. and Eble, C.F. 2016. Late Mississippian vertebrate palaeoecology and
208 taphonomy, Buffalo Wallow Formation, western Kentucky, USA. Lethaia, 49, 199-218.

209 Gregg, J.M., Bish, D.L., Kaczmarek, S.E. and Machel, H.G. 2015. Mineralogy, nucleation and growth of
210 dolomite in the laboratory and sedimentary environment: a review. Sedimentology, 62, 1749-1769.

211 Gregg, J.M., Shelton, K.L., Johnson, A.W., Somerville, I.D. and Wright, W.R. 2001. Dolomitization of the
212 Waulsortian Limestone (Lower Carboniferous) in the Irish Midlands. Sedimentology, 48, 745-766.

213 Greig, D.C. 1988. Geology of the Eyemouth district: Memoir of the British Geological Survey, Sheet 34.

214 Gueriau, P., Charbonnier, S. and Clément, G. 2014a. First decapod crustaceans in a Late Devonian
215 continental ecosystem. Palaeontology, 57, 1203-1213.

216 Gueriau, P., Charbonnier, S. and Clément, G. 2014b. Angustidontid crustaceans from the Late Devonian of
217 Strud (Namur Province, Belgium): insights into the origin of Decapoda. Neues Jahrbuch für Geologie
218 und Paläontologie-Abhandlungen, 273, 327-337.

Gueriau, P., Rabet, N. and Hat, E.D.T. 2018. The Strud crustacean fauna (Late Devonian, Belgium): updated review and palaeoecology of an early continental ecosystem. Earth and Environmental Science Transactions of the Royal Society of Edinburgh, 107, 79-90.

Hodnett, J.P.M. and Elliott, D.K. 2018. Carboniferous chondrichthyan assemblages from the Surprise Canyon and Watahomigi formations (latest Mississippian–Early Pennsylvanian) of the western Grand Canyon, Northern Arizona. Journal of Paleontology, 92, 1-33.

Ivanov, A. 1996. The Early Carboniferous chondrichthyans of the South Urals, Russia. Geological Society, London, Special Publications, 107, 417-425.

Jeffery, J.E. 2006. The Carboniferous fish genera *Strepsodus* and *Archichthys* (Sarcopterygii: Rhizodontida): clarifying 150 years of confusion. Palaeontology, 49, 113–132.

Johnson, G.D. and Thayer, D.W. 2009. Early Pennsylvanian xenacanth chondrichthyans from the Swisshelm Mountains, Arizona, USA. Acta Palaeontologica Polonica, 54, 649-669.

Jones, B. 2013. Microarchitecture of dolomite crystals as revealed by subtle variations in solubility: implications for dolomitization. Sedimentary Geology, 288, 66-80.

Kaiser, S.I., Aretz, M. and Becker, R.T. 2016. The global Hangenberg Crisis (Devonian-Carboniferous transition): review of a first-order mass extinction, in Becker, R.T., Königshof, P. and Brett, C.E., eds. Devonian Climate, Sea Level and Evolutionary Events. Geological Society, London, Special Publications, 423, 387-437.

Kammer, T.W. and Lake, A.M. 2001. Salinity ranges of Late Mississippian invertebrates of the central Appalachian Basin. Southeastern Geology, 40, 99-116.

Kearsey, T., Twitchett, R.J. and Newell, A.J. 2012. The origin and significance of pedogenic dolomite from the Upper Permian of the South Urals of Russia. Geological Magazine, 149, 291-307.

Kearsey, T., Bennett, C.E., Millward, D., Davies, S.J., Gowing, C.J.B., Kemp, S., Leng, M.J., Marshall, J.E.A. and Browne, M.A.E. 2016. The terrestrial landscapes of tetrapod evolution in earliest

Carboniferous seasonal wetlands of the Ballagan Formation in S.E. Scotland. Palaeogeography, Palaeoclimatology, Palaeoecology, 457, 52-69.

Knaust, D. 2013. The ichnogenus *Rhizocorallium*: classification, trace makers, palaeoenvironments and evolution. Earth-Science Reviews, 126, 1-47.

Lamsdell, J.C. 2016. Horseshoe crab phylogeny and independent colonizations of fresh water: ecological invasion as a driver for morphological innovation. Palaeontology, 59, 181-194.

Lamsdell, J.C. and Braddy, S.J. 2010. Cope's Rule and Romer's theory: patterns of diversity and gigantism in eurypterids and Palaeozoic vertebrates. Biology Letters, 6, 265-269.

Lamsdell, J.C., Lagebro, L., Edgecombe, G.D., Budd, G.E. and Gueriau, P. 2019. Stylonurine eurypterids from the Strud locality (Upper Devonian, Belgium): new insights into the ecology of freshwater sea scorpions. Geological Magazine, 156, 1708-1714.

Leeder, M.R. 1973. Lower Carboniferous Serpulid patch reefs, bioherms and biostromes. Nature, 242, 41-42.

Leeder, M.R. 1974. Lower Border Group (Tournaisian) fluvio-deltaic sedimentation and palaeogeography of the Northumberland Basin. Proceedings of the Yorkshire Geological Society, 40, 129-180.

Leeder, M. 1975a. Lower Border Group (Tournaisian) limestones from the Northumberland Basin. Scottish Journal of Geology, 11, 151-167.

Leeder, M. 1975b. Lower Border Group (Tournaisian) stromatolites from the Northumberland basin. Scottish Journal of Geology, 11, 207-226.

Liu, D., Xu, Y., Papineau, D., Yu, N., Fan, Q., Qiu, X. and Wang, H. 2019. Experimental evidence for abiotic formation of low-temperature proto-dolomite facilitated by clay minerals. Geochimica et Cosmochimica Acta, 247, 83-95.

Liu, K.B., McCloskey, T.A., Bianchette, T.A., Keller, G., Lam, N.S., Cable, J.E. and Arriola, J. 2014. Hurricane Isaac storm surge deposition in a coastal wetland along Lake Pontchartrain, southern Louisiana. Journal of Coastal Research, 70, 266-271.

Long, A.G. 1959. The fossil plants of Berwickshire – a review of past work. Part 2. Work mainly done in the present century. History of the Berwickshire Naturalists' Club, 35, 26-47.

Long, A.G. 1960. On the structure of *Samaropsis scotia* Calder (emended) and *Eurystoma angulare* gen. et sp. nov. petrified seeds from the Calciferous Sandstone Series of Berwickshire. Transactions of the Royal Society of Edinburgh, 64, 261-284.

Lumsden, G. I., Tulloch, W., Howells, M. F. and Davis, A. 1967. The geology of the neighbourhood of Langholm: Memoir of the British Geological Survey, Sheet 11.

MacGregor, A.G. 1960. Divisions of the Carboniferous on Geological Survey Scottish maps. Bulletin of the Geological Survey of Great Britain, 16, 127-30.

Maharjan, D., Jiang, G., Peng, Y. and Henry, R.A. 2018. Paired carbonate-organic carbon and nitrogen isotope variations in Lower Mississippian strata of the southern Great Basin, western United States. Palaeogeography, Palaeoclimatology, Palaeoecology, 490, 462-472.

Mángano, M.G. and Buatois, L.A. 2004. Ichnology of Carboniferous tide-influenced environments and tidal flat variability in the North American Midcontinent. Geological Society, London, Special Publications, 228, 157-178.

Marshall, J.E.A., Reeves, E.J., Bennett, C.E., Davies, S.J., Kearsey, T.I., Millward, D., Smithson, T.R. and Browne, M.A. 2019. Reinterpreting the age of the uppermost 'Old Red Sandstone' and Early Carboniferous in Scotland. Earth and Environmental Science Transactions of the Royal Society of Edinburgh, 109, 265-278.

Martel, A.T. and Gibling, M.R. 1991. Wave-dominated lacustrine facies and tectonically controlled cyclicity in the Lower Carboniferous Horton Bluff Formation, Nova Scotia, Canada, in: Anadón, P., Cabrera, L.I. and Kelts, K., eds. Lacustrine Facies Analysis. International Association of Sedimentologists Special Publication, 13, 223-243.

Masdeu, M., Mello, F.T.D., Loureiro, M. and Arim, M. 2011. Feeding habits and morphometry of *Iheringichthys labrosus* (Lütken, 1874) in the Uruguay River (Uruguay). Neotropical Ichthyology, 9, 657-664.

Mather, C.C., Nash, D.J., Dogramaci, S., Grierson, P.F. and Skrzypek, G. 2019. Geomorphic and hydrological controls on groundwater dolocrete formation in the semi- arid Hamersley Basin, northwest Australia. Earth Surface Processes and Landforms, 44, 2752-2770.

McHargue, T.R. and Price, R.C. 1982. Dolomite from clay in argillaceous or shale-associated marine carbonates. Journal of Sedimentary Research, 52, 873-886.

Millward, D., Davies, S.J., Brand, P.J., Browne, M.A.E., Bennett, C.E., Kearsey, T.I., Sherwin, J.R. and Marshall, J.E.A. 2019. Palaeogeography of tropical seasonal coastal wetlands in northern Britain during the early Mississippian Romer's Gap. Earth and Environmental Science Transactions of the Royal Society of Edinburgh, 109, 279-300.

Millward, D., Davies, S.J., Williamson, F., Curtis, R., Kearsey, T.I., Bennett, C.E., West, I.M., Marshall, J.E.A. and Browne, M.A.E. 2018. Early Mississippian evaporites of coastal tropical wetlands. Sedimentology, 65, 2278-2311.

Millward, D., Kearsey, T.I. and Browne, M.A.E. 2013. Norham West Mains Farm Borehole: operations report. British Geological Survey Internal Report IR/13/033.

Ming, G.Y. 2004. Facies characteristics and tiering distributions of Chondrites. Acta Palaeontologica Sinica, 1, 1-8.

Montañez , I.P. and Cecil, C.B. 2013. Paleoenvironmental clues archived in non-marine Pennsylvanian-lower Permian limestones of the Central Appalachian Basin, USA. International Journal of Coal Geology, 119, 41-55.

Moore, C.G., Saunders, G.R. and Harries, D.B. 1998. The status and ecology of reefs of *Serpula vermicularis* L. (Polychaeta: Serpulidae) in Scotland: Aquatic Conservation. Marine and Freshwater Ecosystems, 8, 645-656.

Muchez, P. and Viaene, W. 1987. Dolocretes from the Lower Carboniferous of the Campine-Brabant Basin, Belgium. Pedologie, 37, 187-202.

Narkiewicz, M., Grabowski, J., Narkiewicz, K., Niedźwiedzki, G., Retallack, G.J., Szrek, P. and De Vleeschouwer, D. 2015. Palaeoenvironments of the Eifelian dolomites with earliest tetrapod trackways (Holy Cross Mountains, Poland). Palaeogeography, Palaeoclimatology, Palaeoecology, 420, 173-192.

Ó Gogáin, A., Falcon- Lang, H.J., Carpenter, D.K., Miller, R.F., Benton, M.J., Pufahl, P.K., Ruta, M., Davies, T.G., Hinds, S.J. and Stimson, M.R. 2016. Fish and tetrapod communities across a marine to brackish salinity gradient in the Pennsylvanian (early Moscovian) Minto Formation of New Brunswick, Canada, and their palaeoecological and palaeogeographical implications. Palaeontology, 59, 689-724.

Olanipekun, B.J. and Azmy, K. 2017. In situ characterization of dolomite crystals: Evaluation of dolomitization process and its effect on zoning. Sedimentology, 64, 1708-1730.

Otoo, B.K., Clack, J.A., Smithson, T.R., Bennett, C.E., Kearsey, T.I. and Coates, M.I. 2019. A fish and tetrapod fauna from Romer's Gap preserved in Scottish Tournaisian floodplain deposits. Palaeontology, 62, 225-253.

Owada, M. 2007. Functional morphology and phylogeny of the rock-boring bivalves *Leiosolenus* and *Lithophaga* (Bivalvia: Mytilidae): a third functional clade. Marine Biology, 150, 853-860.

Palma, R.M. and Angeleri, M.P. 1992. Early cretaceous serpulid limestones: Chachao Formation, Neuquen basin, Argentina. Facies, 27, 175-178.

Park, L.E., Siewers, F.D., Metzger, T. and Sipahioglu, S. 2009. After the hurricane hits: recovery and response to large storm events in a saline lake, San Salvador Island, Bahamas. Quaternary International, 195, 98-105.

Petrash, D.A., Bialik, O.M., Bontognali, T.R., Vasconcelos, C., Roberts, J.A., McKenzie, J.A. and Konhauser, K.O. 2017. Microbially catalyzed dolomite formation: From near-surface to burial. Earth-Science Reviews, 171, 558-582.

Pilarczyk, J.E., Horton, B.P., Soria, J.L.A., Switzer, A.D., Siringan, F., Fritz, H.M., Khan, N.S., Ildefonso, S., Doctor, A.A. and Garcia, M.L. 2016. Micropaleontology of the 2013 Typhoon Haiyan overwash sediments from the Leyte Gulf, Philippines. Sedimentary Geology, 339, 104-114.

Platt, N.H. and Wright, V.P. 1992. Palustrine carbonates and the Florida Everglades: Towards an exposure index for the fresh-water environment. Journal of Sedimentary Petrology, 62, 1058-1071.

Plummer, P.S. and Gostin, V.A. 1981. Shrinkage cracks: desiccation or synaeresis. Journal of Sedimentary Petrology, 51, 1147-1156.

Rameil, N. 2008. Early diagenetic dolomitization and dedolomitization of Late Jurassic and earliest Cretaceous platform carbonates: a case study from the Jura Mountains (NW Switzerland, E France). Sedimentary Geology, 212, 70-85.

Ramsbottom, W.H.C. 1973. Transgressions and regressions in the Dinantian: a new synthesis of British Dinantian stratigraphy. Proceedings of the Yorkshire Geological Society, 39, 567-607.

Rejmankova, E., Pope, K.O., Post, R. and Maltby, E. 1996. Herbaceous wetlands of the Yucatan Peninsula: communities at extreme ends of environmental gradients. Internationale Revue der gesamten Hydrobiologie und Hydrographie, 81, 223-252.

Rennie, M.D. and Jackson, L.J. 2005. The influence of habitat complexity on littoral invertebrate distributions: patterns differ in shallow prairie lakes with and without fish. Canadian Journal of Fisheries and Aquatic Sciences, 62, 2088-2099.

Richards, K.R., Sherwin, J.E., Smithson, T.R., Bennion, R.F., Davies, S.J., Marshall, J.E.A. and Clack, J.A. 2018. Diverse and durophagous: early Carboniferous chondrichthyans from the Scottish Borders. Earth and Environmental Science Transactions of the Royal Society of Edinburgh, 108, 67-87.

Rogers, M.J. 1965. A revision of the species of nonmarine Bivalvia from the Upper Carboniferous of eastern North America. Journal of Paleontology, 663-686.

Ross, A.J., Edgecombe, G.D., Clark, N., Bennett, C.E., Carriò, V., Contreras-Izquierdo, R. and Crighton, B. 2018. A new terrestrial millipede (Myriapoda: Diplopoda) fauna of earliest Carboniferous

(Tournaisian) age from the Scottish Borders helps fill 'Romer's Gap'. Earth and Environmental Science Transactions of the Royal Society of Edinburgh, 108, 99-110.

Rygel, M.C., Gibling, M.R. and Calder, J.H. 2004. Vegetation- induced sedimentary structures from fossil forests in the Pennsylvanian Joggins Formation, Nova Scotia. Sedimentology, 51, 531-552.

Rygel, M.C., Calder, J.H., Gibling, M.R., Gingras, M.K. and Melrose, C.S.A. 2006. Tournaisian forested wetlands in the Horton Group of Atlantic Canada. Geological Society of America, Special Publication, 399, 103–126.

Sallan, L.C. and Coates, M.I. 2010. End-Devonian extinction and a bottleneck in the early evolution of modern jawed vertebrates. PNAS, 107, 10131-10135.

Sallan, L.C. and Coates, M.I., 2013. Styracopterid (Actinopterygii) ontogeny and the multiple origins of post-Hangenberg deep-bodied fishes. Zoological Journal of the Linnean Society, 169, 156-199.

Sallan, L.C. and Galimberti, A.K. 2015. Body-size reduction in vertebrates following the end-Devonian mass extinction. Science, 350, 812-815.

Sánchez-Román, M., Vasconcelos, C., Warthmann, R. Rivadeneyra, M. and McKenzie, J.A. 2009. Microbial dolomite precipitation under aerobic conditions: results from Brejo do Espinho Lagoon (Brazil) and culture experiments. Special Publication of the International Association of Sedimentologists, 41, 167-178.

Scotese, C.R. and McKerrow, W.S. 1990. Revised world maps and introduction. Geological Society of London Memoirs, 12, 1-21.

Scott, A.C., Galtier, J. and Clayton, G. 1984. Distribution of anatomically-preserved floras in the Lower Carboniferous in Western Europe. Transactions of the Royal Society of Edinburgh: Earth Sciences, 75, 311-340.

Scott, W.B. 1971. The sedimentology of the dolostone group in the Tweed basin: Burnmouth and the Merse of Berwick. Ph.D. thesis, Sunderland Polytechnic.

Scott, W.B. 1986. Nodular carbonates in the Lower Carboniferous, Dolostone Group of the Tweed Embayment, Berwickshire: evidence for a former sulphate evaporite facies. Scottish Journal of Geology, 22, 325-345.

Searl, A. 1988. Pedogenic dolomites from the Oolite Group (Lower Carboniferous), South Wales. Geological Journal, 23, 157-169.

Shinn, E.A., Lloyd, R.M. and Ginsburg, R.N. 1969. Anatomy of a modern carbonate tidal-flat, Andros Island, Bahamas. Journal of Sedimentary Research, 39, 1202-1228.

Sibley, D.F. and Gregg, J.M. 1987. Classification of dolomite rock textures. Journal of Sedimentary Petrology, 57, 967-975.

Singh, B.P., Srivastava, V.K. and Kanhaiya, S. 2019. Sedimentological and geochemical characteristics of the late middle Eocene dolostone succession, Kachchh, western India. Geological Journal, 54, 3840-3859.

Slaughter, M. and Hill, R.J. 1991. The influence of organic matter in organogenic dolomitization. Journal of Sedimentary Research, 61, 296-303.

Smithson, T.R., Richards, K.R. and Clack, J.A. 2016. Lungfish diversity in Romer's Gap: reaction to the end- Devonian extinction. Palaeontology, 59, 29-44.

Smithson, T.R., Wood, S.P., Marshall, J. E.A. and Clack, J.A. 2012. Earliest Carboniferous tetrapod and arthropod faunas from Scotland populate Romer's Gap. PNAS, 109, 4532-4537.

Somerville, I.D., Strogen, P., Mitchell, W.I., Somerville, H.A. and Higgs, K.T. 2001. Stratigraphy of Dinantian rocks in WB3 borehole, Co. Armagh. Irish Journal of Earth Sciences, 19, 51-78.

Stephenson, M.H., Williams, M., Leng, M.J. and Monaghan, A.A. 2004a. Aquatic plant microfossils of probable non-vascular origin from the Ballagan Formation (Lower Carboniferous), Midland Valley, Scotland. Proceedings of the Yorkshire Geological Society, 55, 145-158.

Stephenson, M.H., Williams, M., Monaghan, A.A., Arkley, S., Smith, R.A., Dean, M., Browne, M.A.E. and Leng, M. 2004b. Palynomorph and ostracod biostratigraphy of the Ballagan Formation, Midland

Valley of Scotland, and elucidation of intra-Dinantian unconformities. Proceedings of the Yorkshire Geological Society, 55, 131-143.

Suarez-Gonzalez, P., Quijada, I.E., Benito, M.I. and Mas, R. 2015. Sedimentology of ancient coastal wetlands: insights from a Cretaceous multifaceted depositional system. Journal of Sedimentary Research, 85, 95-117.

Suttner, T. and Lukeneder, A. 2003. Accumulations of Late Silurian serpulid tubes and their palaeoecological implications (Blumau-Formation; Burgenland; Austria). Annalen des Naturhistorischen Museums in Wien, 105A, 175-187.

Tandon, S.K. and Andrews, J.E. 2001. Lithofacies associations and stable isotopes of palustrine and calcrete carbonates: examples from an Indian Maastrichtian regolith. Sedimentology, 48, 339-355.

Taylor, A., Goldring, R. and Gowland, S. 2003. Analysis and application of ichnofabrics. Earth-Science Reviews, 60, 227-259.

Taylor, P.D. and Vinn, O. 2006. Convergent morphology in small spiral worm tubes ('Spirorbis') and its palaeoenvironmental implications. Journal of the Geological Society, 163, 225-228.

Thorez, J., Dreesen, R. and Streel, M. 2006. Famennian. Geologica Belgica, 9, 27-45.

Törő, B. and Pratt, B.R. 2015. Eocene Paleoseismic Record of the Green River Formation, Fossil Basin, Wyoming, USA: Implications of Synsedimentary Deformation Structures in Lacustrine Carbonate Mudstones. Journal of Sedimentary Research, 85, 855-884.

Trueman, A.E. and Weir, J. 1946. A monograph of British Carboniferous non-marine Lamellibranchs. Palaeontographical Society Monographs 99, pts I-IX.

Turner, M.S. 1991. Geochemistry and diagenesis of basal Carboniferous dolostones from southern Scotland. Ph.D. thesis, University of East Anglia.

Vanstone, S.D. 1991. Early Carboniferous (Mississippian) palaeosols from southwest Britain: influence of climatic change on soil development. Journal of Sedimentary Petrology, 61, 445-457.

Vasey, G.M. 1984. Westphalian macrofaunas in Nova Scotia: palaeoecology and correlation. Ph.D. thesis, University of Strathclyde.

Vasconcelos, C. and McKenzie, J.A. 1997. Microbial mediation of modern dolomite precipitation and diagenesis under anoxic conditions (Lagoa Vermelha, Rio de Janeiro, Brazil). Journal of Sedimentary Research, 67, 378-390.

Vasconcelos, C., McKenzie, J.A., Warthmann, R. and Bernasconi, S.M. 2005. Calibration of the δ18O paleothermometer for dolomite precipitated in microbial cultures and natural environments. Geology, 33, 317-320.

Vaughn, C.C., Nichols, S.J. and Spooner, D.E. 2008. Community and foodweb ecology of freshwater mussels. Journal of the North American Benthological Society, 27, 409-423.

Victor, R., Chan, G.L. and Fernando, C.H. 1979. Notes on the recovery of live ostracods from the gut of the white sucker (*Catostomus commersoni* Lacepede) 1808, (Pisces: Catostomidae). Canadian Journal of Zoology, 57, 1745-1747.

Vinn, O. and Mutvei, H. 2009. Calcareous tubeworms of the Phanerozoic. Estonian Journal of Earth Sciences, 58, 286-296.

Vrazo, M.B., Brett, C.E. and Ciurca, S.J. 2016. Buried or brined? Eurypterids and evaporites in the Silurian Appalachian basin. Palaeogeography, Palaeoclimatology, Palaeoecology, 444, 48-59.

Wacey, D., Wright, D.T. and Boyce, A.J. 2007. A stable isotope study of microbial dolomite formation in the Coorong Region, South Australia. Chemical Geology, 244, 155-174.

Wanas, H.A. and Sallam, E. 2016. Abiotically-formed, primary dolomite in the mid-Eocene lacustrine succession at Gebel El-Goza El-Hamra, NE Egypt: An approach to the role of smectitic clays. Sedimentary Geology, 343, 132-140.

Warren, J. 2000. Dolomite: occurrence, evolution and economically important associations. Earth-Science Reviews, 52, 1-81.

Warren, J.K. 2006. Evaporites: Sediments, Resources and Hydrocarbons. Springer-Verlag, Berlin-Heidelberg, 1035 pp.

Waters, C.N. and Davies, S.J. 2006. Carboniferous: extensional basins, advancing deltas and coal swamps, in Brenchley, P.J. and Rawson, P.F., eds, The geology of England and Wales. Geological Society of London, 173-223.

Williams, H.F.L. 2009. Stratigraphy, Sedimentology, and Microfossil Content of Hurricane Rita Storm Surge Deposits in Southwest Louisiana. Journal of Coastal Research, 25, 1041-1051.

Williams, M., Stephenson, M.H., Wilkinson, I.P., Leng, M.L. and Miller, C.G. 2005. Early Carboniferous (Late Tournaisian-Early Viséan) ostracods from the Ballagan Formation, central Scotland, UK. Journal of Micropalaeontology, 24, 77-94.

Williams, M., Leng, M.L., Stephenson, M.H., Andrews, J.E., Wilkinson, I.P., Siveter, D.J., Horne, D.J. and Vannier, J.M.C. 2006. Evidence that Early Carboniferous ostracods colonised coastal flood plain brackish water environments. Palaeogeography, Palaeoclimatology, Palaeoecology, 230, 299-318.

Wilson, M.A., Vinn, O. and Yancey, T.E. 2011. A new microconchid tubeworm from the Artinskian (Lower Permian) of central Texas, USA. Acta Palaeontologica Polonica, 56, 785-791.

Wilson, M.J., Bain, D.C. McHardy, W.J. and Berrow, M.L. 1972. Clay-mineral studies on some Carboniferous sediments in Scotland. Sedimentary Geology, 8, 137-150.

Wright, D.T. 1999. The role of sulphate-reducing bacteria and cyanobacteria in dolomite formation in distal ephemeral lakes of the Coorong region, South Australia. Sedimentary Geology, 126, 147-157.

Wright, D.T. and Wacey, D. 2004. Sedimentary dolomite: a reality check. Geological Society, London, Special Publications, 235, 65-74.

Wright, V.P. 1990. Equatorial aridity and climatic oscillations during the early Carboniferous, southern Britain. Journal of the Geological Society, 147, 359-363.

Wright, V.P. and Robinson, D. 1988. Early Carboniferous floodplain deposits from South Wales: a case study of the controls on palaeosol development. Journal of the Geological Society, 145, 847-857.

Wright, V.P., Turner, M.S., Andrews, J.E. and Spiro, B. 1993. Morphology and significance of super-mature calcretes from the Upper Old Red Sandstone of Scotland. Journal of the Geological Society, 150, 871-883.

Wright, V.P., Vanstone, S.D. and Marshall, J.D. 1997. Contrasting flooding histories of Mississippian carbonate platforms revealed by marine alteration effects in palaeosols. Sedimentology, 44, 825-842.

Yazdi, M. and Turner, S. 2000. Late Devonian and Carboniferous vertebrates from the Shishtu and Sardar formations of the Shotori Range, Iran. Records of the Western Australian Museum, Supplement 58, 223-240.

Yen, T.C. 1949. Review of Palaeozoic non-marine gastropods and a description of a new genus from the Carboniferous rocks of Scotland. Journal of Molluscan Studies, 27, 235-240.

Yoo, E.K. 1988. Early Carboniferous Mollusca from Gundy, Upper Hunter, New South Wales. Records of the Australian Museum, 40, 233-264.

Zatoń, M., Vinn, O. and Tomescu, A.M.F. 2012. Invasion of freshwater and variable marginal marine habitats by microconchid tubeworms – an evolutionary perspective. Geobios, 45, 603-610.

Ziegler, A.M., Eshel, G., Rees, P.M., Rothfus, T., Rowley, D. and Sunderlin, D. 2003. Tracing the tropics across land and sea: Permian to present. Lethaia, 36, 227-254.

Ziegler, P.A. 1989. Evolution of Laurussia, a study in late Palaeozoic plate tectonics. Dordrecht, The Netherlands, Kluwer academic publishers, 102 p.

Figure Captions

Figure 1. Palaeogeography and location maps. A. Location map of Scotland and northern England. The Ballagan Formation outcrop is within the Tweed Basin (this study), the Midland Valley of Scotland and the Northumberland-Solway Basin. The primary field site of Burnmouth and the location of the Norham Core at Norham are indicated. Maps modified from Smithson et al. (2012); a detailed location map of Burnmouth and the Norham Core is given in Bennett et al. (2017). B. Palaeogeography of Mississippian synsedimentary dolostones. Map is a reconstruction at 335 Ma (modified from Ziegler, 1989). Numbers 1-8 refer to

513 published occurrences of dolostone facies: 1: Kentucky, USA (Barnett et al., 2012) and Tennessee, USA
514 (Caudill et al., 1996); 2-4: Eastern Canada; New Brunswick, Nova Scotia and western Newfoundland (Belt
515 et al., 1967; Martel and Gibling, 1991); 5: Northern Ireland (Clayton, 1986); 6: South Wales (Wright and
516 Robinson, 1988) and South-West England (Vanstone, 1991; Wright et al., 1997); 7: Scottish Borders,
517 Northumberland and Midland Valley of Scotland (Andrews et al., 1991; Freshney, 1961; Ghummed, 1982;
518 Scott, 1971, 1986; Turner, 1991, and this study); 8: Booischot borehole, Campine-Brabant basin of Belgium
519 (Muchez and Viaene, 1987). Dolostones occur within newly rifting basins along the southern margin of
520 Laurussia.

521 Figure 2. The 490-m thick Norham Core showing dolostones. The thickness of each dolostone bed is
522 illustrated with horizontal blue lines and the number of beds per 10 metre rock thickness by a continuous
523 black line. The number of beds per 10 metre thickness decreases on average from the base to the top of the
524 formation and is highest in the basal 80 m of the core. Dolostones are rare within the sandstones of the
525 fluvial facies association. Dolostone facies are: Facies 1: Cemented siltstone and sandstone; Facies 2:
526 Homogeneous micrite; Facies 3: Mixed dolomite and siltstones; Facies 4: Mixed calcite-dolomite; Facies 5:
527 Dolomite with evaporite minerals. Facies 5 is more common at the base of the formation, with other facies
528 types randomly distributed. The detailed section shows an example of a typical facies 2-3 type dolostone
529 dominated sequence from the middle of the Norham Core.

530 Figure 3. Burnmouth section showing dolostones. The thickness and abundance of dolostone beds decreases
531 from the base to the top of the formation. Note that the Burnmouth sequence has fewer dolostone beds
532 identified to a facies level, as only beds that were sampled were assigned to a facies (see Table S1). Detailed
533 section A: Part of the Burnmouth succession with the most abundant dolostone beds, with numerous facies 4
534 beds exhibiting soft sediment deformation. Refer to Figure 2 for the Key.

535 Figure 4. Dolostone facies in the Norham Core. A: Facies 1, cemented sandstone and siltstone, interbedded
536 units that are rooted and bioturbated, two dolostone nodules occur in a siltstone bioturbated by *Chondrites*,
537 230.8 m. B: Facies 2, homogeneous dolomicrite, the bed has a brecciated interior and the basal contact is
538 diffuse into siltstone, 334.95 m. C: Facies 3, interbedded dolomite and siltstone, the middle bed has soft

sediment deformation, 331.1 m. D: Facies 3, interbedded dolomite and siltstone, both units are extensively brecciated, the dolostone hosts ostracods and *Serpula*, 227.1 m. E: Facies 4, a 5 cm thick calcite-rich bed (in the upper part of the photograph) containing abundant fossils (*Serpula*, large bivalves, ?*Schizodus*, *Naiadites*, ostracods, fish fragments and *Spirorbis*, not visible in photograph). Above and below the bed are siltstones bioturbated by *Chondrites*, 473.45 m. F: Facies 5, anhydrite nodules in a dolomite matrix, overlain by dolomite with compacted laminations, 493 m. Scale bars 25 mm.

Figure 5. Key features of dolostone facies in outcrop, thin section scan and photomicrograph. The schematic logs illustrate an average 50 cm thick succession of the facies in outcrop or in core. Facies 1: Thin section scan: cemented siltstone with bivalves and *Serpula*, Norham Core, 336.7 m. Photomicrograph (plane-polars): dolomite crystals cementing a matrix of siltstone and fossil fragments. Facies 2: Thin section scan: micritic homogeneous dolostone with desiccation cracks filled with silt-rich carbonate, Norham Core, 39.95 m. Photomicrograph (plane-polars): small dolomite crystals within a clay matrix. Facies 3: Thin section scan: Interbedded dolomite and finely laminated silt, Norham Core, 321.85 m. Photomicrograph (plane-polars): Boundary between silt and dolomite layers. Facies 4: Thin section scan: micritic calcite and dolomite in patches, oolitic bed, Burnmouth, 209.92 m. Photomicrograph (plane-polars): ooids with dolomite spar in their centre are in a matrix of micritic calcite. Facies 5: Thin section scan: Laminated siltstone with a dolomite nodule bearing large anhydrite crystals, Norham Core, 492.92 m. Photomicrograph (crossed-polars): anhydrite crystals in a dolomicrite matrix. Colours in schematic log: yellow = dolomite, white = siltstone or sandstone, orange = calcite, pink = evaporites. Scale bars: thin section: 5 mm; photomicrograph 100 μm. Symbols: a, anhydrite; b, bivalves; c, calcite ; d, dolomite; q, quartz; s, *Serpula*.

Figure 6. Electron backscatter SEM images of dolostone thin sections. A: Facies 1, sandstone matrix cemented with non-planar anhedral dolomite, Burnmouth, 178.85 m. B: Facies 2, planar euhedral dolomite rhombs in a clay matrix, the rhombs are zoned with calcium-rich centres. One euhedral pyrite crystal is present, Norham Core, 368.07 m. C: Facies 3, planar euhedral dolomite rhombs within a siltstone matrix, no zoning is present, Norham Core, 321.85 m. D: Facies 4, planar euhedral dolomite rhombs and micritic dolomite within a clay matrix, Burnmouth, 184.03 m. E: Facies 4, patches of dolomite and calcite with

abundant bivalve fossils. Pyrite occurs along the rim of fossils, as discrete euhedral crystals and in clusters of small framboids, Norham Core, 473.64 m, this bed is also shown in Figure 4E. F: Facies 4, calcitic ooid partially replaced by dolomite, with a pyrite rim. The ooid has zoned small euhedral dolomite crystals in the interior, and dolomite spar in the matrix, Burnmouth, 209.92 m. G: Facies 5, anhydrite crystals in a dolomicrite matrix, Norham Core, 492.92 m. H: Facies 5, planar euhedral dolomite rhombs within a clay matrix, crystals are zoned with magnesium-rich centres, Norham Core, 449.65 m. Scale bars 50 μm. Symbols: a, anhydrite; b, bivalve; c, calcite; cl, clay minerals; d, dolomite; f, feldspar; p, pyrite; q, quartz.

Figure 7. Secondary alteration and bulbous dolostones. A. The percentage of dolostone samples of each facies from the Norham Core and Burnmouth section, which are brecciated, desiccated or pedogenically modified. Each facies is numbered (1-5), and the circumference of each facies indicates the relative number of beds of each facies. The number of beds of each facies present in the Norham Core are: Facies 1: 52; Facies 2: 85; Facies 3: 95; Facies 4: 9; Facies 5: 38. And at Burnmouth: Facies 1: 48; Facies 2: 40; Facies 3: 58; Facies 4: 13; Facies 5: 6. Internal brecciation is much more common than desiccation cracks. B-D: Facies 2 dolostones with a bulbous top or base. B. Top surface of a dolostone bed with large pillow shaped bulbous dolostone, internally brecciated and rooted, Burnmouth, 128.1 m. C. Basal surface of a dolostone bed with tree trunk impressions and brecciation, Burnmouth, 379.55 m. D. Bulbous top surface of a dolostone bed with a lycopsid root impression, Burnmouth, 334.5 m. Scale bars 5 cm.

Figure 8. Fossil content and bioturbation. In A and C each facies is numbered (1-5), and the circumference of each facies indicates the relative number of beds of each facies as in Figure 7. A: The percentage of dolostone samples of each facies from the Norham Core and Burnmouth which contain fossils. B: Graphs showing the percentage of fossil occurrence per facies. The presence of each fossil group is counted and the percentage calculated, for example, 25% of facies 1 dolostones in the Norham Core contain plant fragments. Of significance are the more common robust bivalves (R. bivalve), *Spirorbis* and *Serpula* burrows within Facies 4 and some Facies 3 beds. Not illustrated are fragments of arthropod cuticle and gastropods, which occur in almost all facies in very low numbers. C: The percentage of dolostone samples of each facies from

590 the Norham Core and Burnmouth, which are bioturbated. Core samples have a higher bioturbation
591 percentage per facies, primarily because bioturbation is more easily seen in the core.

592 Figure 9. Autochthonous and allochthonous *Serpula* within dolostones. Autochthonous *Serpula* colonies are
593 present within the centre of dolostone beds, whereas allochthonous *Serpula* comprises centimetre thick
594 horizons of broken tube fragments that are at random orientations. A: Autochthonous *Serpula* within a
595 dolostone containing siltstone patches, Norham Core, 368.12 m. Ostracods, *Spirorbis*, bivalve fragments,
596 roots and plant fragments were identified in the hand specimen of this bed. B: Autochthonous *Serpula* and
597 ostracods in thin section, within a dolostone, from the Burnmouth field section, 181.83 m height. Thin
598 section scan, *Serpula* tubes are outlined (b1) and shown in a detailed plane-polarised light image (b2). The
599 tube wall is composed of microcrystalline calcite and the tubes are infilled with large sparry calcite crystals.
600 C: Allochthonous *Serpula* within a dolostone that is brecciated, Norham Core, at 227.13 m. A coquina of
601 broken *Serpula* tubes and ostracods fill in the cracks. Thin section scan, crack outline and *Serpula* fragments
602 are outlined in (c). In both B and C *Serpula* tubes are infilled with calcite (white colour) and dolomite
603 crystals (grey) or silt-bearing dolomicrite (brown). Scale: A: 25 mm, B-C: scale bar 5 mm, b2: scale bar 250
604 μm.

605 Figure 10. Microfossil assemblages. Percentage counts of total assemblage microfossil counts for one
606 sample of each facies. Facies 1 (n = 6468 specimens), Facies 2 (n = 779), Facies 3 (n = 1231), Facies 4 (n =
607 1372), and Facies 5 (n = 1853). The full data table of counts for all size fractions and microfossils per gram
608 is detailed in Table S3. Abbreviations: acanth., acanthodian; actin., actinopterygian; chond., chondrichthyan;
609 indet., indeterminate; rhizo., rhizodont.

610 Figure 11. Plate of common dolostone microfossils. A: Actinopterygian lepidotrichia bone, facies 2. B:
611 Hybodont scale with spines that are joined together into a star shape, dorsal oblique view, facies 2. C.
612 Rhizodont tooth with striated ornament, facies 3. D. Actinopterygian scale, exterior surface with a transverse
613 grooved ornament, facies 4. E: Actinopterygian tooth, recurved, facies 4. F. Fish bone (indeterminate), with
614 layered, porous internal structure, facies 4. G. Rhizodont scale with pustular ornament, facies 4. H:

615 *Cavellina* ostracod mould, juvenile, carapace, left lateral view, facies 4. I: Plant fragment, facies 5. Scale
616 bars 250 μm.

617 Figure 12. Dolostone isotope results. Carbon and oxygen isotope results for each dolostone facies from this
618 study and Turner (1991). Dolostone samples from Turner (1991) were classed into the facies scheme of this
619 study based on sample descriptions given. The data are compared with published calcite and dolomite
620 Mississippian isotopic data from a range of settings (numbered 1 to 4) and is most similar to palaeosol-
621 associated ferroan dolomite of the Appalachian and Illinois basins, Kentucky, USA (Barnett et al., 2012).

622 Figure 13. Dolostone depositional environments. The general setting is a tropical, coastal, low-lying
623 floodplain. The location of each dolostone facies (F) is indicated, note that all form in the sub-surface. The
624 main fossils occurring in each facies are highlighted for facies 2-4, with *Spirorbis*, gastropods, *Serpula* and
625 robust bivalves or brachiopods washed into lakes from the shallow-marine environment during storms. Each
626 of these facies can be secondarily modified by rooting, brecciation and pedogenic processes, with the lake
627 environment drying out and evolving to either shallow hypersaline evaporitic pools or to vegetated, brackish
628 coastal marshes.

629 Table 1. Fossil salinity tolerance and taphonomy. Fossils groups present within dolostones are listed from
630 left to right in order of their abundance. Plants are excluded, and so are chondrichthyans, acanthodians,
631 dipnoans, eurypterids, and gastropods, whose taphonomy has not been assessed. The taphonomy is taken as
632 an average for that fossil group, for example 70% of *Serpula* are allochthonous. The salinity tolerance is
633 discussed in the text and is based on published interpretations for that group; Ichnofauna (Bhattacharya and
634 Bhattacharya, 2007; Buatois et al., 2005; Knaust, 2013); Actinopterygian and rhizodont (Carpenter et al., 2014;
635 Greb et al., 2015; Ó Gogáin et al., 2016); Ostracod (Bennett, 2008; Bennett et al., 2012; Williams et al.,
636 2005); Bivalve (*Modiolus*, *Naiadites*) (Ballèvre and Lardeux, 2005; Bennison, 1960; Trueman and Weir,
637 1946); *Schizodus* (Kammer and Lake, 2001); *Spirorbis* (Gierlowski-Kordesch and Cassle, 2015); *Serpula*
638 (Beus, 1980; Braga and López-López, 1989; Palma and Angeleri, 1992; Suttner and Lukeneder, 2003);
639 Brachiopod (Kammer and Lake, 2001). Abbreviations: Auto, autochthonous assemblages; Allo,
640 allochthonous assemblages; Euryh., euryhaline.

641

Palaeontology and palaeoenvironment of Mississippian coastal lakes and marshes

Highlights

- New terrestrial ecosystems established in the Tournaisian after a mass extinction.
- Dolostones and evaporites are common in tetrapod-bearing successions of Scotland.
- Dolomite formed occurred in open and closed saline lakes, brine pans and sabkhas.
- The lakes were a habitat for a diverse vertebrate, mollusc and arthropod fauna.
- Saline lakes may be important in the radiation of life from marine to freshwater.

Figure

Click here to access/download;Figure;Figure 1_palaeogeography and location maps.tif

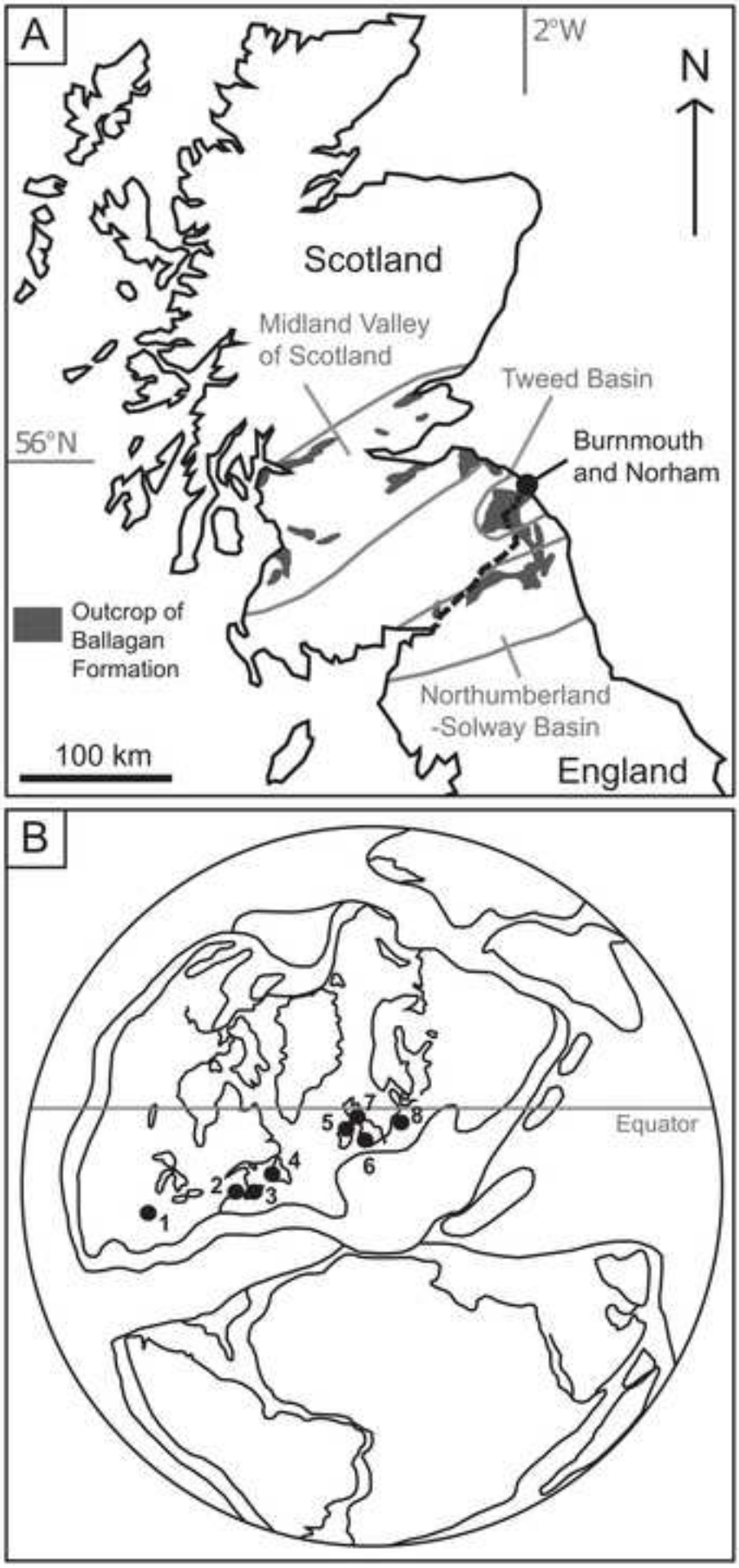

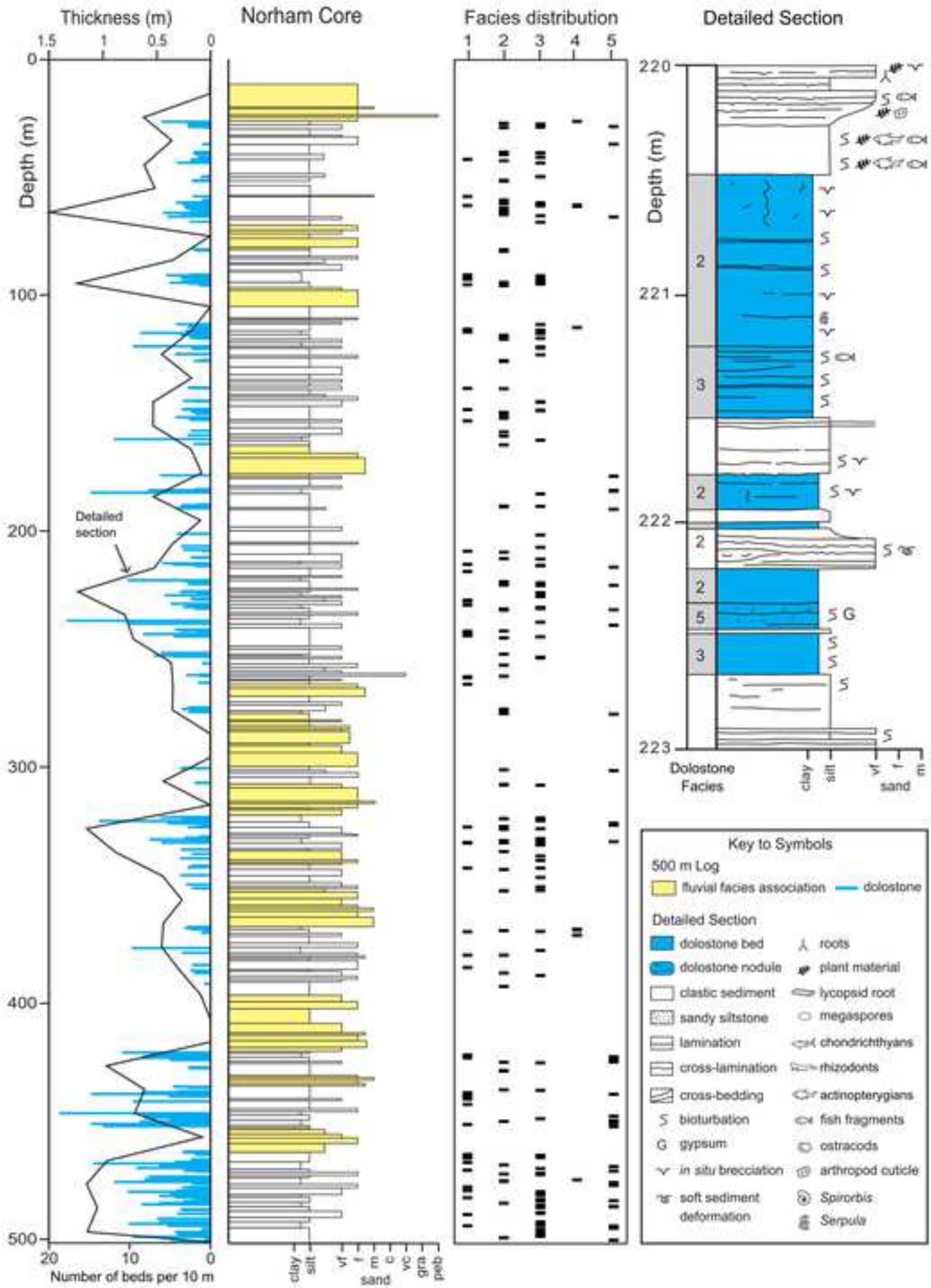

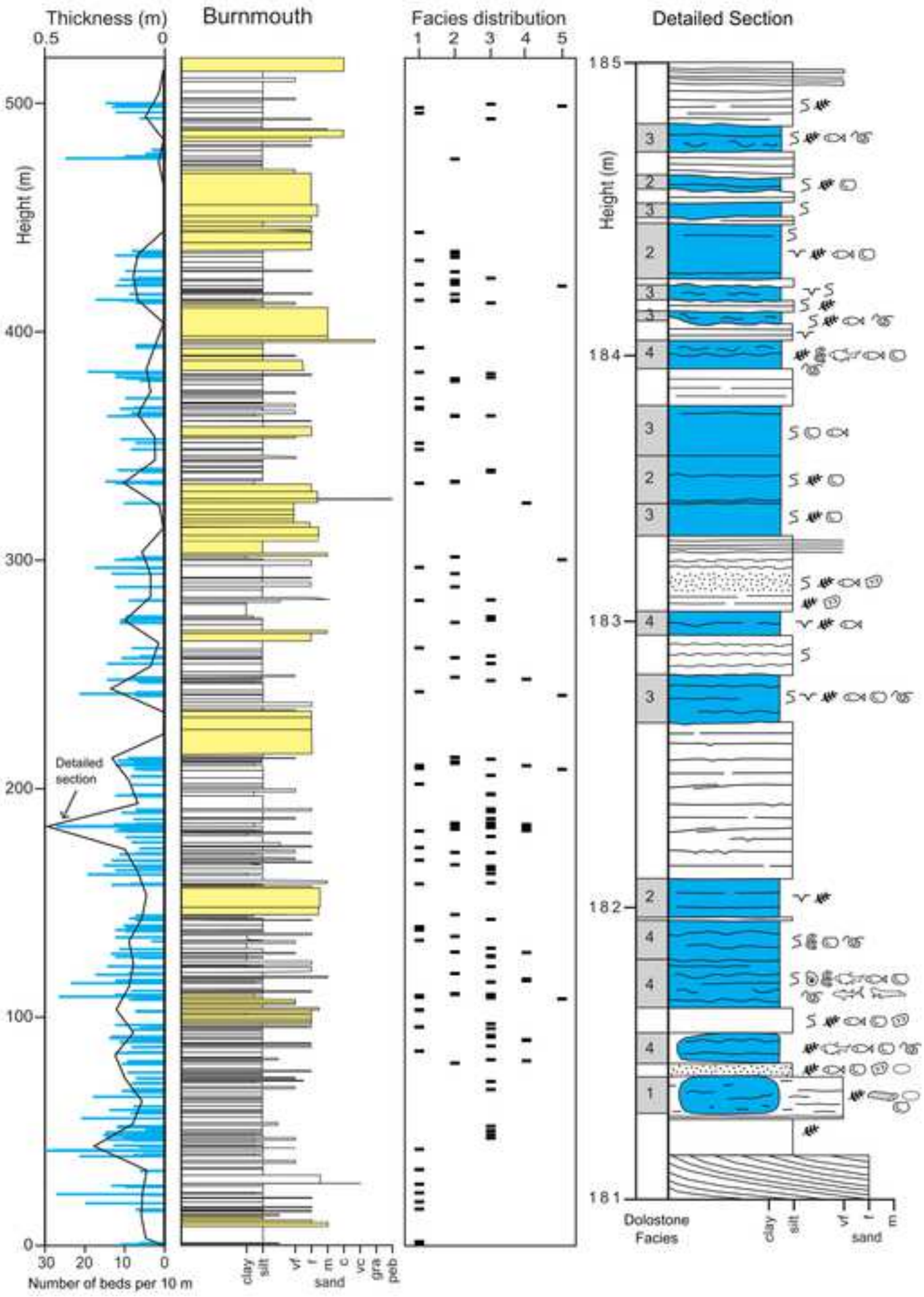

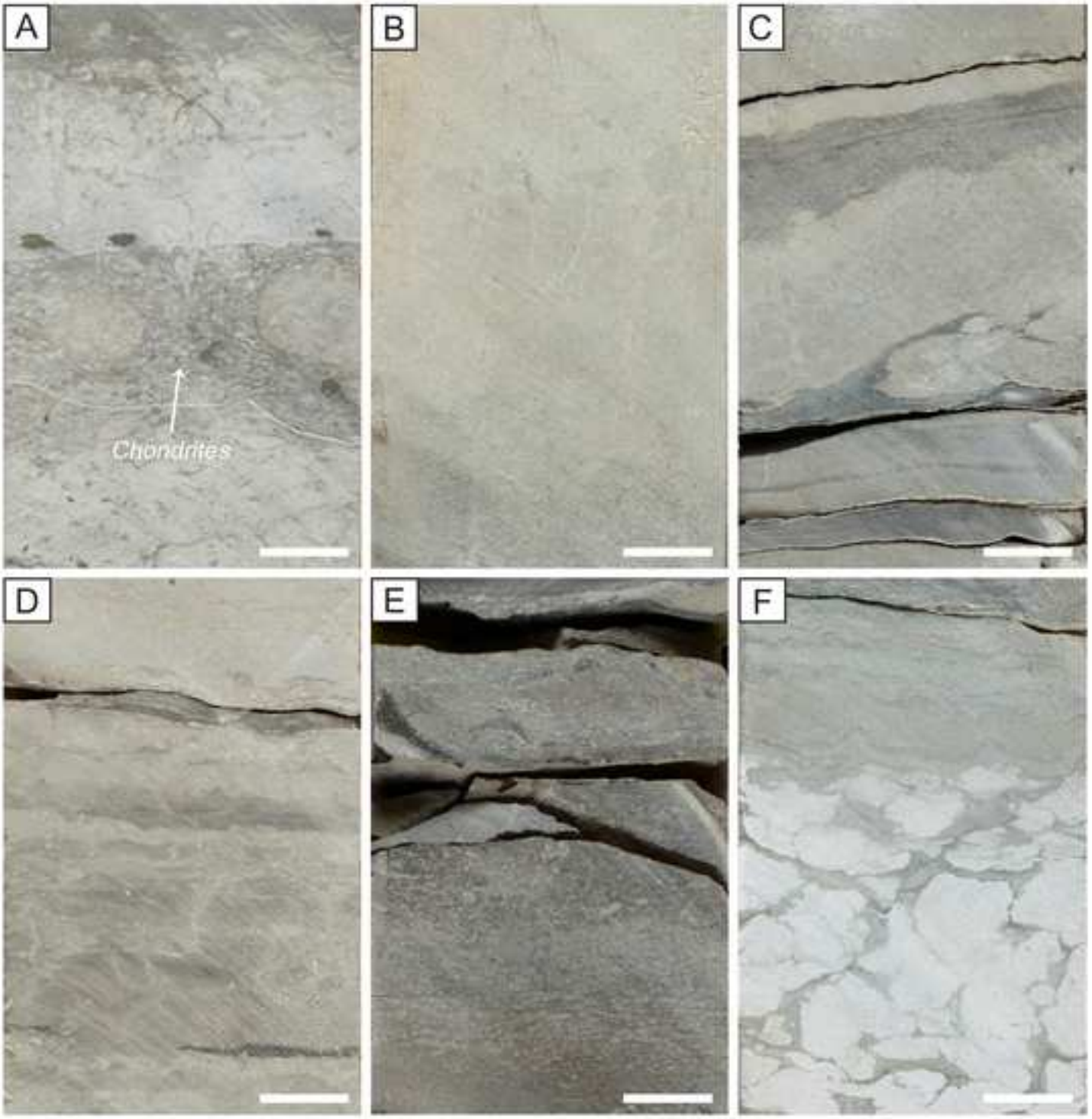

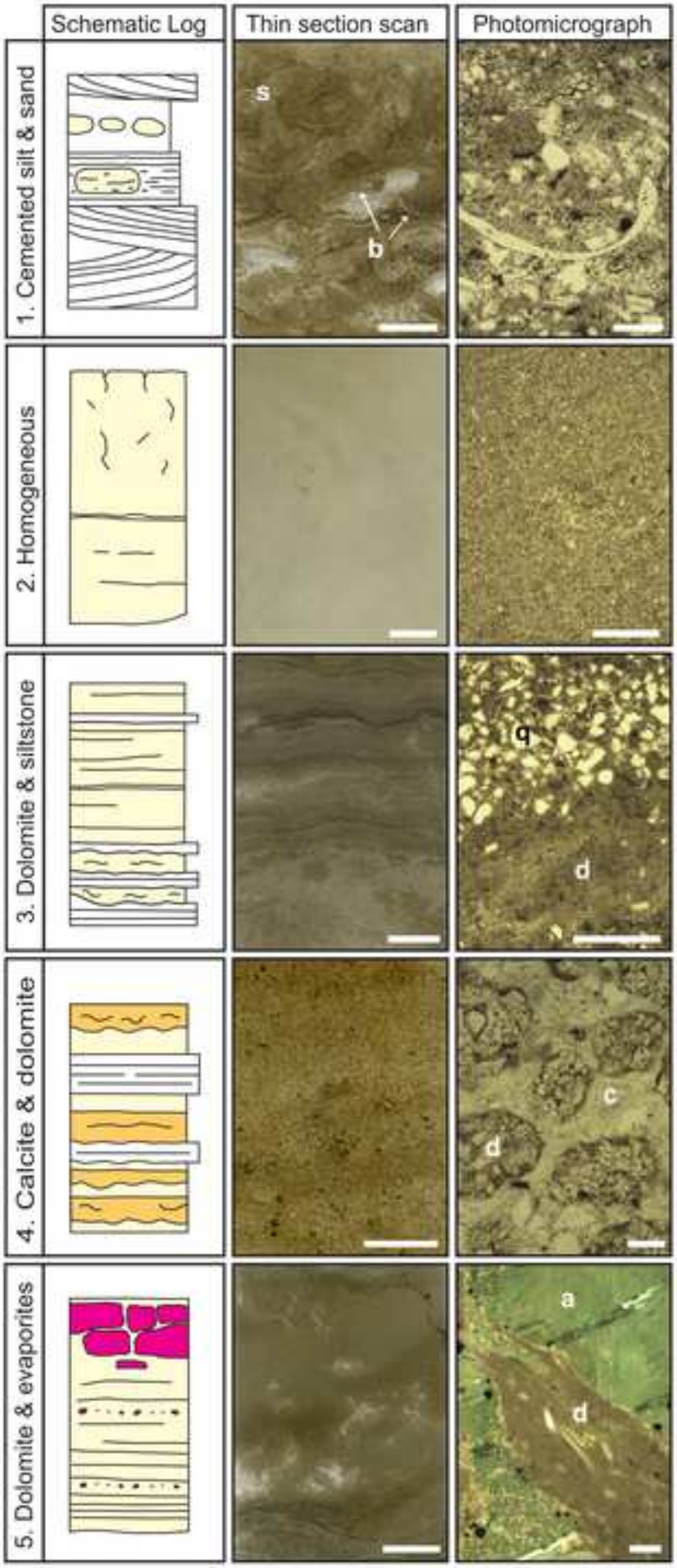

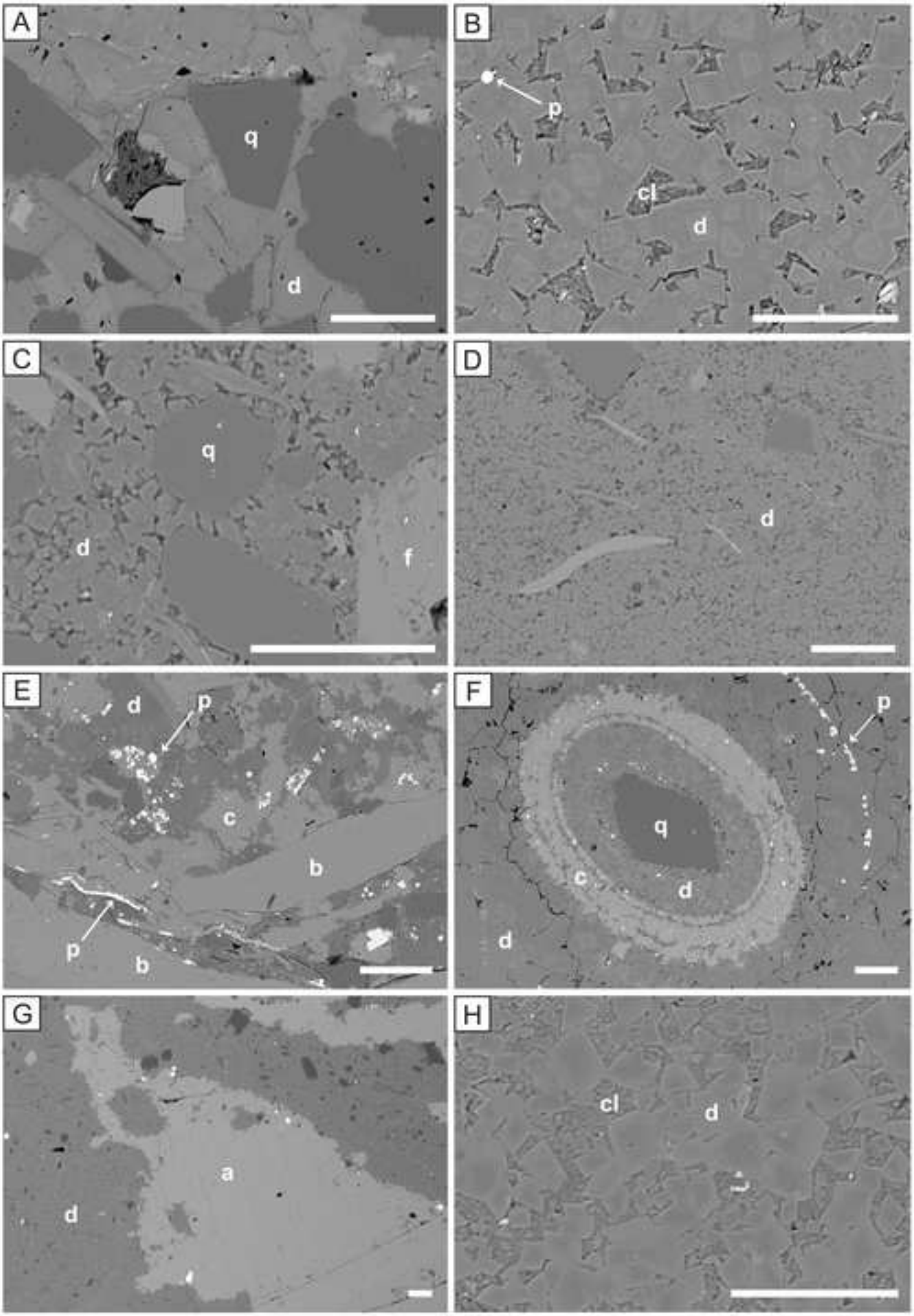

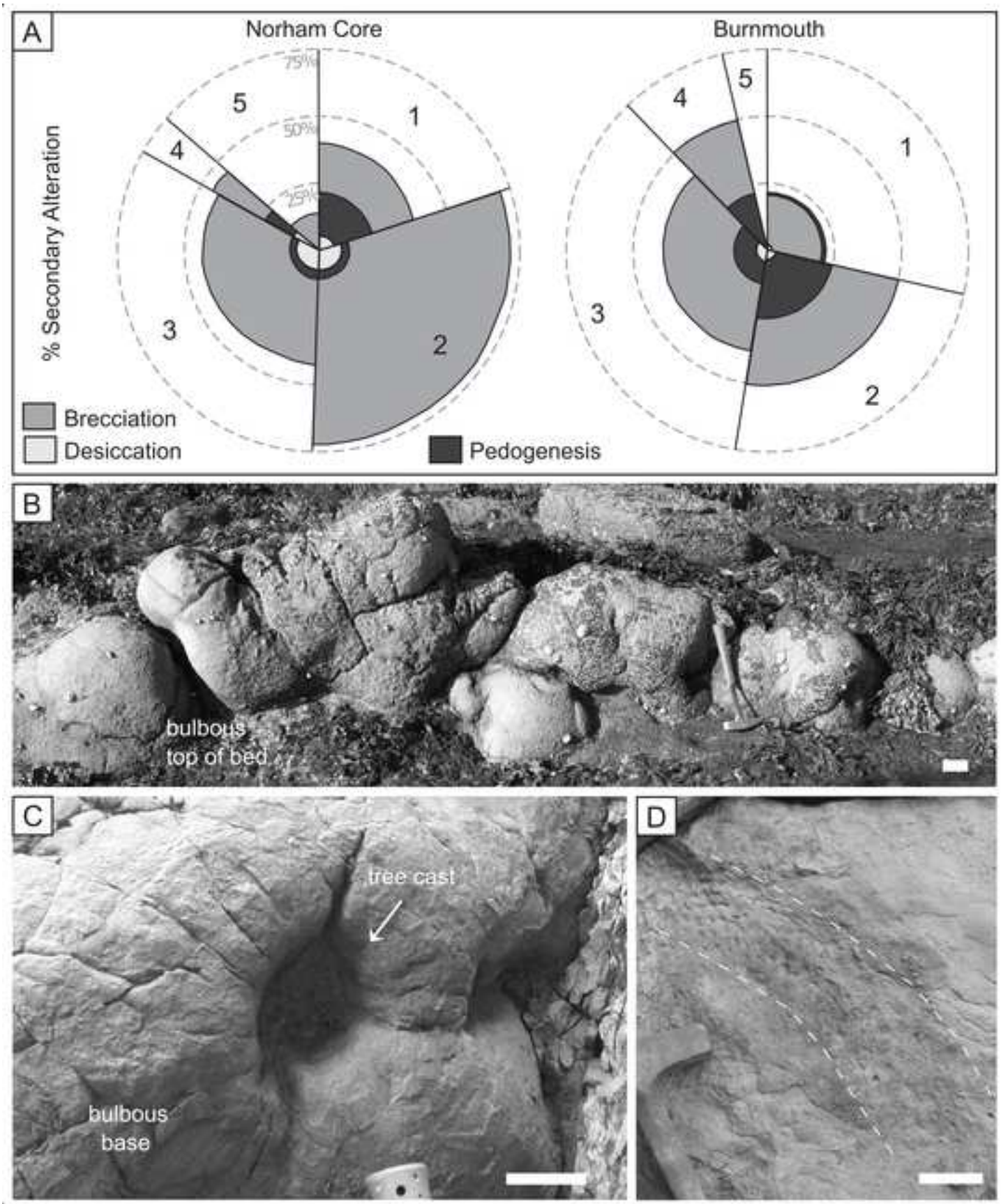

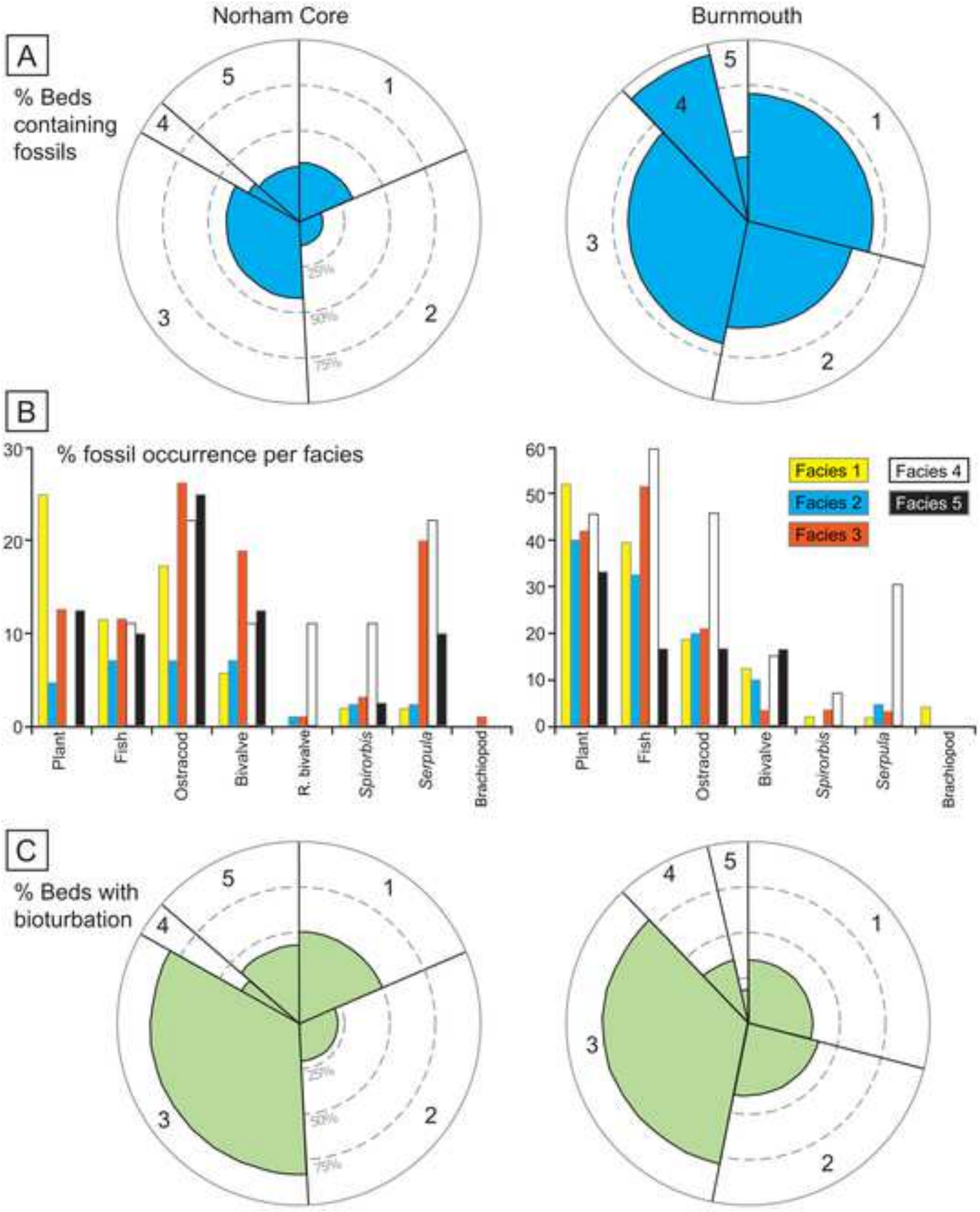

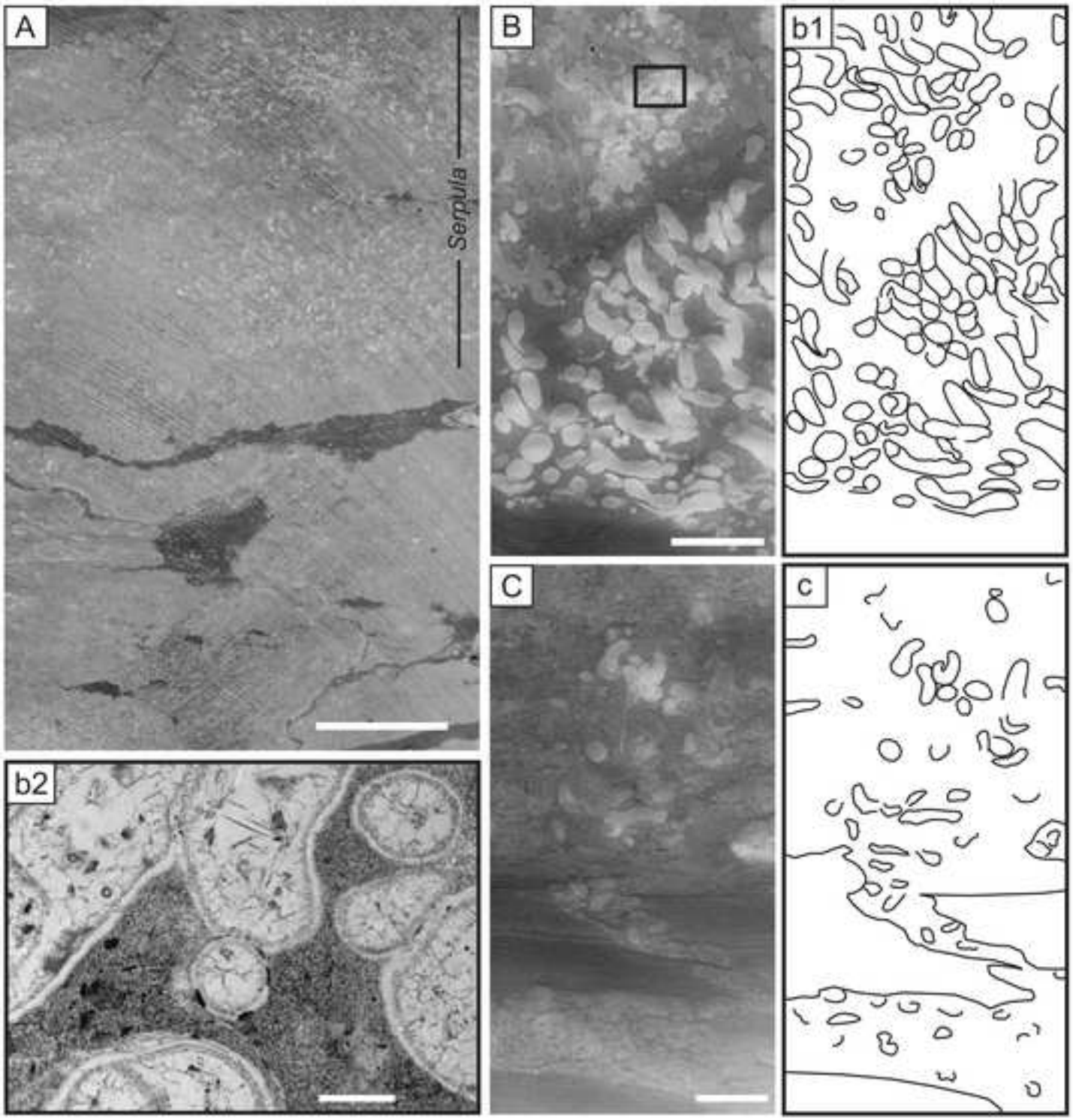

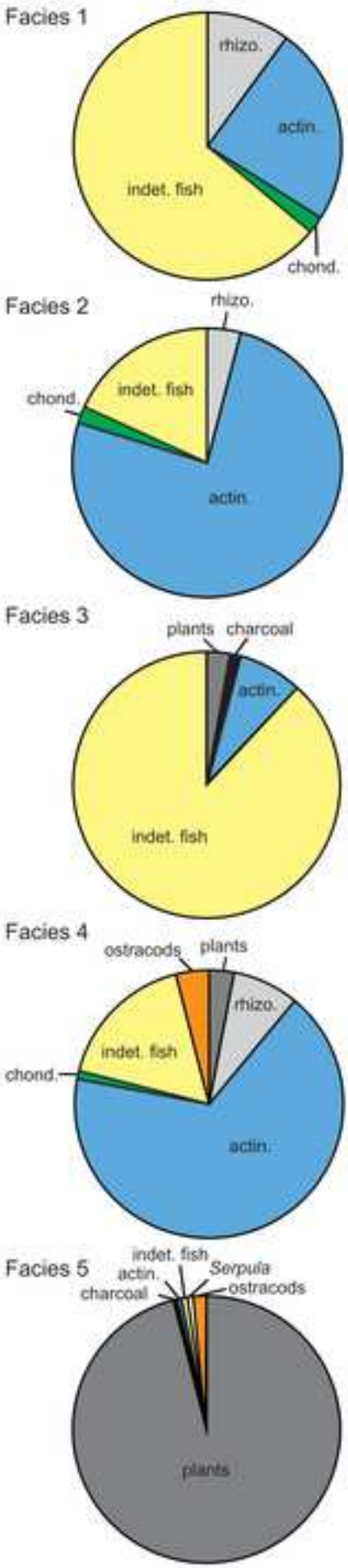

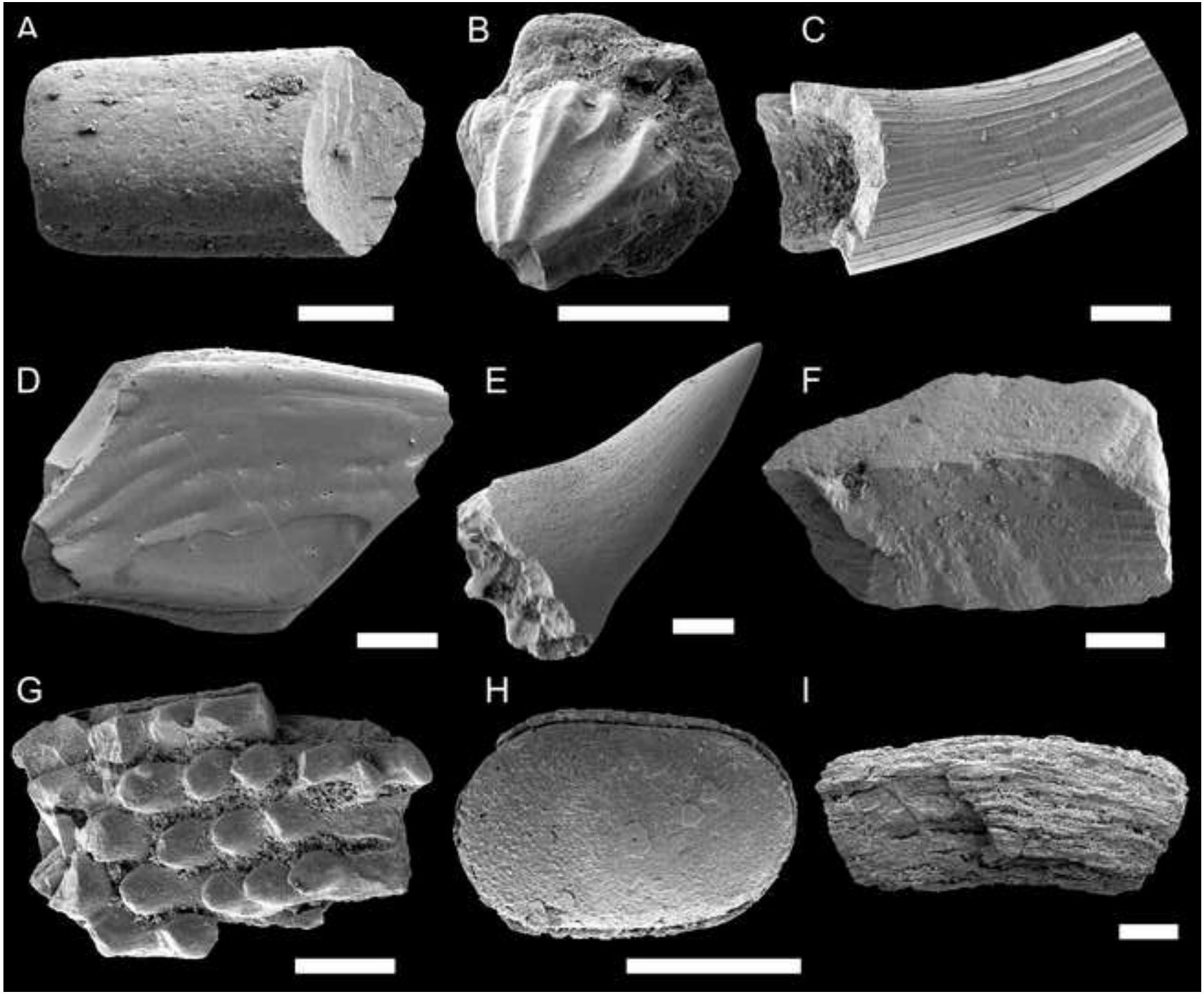

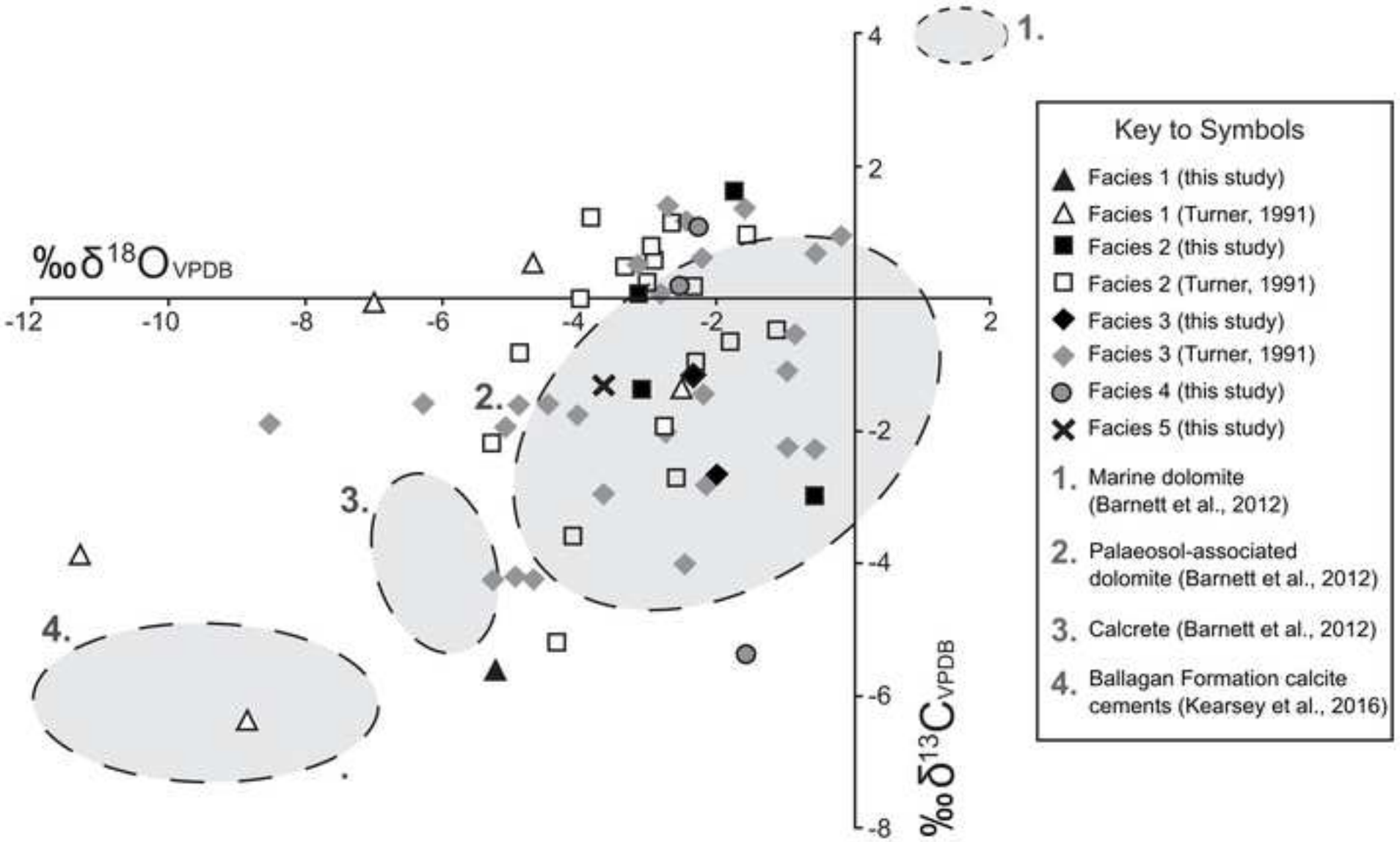

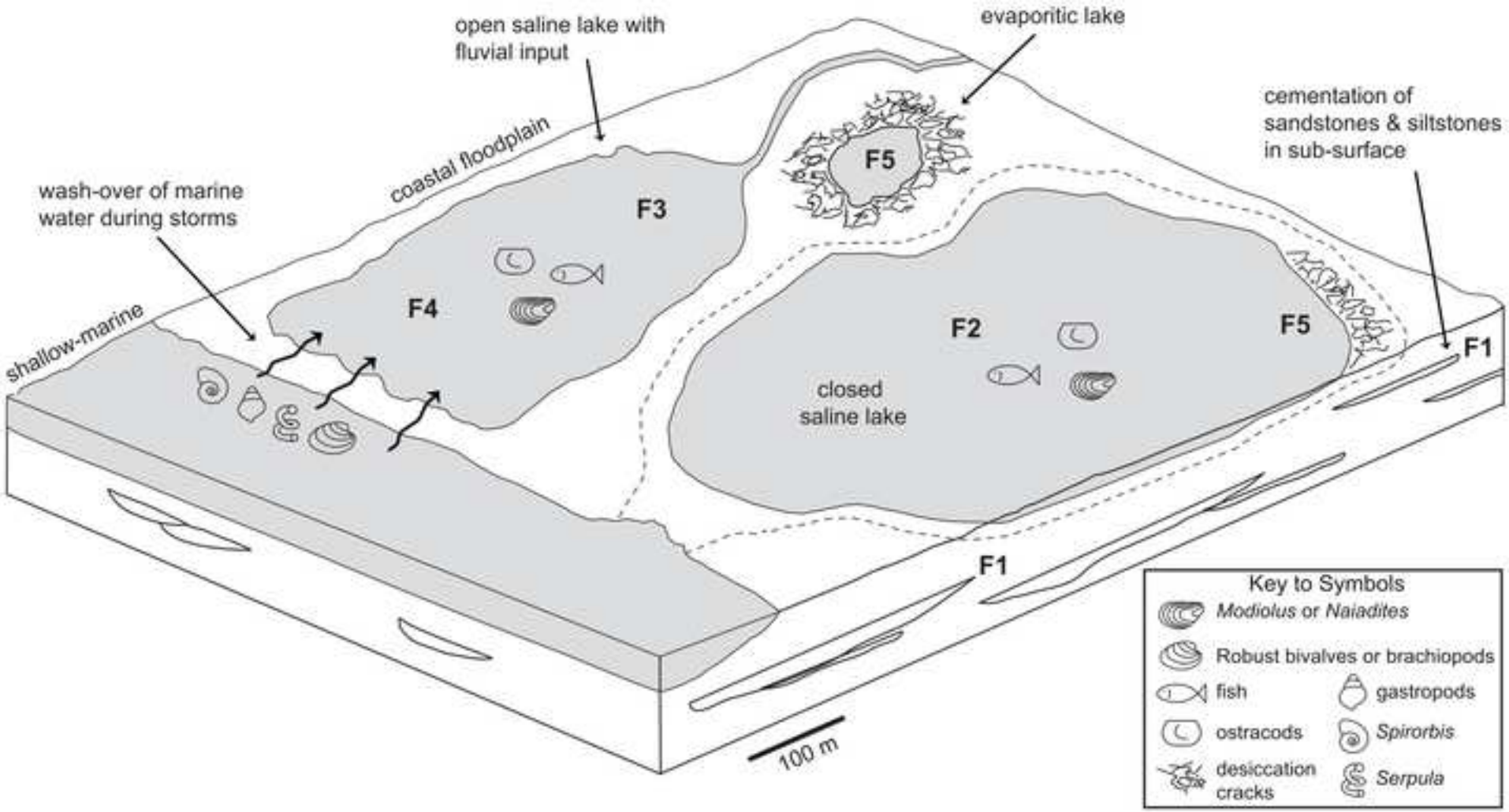

Palaeoecology and palaeoenvironment of Mississippian coastal lakes and marshes during the early terrestrialisation of tetrapods

Table 1. Fossil salinity tolerance and taphonomy.

	Ichnofauna	Actinopterygian, Rhizodont	Ostracod	Bivalves	*Schizodus*	*Spirorbis*	*Serpula*	Brachiopod
Taphonomy	allo	auto	auto	auto	allo	allo	allo	allo
Salinity Tolerance	marine	fresh-brackish	euryhaline	fresh-brackish	euryhaline	marine	marine	marine

Declaration of interests

☒ The authors declare that they have no known competing financial interests or personal relationships that could have appeared to influence the work reported in this paper.

☐The authors declare the following financial interests/personal relationships which may be considered as potential competing interests:

Palaeoecology and palaeoenvironment of Mississippian coastal lakes and marshes during the early terrestrialisation of tetrapods

Bennett, C.E.[1*], Kearsey, T.I.[2], Davies, S.J.[1], Leng, M.J.[3], Millward, D.[2], Smithson, T.R.[4], Brand, P.J.[2], Browne, M.A.E.[2], Carpenter, D.K.[5], Marshall, J.E.A.[5], Dulson, H.[1], Curry, L.[1]

[1] *School of Geography, Geology and Environment, University of Leicester, Leicester, LE1 7RH*

[2]*British Geological Survey, The Lyell Centre, Research Avenue South, Edinburgh EH14 4AP*

[3]*National Environmental Isotope Facility, British Geological Survey, Keyworth, Nottingham, NG12 5GG and School of Biosciences, Centre for Environmental Geochemistry, University of Nottingham, Loughborough, LE12 5RD*

[4]*Department of Zoology, University of Cambridge, Cambridge,* CB2 3EJ

[5] *School of Earth Science, University of Southampton, National Oceanography Centre, European Way, Southampton, SO14 3ZH, UK*

Email addresses: Carys E. Bennett, ceb28@le.ac.uk (corresponding author); Timothy I. Kearsey, timk1@bgs.ac.uk; Sarah J. Davies, Sjd27@le.ac.uk; Melanie J. Leng, mjl@bgs.ac.uk; David Millward, dmill@bgs.ac.uk; Timothy R. Smithson, ts556@cam.ac.uk; Peter J. Brand, peter@pjbrand.plus.com; Michael A.E. Browne, maeb@bgs.ac.uk; David K. Carpenter, dkcarpenter97@gmail.com; John E.A. Marshall, jeam@soton.ac.uk; Hattie Dulson, hattie_d@hotmail.co.uk; Levi Curry, Lc345@live.co.uk.

Abstract

The Ballagan Formation of northern Britain provides an exceptional record of Early Mississippian ecosystems that developed as tetrapods emerged onto land. In this paper, we study two 500-metre sections of the formation near Berwick-upon-Tweed, which are characterised by abundant ferroan dolostone beds. Five lithofacies are identified: cemented siltstone and sandstone, homogeneous dolomicrite, mixed dolomite and siltstone, mixed calcite and dolomite, and dolomite with evaporite minerals. Cemented sediments have non-

planar to planar subhedral dolomite crystals, up to 40 μm in size, whereas other facies predominantly comprise dolomicrite or planar euhedral dolomite rhombs 15 μm in size, with patches of larger rhombs indicating partial recrystallisation. The macro- and microfossil content of the dolostones is dominated by sarcopterygian (rhizodont) and actinopterygian fish, bivalves, *Serpula*, ostracods and *Chondrites* trace fossils; with rarer *Spirorbis*, chondrichthyans (*Ageleodus*, hybodonts and ?ctenacanths, xenacanths), non-gyracanth acanthodians, gastropods, eurypterids, brachiopods, plant debris, wood, lycopsid roots, charcoal, megaspores, phycosiphoniform burrows, *Zoophycos*? and *Rhizocorallium*. The oxygen and carbon isotope composition of dolomites range from –3.6‰ to –1.7‰ (for $\delta^{18}O$) and –2.6‰ to +1.6‰ (for $\delta^{13}C$) respectively indicating dolomite growth in mixed salinity waters. Frequent marine storm-surge events transported marine waters and animals into floodplain lakes, where evaporation, interstitial sulphate-reducing bacteria, iron reduction and methanogenesis allowed dolomite growth in the shallow sub-surface. Secondary pedogenic modification (by roots, brecciation, desiccation, and soil forming processes) is common and represents lake evaporation with, in some cases, saline marsh development. The dolostone facies are part of a complex environmental mosaic of sub-aerial dry floodplain, wet marshy floodplains, rivers, and lakes ranging in salinity from freshwater to hypersaline. Marine influence is strongest at the base of the formation and decreases over time, as the floodplain became drier, and forested areas became more established. Coastal lakes were an important habitat for animals recovering from the end-Devonian Hangenberg Crisis and may have acted as a pathway for euryhaline fishes, molluscs and arthropods to access freshwater environments.

Keywords: Carboniferous; dolostone; lake; hypersaline; floodplain; tetrapods

1. Introduction

Following the end-Devonian mass extinction (the Hangenberg Crisis), new terrestrial habitats developed related to changes in plant cover and river morphology (Davies and Gibling, 2013; Kaiser et al., 2016). The extinction resulted in changes in body size of fishes (Challands et al., 2019; Sallan and Galimberti, 2015), while tetrapods evolved pentadactyl limbs for terrestrial locomotion (Smithson et al., 2012). In continental brackish to freshwater environments dipnoans and gyracanthid fish occupied the niches left vacant by extinct placoderms and porolepiformes (Friedman and Sallan 2012). The late Devonian to early Carboniferous was a time of marine to freshwater radiation for many animal groups, including elasmobranch chondrichthyans (Cressler et al., 2010), xiphosurans (Bicknell and Pates, 2019; Lamsdell, 2016), eumalacostracans and branchiopods (Gueriau et al., 2014a,b, 2018), ostracods (Bennett, 2008), gastropods (Yen, 1949) and bivalves (Ballèvre and Lardeux, 2005; Bridge et al., 1986).

The Tournaisian Ballagan Formation of the Scottish Borders preserves some of the most continuous and important records of the evolution of early terrestrial ecosystems during recovery from the Hangenberg Crisis. The formation hosts rare terrestrial tetrapods (Clack, 2002; Clack et al., 2016, 2018, 2019; Otoo et al., 2019), fishes (Carpenter et al., 2014; Challands et al., 2019; Richards et al., 2018; Sallan and Coates 2013; Smithson et al., 2012, 2016), shrimps (Cater et al., 1989), xiphosurans (Bicknell and Pates, 2019), millipedes (Ross et al., 2018), ostracods (Williams et al., 2005, 2006), plants (Bateman and Scott, 1990; Scott et al., 1984) and palynomorphs (Stephenson et al., 2004a, b; Marshall et al., 2019). Dolostone and evaporite beds are common in the formation and comprise 17% of the total thickness (Bennett et al., 2016). Primary micritic dolomite formation at the present day is fairly rare and occurs in sabkhas (Bontognali et al., 2010), hypersaline lakes (Wright, 1999) or lagoons (Vasconcelos and McKenzie, 1997), deposited from groundwater (Mather et al., 2019), and in peritidal or deep marine environments (Warren, 2000). Micritic dolomite in the geological record has been associated with these environments, as well as with palaeosols

(Kearsey et al., 2012) and marshes (Barnett et al., 2012). The Mississippian was an interval of globally low levels of dolomite abundance, especially compared with very high dolomite abundance episodes in the Ordovician, Silurian and Cretaceous (Given and Wilkinson, 1987). Yet dolostones are a key component of the Ballagan Formation and part of the story of the diverse environments that existed when tetrapods first evolved to walk on land.

Until recently, the fossil record in dolostones has not been examined in detail, and both Belt et al. (1967) and Ghummed (1982) noted the paucity of fossils within the dolostones. New work is challenging the previous conception of dolostones as rather barren rocks: a mesofossil study on two dolostone beds from the Isle of Bute identified a diverse fish fauna (Carpenter et al., 2014), and common *Chondrites* burrows were found in dolostones from the Norham Core (Bennett et al., 2017). Our study continues the palaeontological analysis of the dolostones and is the first to integrate palaeontology with detailed sedimentological and geochemical analysis. The aim of this study is to interpret the palaeoenvironment of these dolostone-bearing successions, using an extensive dataset of more than 500 dolostone samples from the Ballagan Formation. The study interprets a mosaic of coastal lake environments, which may have been influential in the radiation of fish and aquatic invertebrates from marine to freshwater environments as new ecosystems developed.

2. Geological background

The Ballagan Formation crops out across the Midland Valley of Scotland and in the Borders region between Scotland and England (Figure 1A), and spans most of the Tournaisian stage and early Visean (Marshall et al., 2019). Formerly placed within the Dolostone Group in the Scottish Borders (Greig, 1988), the Calciferous Sandstone Measures in Midland Valley of Scotland (MacGregor, 1960), and the Lower Border Group in the Langholm area (Lumsden et al., 1967), the Ballagan Formation is now part of the Inverclyde Group (Browne et al., 1999). The entire formation is exposed in a 513-metre-thick, vertically-dipping coastal section at Burnmouth, bound by sandstone units of the upper Devonian Kinnesswood Formation at the base and the Visean Fell Sandstone Formation at the top (Kearsey et al., 2016; Marshall et

al., 2019). A new palynological analysis at Burnmouth revealed that the section does not span just the CM spore zone as previously thought, but it encompasses the VI, HD, Cl 1 and CM spore zones, spanning the early Tournaisian to early Visean (Marshall et al., 2019).

The Ballagan Formation comprises ten facies and three facies associations, each of which occurs throughout the formation: 1) fluvial facies association (sandstones, deposited in meandering to anastomosing fluvial channels); 2) overbank facies association (fine-grained siliciclastic sediments and conglomerate lenses, deposited in temporary floodplain lakes, streams and sub-aerial vegetated land surfaces); and 3) saline-hypersaline lake facies association (dolostones and evaporites, the focus of this study) (Bennett et al., 2016). Dolostones (locally referred to as 'cementstones'; Bennett et al., 2016) are present only in the saline-hypersaline lake facies association, together with evaporites. They occur interbedded within the siltstones, palaeosols and sandstones of the overbank facies association, and represent time periods when the coastal floodplain was covered in extensive lakes.

Ballagan Formation dolostones from Scotland have been studied from the East Lothian Cockburnspath Outlier, including Cove and Pease Bay (Andrews et al., 1991; Andrews and Nabi, 1994, 1998), the western Midland Valley of Scotland (Freshney, 1961; Ghummed, 1982), the River Tweed area at Burnmouth (Scott, 1971, 1986), Foulden (Anderton, 1985), the Firth of Tay boreholes (Browne, 1980), Ballagan Burn, Gairney Burn field sections, and the Glenrothes, Little Freuchie and Knowehead boreholes (Turner, 1991). Tournaisian dolostones of Scotland and Canada have a composition of ferroan dolomite with minor calcite and a siliciclastic component (clays and silts) of 6 to 30% (Belt et al., 1967). In the Midland Valley of Scotland, Tweed Basin and Northumberland-Solway Basin, dolostones can be associated with evaporites (Armstrong et al., 1985; Millward et al., 2018, 2019; Scott, 1986). Dolostones have been interpreted to represent deposition in floodplain lakes (Anderton, 1985; Andrews et al., 1991; Andrews and Nabi, 1994, 1998; Scott, 1971), and as marginal marine deposits (Belt et al., 1967), or continental sabkha (Scott, 1986). Ferroan dolostones from the Tournaisian of New Brunswick, Newfoundland, Northumberland and Scotland have similar characteristics, including homogeneous, layered, hummocky, nodular and brecciated or pedogenic (rooted) forms (Belt et al., 1967; Andrews, 1991; Freshney, 1961; Leeder, 1974; Scott, 1971,

1986). Dolostones from eastern Canada are primarily associated with alluvial successions with fewer marine indicators than British examples (Belt et al., 1967), with the Maritimes Basin isolated from marine influence for much of the Carboniferous (Falcon-Lang et al., 2015a).

In the Tournaisian, Scotland and Northern England were situated 4ºS of the palaeo-equator (Scotese and McKerrow, 1990). The climate was tropical and evidence from sandy siltstones, palaeosols and tree rings indicates seasonal flooding or monsoon-like heavy rainfall (Bennett et al., 2016; Falcon-Lang, 1999, Kearsey et al., 2016). Mississippian deposition took place in a number of NE-trending transtensional basins along the southern margin of Laurussia which formed as a consequence of oblique dextral collision between Laurussia and Gondwana (Figure 1B; Coward, 1993; Waters and Davies, 2006). The hypothesis of a marine influence from the east (Cope et al., 1992) is confirmed by a detailed analysis of the occurrence of evaporites, marine fossils, and other indicators, in boreholes across the Midland Valley of Scotland, Tweed Basin and Northumberland-Solway Basin (Millward et al., 2019).

3. Materials and methods

Dolostones were studied from a coastal field site at Burnmouth (British National Grid NT 95797 60944) and a fully cored borehole drilled at Norham West Mains Farm, known as the Norham Core, (British National Grid NT 91589 48135), near Berwick-upon-Tweed (Millward et al., 2013). The entire Ballagan Formation (513 m thick) is exposed at Burnmouth, and the 490 m thick Norham Core fully cores the Ballagan Formation, but did not penetrate the base, suggesting the total thickness of the formation is variable. The two sections complement each other: the field exposure at Burnmouth reveals the extensive lateral continuity of the dolostone beds and the Norham Core provides fine detail of the internal structures of the dolostones and their relationship with underlying and overlying beds. The Norham Core palynostratigraphy has not been published yet, and whilst it isn't possible to correlate the two sections based on individual beds, they host the same facies and facies associations (Bennett et al., 2016). Core and field sections were recorded by sedimentary logging, and samples were taken approximately every 1 metre.

Dolostones are described from hand specimens, field exposures, core photographs and thin sections: 278 dolostone beds are recorded in the Norham Core and 267 at Burnmouth. Beds at Burnmouth were not identified to facies level unless they were sampled (166/267 beds), because weathering obscures the detail at outcrop. Standard-sized polished thin sections, 30 μm thick, were made from 70 Burnmouth and 52 Norham Core samples. Thin sections were examined using a Leica petrographic microscope to identify dolostone facies and mineralogy. The Hitachi S-3600N SEM at the University of Leicester was used to determine between calcite and dolomite using the Back Scattered Electron detector and identify ferroan dolomite and zoned crystal compositions using energy dispersive X-ray (EDX) spot analysis. X-ray Diffraction (XRD) geochemistry of 49 dolostone powder samples were analysed using a Bruker D8 Advance with DaVinci and DIFFRACplus data analysis software at the University of Leicester.

Fossil material was identified from surface-sampling and micropalaeontological residues. Five samples from the Burnmouth section, one from each facies, of weights varying from 390-500 g per sample, were processed for micropalaeontology. Each sample was broken into centimetre size pieces and placed in a plastic sieve in a bucket to aid breakdown. The samples were repeatedly immersed in a 5% solution of acetic acid, buffered using tricalcium diorthophosphate and spent acid from each cycle. Each processing cycle comprised a one week immersion in the acid solution, followed by an hour long rinse in water. Then disaggregated sediment residue was wet sieved at 1000, 425, 250, 125, 65 μm fractions and oven dried at 40^{o}C. The cycle was repeated until all the rock had broken down. The 1000, 425, and 250 μm fractions were fully picked, and total fossil counts recorded. Microfossil components were identified from literature records, or through direct comparison with macrofossil specimens from the Ballagan Formation.

A representative set of eleven samples were analysed for carbon and oxygen isotopes. Dolomite samples were ground to a fine powder in agate, and an aliquot of the powder (c. 20 mg) was reacted with anhydrous phosphoric acid *in vacuo* at 25.2°C for 72 hours. The CO_2 liberated was cryogenically separated from water vapour and collected for analysis. Measurements were made on a VG Optima mass spectrometer. Isotope values ($\delta^{13}C$, $\delta^{18}O$) are reported as per mille (‰) deviations of the isotopic ratios ($^{13}C/^{12}C$, $^{18}O/^{16}O$) calculated to the VPDB scale using a within-run laboratory dolomite standard calibrated against NBS-19.

The dolomite-acid fractionation factor applied to the gas values is 1.01109. The Craig (1957) correction is also applied to account for ^{17}O. Overall analytical reproducibility for these samples is on average better than 0.1‰ for $\delta^{13}C$ and $\delta^{18}O$ (1σ).

4. Results

4.1. Dolostone characteristics and distribution

Dolostones comprise 14% of the total sedimentary rock thickness in the Norham Core and 8% at Burnmouth. Typically, pale grey internally, with a pale yellow weathered surface at outcrop, dolostones are present within repeating successions that include siltstones, thin sandstone beds and palaeosols. Dolostone beds are distributed fairly evenly throughout both successions (Figures 2-3) and it is not possible to correlate individual beds between the two. At Burnmouth dolostones are generally parallel-bedded and can be traced the entire length of the foreshore at low tide (~500 m), without any significant changes in thickness or structure. We estimate that the true lateral extent of individual beds is of the order of 1 km or more based on the common occurrence of dolostones across the region (Millward et al., 2019).

Dolostones are categorised into five facies. Facies 1: Cemented siltstone and sandstone; Facies 2: Homogeneous dolomicrite; Facies 3: Mixed dolomite and siltstone; Facies 4: Mixed calcite and dolomite; Facies 5: Dolomite with evaporite minerals. Facies 2 and 3 represent approximately 60% of the dolostone beds. For each facies bed thickness is highly variable (Table S1), with average (mean) bed thickness of 14 cm (Burnmouth) to 26 cm (Norham Core) for Facies 1-4. Facies 5 comprises thicker beds in the Norham Core (mean thickness 37 cm), but is poorly represented at Burnmouth due to the effects of weathering.

Dolostones are thickest and most common in the lowermost 200 m of the Burnmouth section, and the lowest 80 m of the Norham Core (Figures 2-3). There are high abundance peaks, and thick dolostone beds in the Norham section at 320 m and 220-230 m depth. High-abundance peaks at 60 and 100 m depth

correspond to a section with closely-spaced but thin dolostone beds. Dolostone bed abundance variations in both sections are primarily controlled by the occurrence of sandstone beds of the fluvial facies association. Where thick fluvial sandstone units are present dolostones are absent or very rare. Removing the sandstone bodies from the sequence shows a trend of a reduction in the number of dolostone beds over time in both sections. Dolostone facies 5 is most common at the base of the Norham Core, but there are no other apparent trends in facies variation in progressively younger rocks.

At Burnmouth 77% of dolostone beds are laterally continuous over hundreds of metres. Of the discontinuous beds studied (n = 40), many are nodular (n = 23), or have a lateral extent of a few metres to tens of metres. Each dolostone facies contains some discontinuous beds, with Facies 1 the greatest (35% of beds are discontinuous). Nodule associations are varied: some occur within organic-rich black siltstones and preserve dolomitised anatomically-preserved plant fossils, whereas others comprise homogeneous dolomicrite or are associated with palaeosols or evaporites. Nodules composed of calcite and calcite-cemented sandstone beds are observed more rarely.

4.2. *Sedimentology of dolostone facies*

Dolostone photographs, outcrop profiles, microfacies and microtextures are shown in Figures 4-6 and Table S2.

4.2.1. Facies 1: Cemented siltstone and sandstone

The facies comprises siliciclastic sediments that have been cemented by dolomite. At outcrop and in core they are typically nodular and interbedded with sandstone or siltstone (Figure 3, Section A; Figure 4A). Bed boundaries between dolostone and surrounding rocks are sharp. Original sedimentary structures such as laminae, cross-lamination and clasts remain visible. The siliciclastic component dominates (approximately 90% sediment volume), with dolomite typically cementing quartz, feldspars and clays (Figure 5; Figure 6A). Dolomite crystal textures are non-planar anhedral to planar, interlocking subhedral, with crystal size ranging

from 5-40 μm. Crystals can be zoned, with calcium-rich cores, and zoned and unzoned crystals can occur in the same sample. Fossil voids can be filled with dolomite or calcite spar. One facies 1 sample is cemented by calcite instead of dolomite, and in another sample, burrows and plant material are pyritised.

4.2.2. Facies 2: Homogeneous dolomicrite

The facies comprises dolomite, clays (20-50% volume) and silt. Facies 2 units have a homogeneous structure, bedding is usually absent, though thin clay-rich partings are rarely present (Figure 5). Diffuse bed boundaries that are transitional into siltstone at the top and base of dolostones are recorded in 11% of facies 2 beds in the core (Figure 4B), but are not observed in field exposure. *In situ* brecciation structures and desiccation cracks are common and mudstone occurs within the cracks (see section 4.3). Dolomicrite patches or evenly distributed dolomite rhombs occur within a matrix of clays (Figure 6B). Rhombs are usually planar euhedral, have a unimodal size distribution (Sibley and Gregg, 1987), and size range of 2-15 μm. No dolomite overgrowth fabrics or cements are present. In samples where a brecciation crack is filled with silt-rich mudstone, the dolomite rhombs are larger within the silt matrix than in the underlying clay matrix. Dolomite rhombs can be zoned, with calcium-rich centres (Figure 6B). Dolomicrite (<4 μm size dolomite crystals) content of samples is variable, from none, to comprising significant proportions of a sample. Sparse euhedral pyrite crystals and rare pyrite framboids are present in some samples (Figure 6B).

4.2.3. Facies 3: Mixed dolomite and siltstone

The facies comprises laminated or bedded alternations of dolostone and siltstone, with a minor component of sandstone. In the Norham Core 34% of facies 3 beds comprise thick composite units of interbedded dolostone and siltstone, bioturbated by *Chondrites* (Bennett et al., 2017). Diffuse bed boundaries into siltstone are present in 12% of facies 3 beds in the core, and it is likely that bioturbation obscures in others. Soft-sediment deformation structures (Figure 4C), brecciation (Figure 4D) and desiccation cracks are

recorded in some samples. Siltstone laminae or beds are cemented by large dolomite rhombs, whereas the dolostone layers comprise micritic dolomite or planar euhedral rhombs of 5-20 μm size (Figure 6C), some of which are zoned with calcium-rich centres. In three samples laminated dolostone resembles the structure of microbial laminites, due to the millimetre-scale spacing of the planar and wavy laminae (cf. Narkiewicz et al., 2015), but no organic structures are preserved. One of these putative microbial samples has a lamina that is pyritised, but in general the occurrence of pyrite is rare in samples of this facies.

4.2.4. Facies 4: Mixed calcite and dolomite

The facies is characterised by pale yellow calcite-rich beds interbedded with pale grey dolomite and clastic components. Beds can contain an abundant shelly fauna (Figure 4E). Soft-sediment deformation structures such as convolute lamination (cf. Törö and Pratt, 2015) are present within 7 out of 14 beds of this facies at Burnmouth (Figure 3) and there are rip-up clasts in one bed. Diffuse bed boundaries have not been observed in this facies and the bases of the beds sometimes exhibit load structures into underlying siltstones. The calcite component has mostly been replaced by dolomite and is absent in some samples. Where present, micritic calcite occurs as patches, surrounded by a matrix of dolomicrite (Figure 6D) or patches of dolomite rhombs (Figure 6E) or dolomite spar. Calcite crystals form inter-crystalline textures or the cores of larger dolomite crystals. Dolomite textures range from non-planar anhedral to planar euhedral or subhedral, crystals are 5-50 μm in size. Rhombs can be zoned and some have magnesium-rich centres and micropores. One sample contains calcitic ooids that are partially replaced by dolomite, and some ooids have a rim of euhedral pyrite crystals (Figure 6F). The matrix between the ooids comprises patches of micritic calcite and dolomite spar. Pyrite is rare, occurring as sparse euhedral crystals in the matrix. In two fossil-rich samples it occurs in greater abundance, as discrete euhedral crystals, small framboid clusters, fine crystal drapes over quartz grains, or along the rim of fossils (Figure 6E).

4.2.5. Facies 5: Dolomite with evaporite minerals

Millward et al. (2018) detailed the complex variety of evaporite-bearing rocks in the Norham Core, comprising 12 gypsum-anhydrite forms and seven facies, some of which are also associated with dolostone. Herein, facies 5 is identified as dolostone units containing any type of evaporite form. Rarely seen in surface exposures, where gypsum is replaced by calcite or dolomite, six beds are identified at Burnmouth. They are either localised or nodular, and one evaporite bed changes laterally into a facies 2 dolostone. Facies 5 beds in the Norham Core (n = 38) are well preserved (Figure 4F), have sharp bed boundaries, and are commonest in the lowest 80 m of the core (Figure 2). Some of the evaporite occurrences are within composite successions of dolostone and siltstone with nodular (Figure 5; Figure 6G), chicken-wire and massive evaporite (Millward et al., 2018). Uncommon units of thinly laminated siltstone and dolostone with small evaporite nodules were interpreted by Millward et al. (2018) as preserved microbial mats. Micron-sized pyrite crystals and larger pyrite framboids were observed in evaporite-bearing dolostones by Millward et al. (2018). The dolostone is usually homogeneous, comprising planar euhedral rhombs of 40-140 μm, or in some rocks 12-15 μm size (Figure 6H), evenly distributed within a clay matrix, similar to facies 2; a few examples comprise rhombohedral grains <5 μm. Evidence for the synsedimentary growth of dolomite and evaporite minerals include prismatic aggregates of aphanitic anhydrite inferred as pseudomorphs after primary gypsum, soft-sediment deformation and de-watering structures, diffuse small (<1 cm size) irregularly shaped gypsum nodules within dolomicrite, and the compaction of siltstone lamination associated with nodule growth.

4.3. *Post-depositional features*

Previously, similar dolostones have been categorised using the presence of brecciation or pedogenic alteration as defining features (Barnett et al., 2012; Turner, 1991). While not reflecting original deposition, brecciation and pedogenic alteration have been identified in all facies in this study, and are important in understanding post-depositional environmental conditions.

Brecciation, desiccation cracks and pedogenic modification of dolostone beds are common throughout both sections. Brecciation is the most common, observed in 47% of dolostones in the core and 36% at Burnmouth. Brecciation is usually *in situ*, occurring internally within a bed, without a connection to the top surface. Facies 2 and 4 have the highest percentage of brecciation, whereas facies 5 has the least (Figure 7A). In the core, brecciated dolostones are more common towards the top of the borehole, but this trend is not seen in Burnmouth. Brecciation and pedogenic modification are not mutually exclusive, brecciation associated with roots or pedogenic modification occurs in both the core (8% of dolostones) and Burnmouth (9% of dolostones sampled).

Desiccation cracks and internal brecciation (synaeresis cracks cf. Plummer and Gostin, 1981) are quite difficult to distinguish, due to erosion of the top of the bed in the field, and the small volume exposed in the borehole. Approximately 20% brecciation observed in dolostone beds is at the top of the bed, but verifiable desiccation cracks with polygonal structures are only observed in much lower numbers (Figure 7A; Table S1), and are not recorded in facies 5. Stylolites are also occasionally present and are most common within thick facies 2 beds.

Pedogenic modification features include roots, red-staining, mottling, iron-oxide or carbonate nodules (Table S1). Overall, 11% of dolostones in the Norham Core and 18% of dolostones at Burnmouth are pedogenically altered. In both sections, facies 1, 2 and 4 exhibit the highest percentage of pedogenic modification, and facies 5 has none (Figure 7A). Despite the presence of these features, none of the pedogenically altered dolostones show the development of sub-soil horizons, such as a clay-rich B horizon (cf. Kearsey et al., 2016). Developed palaeosol levels within the Ballagan Formation are not associated with dolostones (Kearsey et al., 2016). The palaeosols of the overbank facies association are siltstones and only rarely contain small carbonate nodules (Kearsey et al., 2016). They represent a range of floodplain environments including woodland (Vertisols), scrubby vegetation (Entisols, Inceptisols) and saline marshes (gleyed Inceptisols) (Kearsey et al., 2016). The pedogenic modification of the dolostones can be considered as minor because it does not completely destroy primary lamination, where present. In addition, rooting is sparse and often forms vertical root cavities indicative of single-colonization events.

4.4. *Plant fossils*

Twelve dolostones at Burnmouth have a bulbous basal or top surface and are rooted (Figure 7B-D). The facies of these bulbous beds is variable; 8/12 beds are facies 2, the others are facies 1 and 3. Four of these bulbous beds preserve ~10 cm diameter circular depressions (Figure 7C) similar to vertical arborescent trunk traces (Rygel et al., 2004). One Burnmouth facies 2 bed with a bulbous top contains an *in situ* lycopsid root impression on the top surface (Figure 7D). Lycopsid rhizomorph impressions are also recorded from one facies 1 sample each at Burnmouth and in the core. The specimens have spirally arranged roots and closely resemble *Protostigmaria* as described (Rygel et al., 2006) from the correlative Blue Beach Member of the Horton Bluff Formation in Nova Scotia and in the Albert Formation of New Brunswick (Falcon-Lang, 2004). Significantly these rhizome systems supported trees attributed to *Lepidodendropsis* which formed substantive *in situ* forests at Blue Beach. Similar large lycopods are not uncommon (Long, 1959) in the Tournaisian of the Borders implying the presence of analogous forests. However, further work is needed on better preserved specimens to confirm these identifications as they are quite rare at the Burnmouth section. Internal brecciation, sparse fish and plant fragments are observed. Dolostones with a hummocky or bulbous base are described from boreholes in the Gargunnock area of Scotland (Belt et al., 1967; Francis et al., 1970). Anatomically preserved plant fossils occur within dolostones in two horizons at Burnmouth (facies 1 nodules) and one in the Norham Core (facies 2 dolostone). In these nodules dolomite permineralises plant structures in three dimensions, but plant identification has not been accomplished in this study. Anatomically preserved fossils are identified by Scott et al. (1984) and the extensive work of Albert Long (first published in Long 1960, and in ten subsequent papers, see Scott et al., 1984 for full details). Long's specimens were largely recovered from loose blocks or recorded *in situ* at Partanhall, which is a locality 500 m along-strike, but at the same stratigraphic position, as the Burnmouth specimens reported herein. They identified ferns, lycopods, pteridosperms, and gymnosperms. Small plant fragments comprising fibrous, elongate, broken pieces, probably originating from plant stems, are present in 111 hand specimen samples, encompassing all dolostone facies. Rarer wood fragments (10 samples), charcoal (3 samples) and

indeterminate megaspores (5 samples) are present. Charcoal specimens are identified by their brittle texture, fibrous external structure, and hollow internal structure of preserved cellular tissue. The specimens herein have not been identified, but charcoal from a conglomerate bed at Burnmouth was identified as arborescent pteridosperm wood (Clack et al., 2019).

4.5. *Vertebrate Palaeontology*

The fossil content of each dolostone bed observed from hand specimens is reported in Table S1 and is presented by facies in Figure 8 in order to assess ecological differences. The macrofossil vertebrate content of the dolostone hand specimen samples is dominated by indeterminate fish fragments (present in 79 samples), actinopterygian scales, teeth and bones (36 samples) and rhizodont scales and teeth (12 samples). Rarer fossils include two *Ageleodus* teeth and two samples with dipnoan bones and scales. Additional vertebrate groups are recorded in microfossil samples. Tetrapods have not been reported or identified in dolostones from Burnmouth or the Norham Core.

4.6. *Invertebrate Palaeontology*

An assemblage of fish, ostracods, bivalves and *Serpula* are present within most dolostone facies. Ostracods are most common, identified in 112 hand specimen samples. *Shemonaella, Paraparchites* and a putative *Cavellina* are recorded, but most are poorly preserved (recrystallised to dolomite) and cannot be identified. The three identified ostracod genera have a benthic mode of life (Crasquin-Soleau et al., 2006). Indeterminate, thin-shelled bivalves are present in 37 samples. Small *Modiolus* (18 samples) and *Naiadites* (14 samples) bivalves are recorded, with one thick-shelled ?*Schizodus* and two unidentified large bivalves (referred to herein as robust bivalves). Both *Modiolus* and *Naiadites* are thought to have a semi-infaunal to benthic mode of life (Owada, 2007; Vasey, 1984).

Serpula is common, recorded from 39 hand specimen samples. It comprises calcified polychaete worm tubes, loosely coiled helical cylinders that are 1-2 mm in diameter (Figure 9). In the Ballagan Formation these fossils are exclusively present in dolostones. The spiral tubes have a similar morphology and size to those described from peritidal carbonates of the late Tournaisian of Northern England, the Scottish Borders and Wales (Burchette and Riding, 1977; Leeder, 1973). Burchette and Riding (1977) interpreted these as gastropod in origin, but the absence of internal septa and a planispiral-shaped basal part of the tube (cf. Vinn and Mutvei, 2009) precludes a gastropod affinity. *Serpula* sometimes co-occurs with, but are distinct from, the microconchid '*Spirorbis'*, which is less abundant (11 samples). *'Spiroribis'* has a lamellar skeletal microstructure, micropores and bulb like (rather than open) tube origin (Wilson et al., 2011; Taylor and Vinn, 2006).

Fragments of arthropod cuticle (7 samples) and gastropods (6 samples) occur in almost all facies in very low numbers. Cuticle is not complete enough to identify, but is likely to be eurypterid in origin as these are the most common arthropods in the Ballagan Formation (Ross et al., 2018; Smithson et al., 2012). Gastropod identification is limited by poor preservation but may belong to *Naticopsis scotoburdigalensis* which has been recorded in the Ballagan Formation (Brand, 2018). Small brachiopods putatively identified as rhynchonellids occur in three beds.

Fossil content is not evenly distributed between facies, with facies 2 and 5 having the lowest content (Figure 8A). The distribution of each fossil group is illustrated in Figure 8B. Key points include: 1) thick-shelled robust bivalves are most common in facies 4 in the Norham Core; 2) *Spirorbis* and *Serpula* are most common in facies 4, then facies 3; 3) while lower in abundance, the faunal composition of facies 5 is no different from that from other facies. To further examine the differences between each facies, one sample of each was processed for micropalaeontology.

4.7. *Ichnology*

Bioturbation is observed in 191 samples, in all dolostone facies, and is most common in facies 3 where more than 75% of samples are bioturbated (Figure 8C). Within Burnmouth and the Norham core there are 71 intervals of *Chondrites* bioturbation within dolostones (Table S1). A detailed ichnofauna study by Bennett et al. (2017) described *Chondrites* traces as sub-vertical, branching with a dendritic pattern and have a burrow diameter range of 0.5–3 mm (Figure 4A). *Chondrites* is horizons are usually monospecific, but are associated with phycosiphoniform burrows (13 horizons), *Zoophycos*? (5 horizons) and *Rhizocorallium* (1 horizon). Bennett et al. (2017) reported that *Chondrites* horizons range in thickness from 1 to 37 cm, with a mean of 10 cm, and are mostly single-colonisation, simple-tier, with a high bioturbation intensity (bioturbation index of 5 or 6). Phycosiphoniform burrows are oblique to sub-horizontal, sinuous, of 2 mm burrow diameter, and have a bioturbation index of 4. Some *Chondrites* occurrences in siltstone rocks were reported in Bennett (et al., 2017) to be associated with orthocone fragments and scolecodonts.

4.8. *Micropalaeontology*

The microfossil composition of a representative sample from each facies (total present in all size fractions) is shown in Figure 10. The majority of specimens picked are below 1 mm in size and comprise small fragments of bones, scales, teeth, plant material or ostracod shells, which have the greatest occurrence in the 250 μm size fraction (Table S3). Examples of more complete specimens of the most abundant microfossils are illustrated in Figure 11. The amount of unidentified vertebrate bone and scale material strongly varies per sample (Facies 1: 64%; Facies 2: 18%; Facies 3: 87%; Facies 4: 17%; Facies 5: 1%). In all facies microfossils are well-preserved with no wear or abrasion identified. The microfossil results reveal the following groups that are not identified in hand specimen: chondrichthyan denticles and elasmobranch teeth (hybodonts and ?ctenacanths, xenacanths) and non-gyracanth acanthodian scales.

Facies 1 – This sample has by far the highest fossil concentration of the five samples analysed, at 16.6 fossils/g, but no fossils are present within the 1 mm size fraction (Table S3). The assemblage is dominated by indeterminate fish fragments, but also includes actinopterygian, rhizodont and rarer

chondrichthyan microfossils. Indeterminate fragments have a range of textures and colours, but are generally thin plates resembling fragments of fish scales, or chunky bone fragments. Actinopterygian components comprise scales, dermal bones, lepidotrichia bones and teeth. Actinopterygian scales have a rhombic shape with a smooth interior surface with keel, and a shiny exterior outer surface layer (ganoine mineralised tissue). The external ornament is typically transverse ridges and grooves of various heights, with small pores. Straight and recurved conical actinopterygian teeth occur in both size fractions and are identified by their transparent apical caps and cross-hatched ornament on the shaft (Carpenter et al., 2011). Only a few specimens are broken with a missing cap. Eleven of the 66 actinopterygian teeth identified are pharyngeal – rows of small, unornamented, curved, blunt teeth. Actinopterygian dermal bone has a pustulate ornament on one side, and a shiny, ganoine surface texture (cf. Clack et al., 2019). The lepidotrichia bones are most common in the 250 μm size fraction and are small, so are more likely to be actinopterygian than rhizodont. They have a range of surface textures ranging from smooth to longitudinal striations or ridges.

Rhizodont scale fragments and teeth are present. The exterior surface of rhizodont scales is cream coloured, with a fibrous structure, whereas the interior layers of broken scales have a range of structural elements characteristic of rhizodonts, including sheets of tubercules, pits or interlocking ridges and grooves. Curved rhizodont teeth fragments have ornament of well-defined striae similar to that of *Archichthys* (Jeffery, 2006). Eight dipnoan scales are identified by their cream coloured exterior surface with regularly spaced pits, a characteristic of macrofossil specimens from the Ballagan Formation. One putative dipnoan toothplate fragment has three aligned rounded teeth.

Chondrichthyan material comprises 10 *Ageleodus* teeth, one small xenacanth tooth and 90 chondrichthyan denticles. The *Ageleodus* teeth have a flat root with 4-8 tooth cusps, which is within the mean cusp count range of the genus (Downs and Daeschler, 2001). Some of the tooth cusps are broken off, and all specimens are small (less than 1 mm in length), likely to be from juvenile animals. One chondrichthyan tooth of the order Xenacanthiformes is identified by two principal cusps, with a smaller intermediate cusp in the centre (Johnson and Thayer, 2009). Chondrichthyan denticles are identified as hybodont (n = 36), ?ctenacanth (n = 7), and indeterminate elasmobranch specimens (n = 47). Hybodont

scales have a concave base, spinose top and distinctive grouping of spines which form a single flat star-shape, or multiple star-shaped clusters in dorsal view (Garvey and Turner, 2006; Yazdi and Turner, 2000). Putative ctenacanth scales have a flat base, spinose top, with numerous strongly curved spines of irregular height (Ivanov, 1996; Yazdi and Turner, 2000). Indeterminate elasmobranch scales have a flat or concave base and a top of curved spines which in dorsal view form clusters of irregular height, or individual spines (Burrow et al., 2009; Carpenter et al., 2011).

Facies 2 – The sample has the lowest fossil concentration of the five samples, at 1.9 fossils/g, but the assemblage is not notably different from facies 1. It is dominated by actinopterygians and indeterminate fish fragments, with chondrichthyans and rhizodonts a minor component. Actinopterygian scales are most numerous in the 250 μm size fraction. 25 actinopterygian teeth of various sizes are present, of which three are pharyngeal. One actinopterygian lepidotrichia bone has a smooth surface ornament (Figure 11A). Indeterminate fragments mostly comprise scale fragments of various textures and colours. One large *Ageleodus* tooth (3 mm in length) has a large flat root and nine tooth cusps. Chondrichthyan denticles are assigned to hybodont (n = 5, see Figure 11B), ?ctenacanth (n = 1), and indeterminate elasmobranch specimens (n = 11). Rarer rhizodont material comprises scale and teeth fragments.

Facies 3 – Indeterminate fish fragments dominate the assemblage. They are dark brown, chunky, with small pores, and some specimens have internal layers. There is a minor component of actinopterygian scales, lepidotrichia bone and small teeth. One rhizodont tooth fragment is identified by its well-defined striae (Figure 11C). Four acanthodian scales are diamond shaped, with a flat base and convex, asymmetrical top. Rare plant fragments and charcoal are present. One indeterminate megaspore and three ostracod moulds (podocopid in shape, two are tentatively assigned to *Cavellina*) are present.

Facies 4 – Actinopterygian fragments comprise two-thirds of the microfossils present and indeterminate fish fragments one quarter. Actinopterygian scales are abundant, most common in the 250 μm size fraction, and many specimens have transverse grooves (Figure 11D), and a shiny exterior surface. Small numbers of actinopterygian lepidotrichia bone occur in the 250 μm size fraction. Also present are 12

actinopterygian teeth (Figure 11E), four of which are pharyngeal. Indeterminate fish material comprises mostly scales but some bone material with a layered, porous internal structure (Figure 11F). Lower numbers of rhizodont scales are present (Figure 11G), and rhizodont teeth fragments. Moulds of 61 adult and large juvenile ostracods were recorded, most of which are carapaces. The following were identified: *Acutiangulata, Carbonita?, Cavellina* (Figure 11H), *Geisina, Sansabella* and palaeocopid ostracods, but most are too poorly preserved to identify. Low numbers of hybodont, ?ctenacanth and indeterminate elasmobranch scales are present, along with plant fragments.

Facies 5 – The assemblage is dominated by plant stem fragments with a fibrous structure, comprising 96% of the microfossils present (Figure 11I). Seven charcoal fragments are identified. Light brown actinopterygians scales and indeterminate fish scales of varying colour are present. Moulds of 32 adult and juvenile ostracod carapaces, and some single valves composed of sparry dolomite are recorded, including *Shemonaella, Sansabella* and palaeocopids. Rare broken fragments of the internal moulds of *Serpula* tubes are preserved.

4.9. *Taphonomy*

Taphonomic data are important for an assessment of which animals were living in the environment (autochthonous assemblages), or those that have been transported from other environments (allochthonous assemblages). There are no major differences identified in fossil presence/absence between the processed microfossil samples of different facies, but there are large differences in abundance. These could be attributed to local effects, for example an abundance of actinopterygian scales may mean that an actinopterygian macrofossil occurs within the same sample. Sample size can, of course, bias faunal diversity. For example, *Megalichthys* and Climatiiformes acanthodians occur in dolostones of the Isle of Bute (Carpenter et al., 2014), but are absent here, perhaps due to the smaller sample sizes analysed (500g versus 15 kg sample size). The larger hand specimen samples from Burnmouth (approximately double the

493 size of samples from the Norham Core) mean that there is a higher fossil presence per facies recognised at
494 Burnmouth (Figure 8A).

495 Facies 1 contains an abundant fossil assemblage, but an absence of fossils in the 1 mm fraction, indicates
496 size-sorting during deposition. The sample is a sandy siltstone that has been dolomitised. This is the most
497 fossil-rich facies of the Ballagan Formation, it commonly contains clasts of millimetre size or less, and it
498 formed as a cohesive debris flow due to meteoric flooding over a vegetated, often dry floodplain (Bennett et
499 al., 2016). As is characteristic for the sandy siltstone facies, the fossils are well-preserved and bones are
500 often still articulated (Otoo et al., 2019). Here, most actinopterygian teeth are intact, indicating only local
501 transportation. Facies 2-5 dolostones also contain microfossils that are well-preserved with no abrasion
502 observed. The only broken microfossils present are *Serpula* tubes within facies 5. Ostracod assemblages
503 comprise a range of adults and juveniles, and significant numbers of carapaces to single valves, indicative of
504 autochthonous assemblages (Boomer et al., 2003).

505 The analysis of over 400 dolostone hand specimen samples from Burnmouth and the core provides a
506 more comprehensive overview of fossil taphonomy. Table 1 summaries the taphonomy of each fossil group,
507 where known. No complete vertebrates are identified within the dolostones, so fossil fish taphonomy is
508 difficult to assess, although other studies of dolostones interpret that they were living in this environment
509 (Carpenter et al., 2014). *Naiadites* and *Modiolus* bivalves are usually sparsely distributed on bedding planes,
510 represent juvenile and adult stages and are un-broken, indicating minimal transport. In contrast, robust
511 bivalves (*Schizodus*) and brachiopods are concentrated, with stacked broken valves indicative of
512 transportation. All occurrences of the microconchid *Spirorbis* are as broken, isolated and often juvenile
513 forms, with no colonial or accumulation structures.

514 The taphonomy of *Serpula* occurrences in the Norham Core is recorded in Table S4. Autochthonous
515 *Serpula* colonies are present within the centre of dolostone beds (Figure 9A-B) and comprise orientated
516 tubes of varying size. Facies 3 contains the highest proportion of samples with *Serpula* colonies. But in total,
517 70% of all *Serpula* assemblages are allochthonous, forming centimetre thick horizons of broken tube
518 fragments that are at random orientations (Figure 9C). The taphonomy of chondrichthyans, acanthodians,

519 eurypterids, and gastropods has not been assessed, because of low specimen numbers. Future work to
520 enhance the taphonomy interpretation could be to analyse freshly exposed dolostone bedding surfaces at
521 Burnmouth and identify either trackways, or trace fossil evidence of transport or hostile environmental
522 conditions, such as eccentric xiphosuran trails (Falcon-Lang et al., 2015b).

523

524 ***4.10.*** *Geochemical and isotope composition*

525 EDX and XRD analysis reveal a ferroan dolomite composition for all facies. The XRD spectra
526 differentiated ordered dolomite from high-magnesium calcite (cf. Gregg et al., 2015). Facies 1 and 4 also
527 contain calcite and all samples contain minor amounts of mixed clays, quartz and feldspar (most common in
528 facies 1). Facies 5 samples contain gypsum, anhydrite, and in some samples calcite as a secondary
529 replacement of gypsum. Clay mineralogy is not examined in detail here, but Wilson et al. (1972) identified
530 illite within homogeneous type dolostones. An extensive carbonate geochemical analysis has not been
531 undertaken here, but previous studies report an average 10 wt% Mg and 2-3 wt% Fe for homogeneous
532 dolostones from the Cockburnspath area, analysed by electron microprobe (Andrews et al., 1991). XRD
533 analysis identified the presence of pyrite in one sample each of facies 1, 3 and 5.

534 Facies 2-5 dolostones examined in this study have a range of $\delta^{18}O$ and $\delta^{13}C$ from –8.5‰ to –0.2‰ (for
535 $\delta^{18}O$, mean –3.0‰) and –5.4‰ to 1.6‰ (for $\delta^{13}C$, mean –1.2‰) (Figure 12, Table S5). There is a large
536 degree of overlap between the different facies, and the isotope ranges fall within the results of a more
537 extensive isotope study into the Ballagan Formation dolostones by Turner (1991), also shown on Figure 12.

538

539 **5. Interpretation**

540 ***5.1.*** *Mechanism of dolomite formation*

541 The presence of marine fauna and ichnofauna in each dolostone facies indicate that dolomite formation
542 is likely to have originated from a marine water source. Previous studies interpreted that dolomite formed

543 from the alteration of primary calcite or aragonite (Belt et al., 1967; Leeder, 1974). The dolostones in this
544 study have no features typically associated with dolomitised limestones such as relict bioclastic fabric
545 (Searl, 1988), loss of internal structures (Muchez and Viaene, 1987), large crystal size (Gregg et al., 2001),
546 or a red rusty colour (McHargue et al., 1982). Storm surges were proposed as the mechanism to explain how
547 marine waters were transported into floodplain lakes (Bennett et al., 2017), yet did not form established
548 marine incursions across the floodplain. Modern storm surges can transport sand, mud and marine fauna
549 many river kilometres upstream and deposit across floodplain lakes (Donnelly et al., 2004; Goodbred and
550 Hine, 1995; Liu et al., 2014; Pilarczyk et al., 2016; Park et al., 2009; Williams, 2009). The taphonomic
551 evidence of disarticulated marine fauna and presence of a restricted marine ichnofauna (Bennett et al., 2017)
552 are also consistent with the storm surge model.

553 Facies 1 beds were deposited as fluvial to floodplain sediments that are interpreted to have been
554 cemented during early diagenesis, where eogenetic dolomite precipitated from solution within sediment pore
555 spaces, after the lithification of the sediment. The cementation of these deposits likely occurred at relatively
556 shallow burial depths, prior to significant sediment compaction, due to the presence of 3D plant remains and
557 sedimentary structures such as cross-lamination.

558 Facies 2, 3 and 5 dolostones are interpreted as synsedimentary dolomite, where dolomite crystals
559 precipitated from solution within the pore spaces of soft sediment, before lithification. Evidence for this
560 includes: 1) the preservation of 3D plants within nodules; 2) the presence of dolostone clasts within
561 conglomerate lags of the fluvial sandstone units in the Ballagan Formation (Bennett et al., 2016); 3) the even
562 distribution and abundance of dolomite crystals within a clay matrix indicates that dolomite grew when there
563 was a high sediment porosity; 4) some dolomite bed boundaries are gradational into siltstone, indicating a
564 transitional micro-environment zone of dolomite formation in the subsurface: 5) beds and laminae of
565 rhombohedral dolomite grains <5 μm, interpreted as either primary precipitates, or more probably, early
566 replacement of high-Mg calcite (Millward et al., 2018; Vasconcelos and McKenzie, 1997). In experimental
567 studies of microbially mediated (Petrash et al., 2017) and abiotic dolomite formation (Liu et al., 2019),
568 proto-dolomite (or disordered dolomite) first forms as micron or sub-micron sized spherulitic, cauliflower-

shaped crystals or aggregates, which then transforms to ordered euhedral dolomite rhombs with burial. Wanas and Sallam (2016) described 20–30 μm size euhedral dolomite rhombs within a clay matrix in Eocene saline lake sediments, interpreted as primary dolomite. This is similar to the microtextures observed in the facies 2 Ballagan Formation dolostones. Zoned euhedral dolomite rhombs are common in dolomitised limestones (Olanipekun and Azmy, 2017; Rameil, 2008), but can also occur due to a change in the composition of the dolomitising fluid rather than due to diagenesis (Jones, 2013).

Some facies 2-5 samples also host eogenetic dolomite, evidenced by the presence of some planar subhedral dolomite crystals 30 μm in size (facies 2), larger size dolomite rhombs within siltstone interbeds (facies 3), or in some homogeneous dolomite associated with evaporites (facies 5). In facies 2, 3 and 5 eogenetic microcrystalline dolomite may have formed due to the neomorphic replacement of original dolomicrite, as suggested by Ghummed (1982). The timing of this recrystallisation is difficult to ascertain. Primary dolomite precipitation likely occurred below the sediment surface, within the top metre of sediment, as has been proposed for nodular dolostones (Andrews et al., 1991). In addition, sub-surface synaeresis cracks in clay-rich sediments have been interpreted as forming due to de-watering or salinity changes (Plummer and Gostin, 1981), and internal brecciation is a common feature of the dolostones. Dolostone recrystallisation may have occurred in the near sub-surface prior to burial compaction. Eocene dolomitised limestones of the Kachchh Basin, western India, with planar euhedral, 40–100 μm size zoned rhombs are interpreted to have formed by diagenesis in a shallow marine environment in low temperature and salinity conditions (Singh et al., 2018).

In facies 4 samples, dolomite forms as a replacive secondary stage to calcite, indicated by the non-planar to planar-subhedral crystal textures, rhombs with micropores, patches of large sized dolomite rhombs or spar. The loading structures, rip-up clasts and soft-sediment deformation present in some facies 4 beds indicates the transport of carbonate into the lakes from a marine source. The facies 5 mineralogy of dolomite, gypsum and anhydrite along with trace amounts of celestine and barite is more commonly recorded in marginal marine settings rather than continental deposits (Millward et al., 2018; Warren, 2006; Chagas et al., 2016).

595 The dolomite-precipitating fluid may have derived from the evaporative enrichment of marine brines, a
596 common mechanism in modern day lagoons (Bahniuk et al., 2015). Why was dolomite precipitated instead
597 of calcite? Dolomite precipitation requires a concentration of calcium and magnesium ions, with low
598 concentrations of dissolved-sulphate (Baker and Kastner, 1981). Calcium and magnesium originated from
599 seawater, and the minor presence of pyrite within the dolostones indicates that some sulphate input.
600 Sulphate-reducing bacteria mediate the formation of ferroan dolomite in modern lakes in both oxic
601 (Sánchez-Román et al., 2009; Shinn et al., 1969) and anoxic (Vasconcelos and McKenzie, 1997; Wright,
602 1999; Wright and Wacey, 2004) conditions. The Ballagan Formation evidences semi-infaunal bivalves and
603 benthic ostracods living on the lake bottom, so conditions were likely to be oxic. Organic matter decay
604 would produce favourable conditions for dolomite formation by sulphate-reducing bacteria by reducing the
605 alkalinity and pH of pore waters (Slaughter and Hill, 1991). These reducing conditions would also allow the
606 incorporation of ferrous iron into the dolomite lattice (Barnett et al., 2012; Wright et al., 1997).

607 An abiotic primary dolomite formation model involving smectite is proposed by Wanas and Sallam
608 (2016). Eocene saline lake sediments comprised of clays with a gel-like highly viscous smectitic medium,
609 low sedimentation rate, high evaporation rate, and an alkaline solution, allowed for dolomite precipitation in
610 the absence of microbes. Due to diagenesis the original amount of smectite in the Ballagan Formation is
611 unknown (Kearsey et al., 2016), but illite has been identified in dolostones (Wilson et al., 1972) and
612 palaeosols (Kearsey et el., 2016). In addition, an experimental study demonstrated that illite can aid the
613 precipitation of abiotic dolomite under ambient conditions (Liu et al., 2019). However, the presence of
614 microbial mats, and pyrite hints that some biotic mediation was involved in forming the dolostones. An
615 alternative mechanism to explain the low pyrite levels in the dolostones was put forward by Andrews et al.
616 (1991). Organic matter decay and anaerobic oxidation via iron reduction and methanogenesis would have
617 created suitable alkaline conditions for ferroan dolomite growth.

618

619 ***5.2.*** *Palaeosalinity interpretation - fauna*

620 The fauna, microfauna and ichnofauna in the dolostones indicate a range of palaeosalinities were
621 encountered during the development of these intervals, summarised in Table 1. Each dolostone facies
622 contains fauna which can be interpreted as living in marine to freshwater environments.

623

624 5.2.1. Fossils with a marine origin

625 Rhynchonellid brachiopods are interpreted as stenohaline (Kammer and Lake, 2001). *Naticopsis*
626 *scotoburdigalensis* is described from a non-marine assemblage of *Modiolus, Curvirimula, Spirorbis,*
627 *Promytilus?, 'Estheria'* and ostracods from the Visean of Edinburgh (Chisholm and Brand, 1994). However,
628 *Naticopsis* is usually associated with marine conditions, for example in reef limestones of the Frasnian to
629 Tournaisian of Australia (Cook et al., 2003; Yoo, 1988). Palaeozoic *Spirorbis* has been interpreted as
630 tolerant of a wide salinity range (Zatoń et al., 2012); however, an extensive review by Gierlowski-Kordesch
631 and Cassle (2015) provided good evidence to suggest a marine origin, with larval spirorbids readily
632 transported into non-marine environments by tidal currents or storm deposits. Modern *Serpula* encrusts
633 bivalves, stones and substrates or forms colonial reefs along the sub-littoral zone of the British coast (Moore
634 et al., 1998). One record of a brackish-water serpulid colony occurs in the Holocene (Ferrero et al., 2005),
635 although most evidence points to a marine origin: In the geological record, *Serpula* forms in colonial
636 bioherm structures within shallow marine carbonates (Beus, 1980; Braga and López-López, 1989; Suttner
637 and Lukeneder, 2003) and Cretaceous serpulid bioherms are recorded from carbonate ramps (Palma and
638 Angeleri, 1992). The salinity tolerance of *Serpula* in the Palaeozoic has not been rigorously examined,
639 although most serpulid occurrences in the Ballagan Formation indicate significant transport and thus implies
640 they were washed-in from a marine environment. Despite this, some of them (30%) were able to survive and
641 colonise the sediment within the coastal lakes. The marine faunal diversity is low compared with other
642 Mississippian ferroan dolostones which host echinoderms, brachiopods and bryozoans (Barnett et al., 2012)
643 and conodonts (Somerville et al., 2001).

The ichnofacies that would be expected in the Ballagan Formation based on palaeoenvironment of *Scoyenia* (floodplains), *Skolithos* (river channels), and *Mermia* (coastal lakes) are absent. There are no arthropod, annelid, mollusc, fish or tetrapod traces or trackways, as reported from the Lower Pennsylvanian Tynemouth Creek Formation (Falcon-Lang et al., 2015b). Bennett et al. (2017) discussed that the absence could be due to a combination of few freshly exposed bedding-plane surfaces in the field succession, poor preservation, overprinting of these traces by *Chondrites*, or true absence. The ichnotaxa present within dolostones (*Chondrites*, phycosiphoniform, *Zoophycos*? and *Rhizocorallium*) are all indicator species of normal marine salinities (Bhattacharya and Bhattacharya, 2007; Buatois et al., 2005; Knaust, 2013). But because the ichnoassemblages are usually monospecific or of low diversity, they do not represent normal marine assemblages. Low diversity assemblages can be recorded in brackish settings (Mángano and Buatois, 2004), or deep marine turbidites (Carvalho et al., 2005). The Ballagan Formation ichnoassemblages indicate unusual environmental conditions. The high-bioturbation intensity but shallow burrowing depth of *Chondrites* represents rapid but short-lived colonisation of the sediment. Either normal marine conditions were never sustained in the lakes, or it was too hostile for most marine burrowing organisms to exploit successfully.

5.2.2. Euryhaline

Based on their facies distribution during the Mississippian, Carpenter et al. (2014) interpreted the following taxa as euryhaline: ctenacanths, acanthodians and *Ageleodus;* while rhizodonts and dipnoans favoured brackish to freshwater conditions. Xenacanths are more commonly associated with freshwater sedimentary deposits than contemporaneous holocephalan chondrichthyans (Friedman and Sallan, 2012). Xenacanths, rhizodonts, *Ageleodus*, actinopterygians and dipnoans have all been recorded in fluvial (oxbow lake) facies in the Late Mississippian (Greb et al., 2016). A study of fish palaeoecology from Pennsylvanian rocks deposited across a marine-brackish salinity gradient demonstrated that out of all these groups, chondrichthyans (xenacanths and *Ageleodus*) were able to live in the widest range of salinity (Ó Gogáin et al., 2016). Holocephalan teeth are numerically dominant over elasmobranch teeth in lagoonal dolostones

from Whitrope Burn (Richards et al., 2018). This site, in the Northumberland-Solway Basin, had a stronger marine connection than the Tweed Basin (Millward et al., 2019). Carboniferous hybodonts occur in non-marine to marginal marine assemblages (Garvey and Turner, 2006). Xenacanths, hybodonts and cteanacanths are reported from a shallow marine environment at Late Mississippian age localities in Arizona (Hodnett and Elliott, 2018). *Shemonaella*, *Paraparchites* and *Cavellina* are common euryhaline Mississippian ostracods (Bennett, 2008; Bennett et al., 2012) that are typical of the Ballagan Formation ostracod assemblage (Williams et al., 2005). The thicker-shelled *Schizodus* bivalves are likely euryhaline (Kammer and Lake, 2001).

5.2.3. Brackish to freshwater

The most common fish in the Ballagan Formation (actinopterygians, rhizodonts and dipnoans) are interpreted as euryhaline, or brackish-freshwater tolerant (Carpenter et al., 2014). Actinopterygians, rhizodonts and dipnoans have occupied freshwaters for the entire Devonian period (Friedman and Sallan, 2012). But there may be differences within groups. In a study of vertebrate fossil distribution in the Pennsylvanian Minto Formation of New Brunswick, Canada, Ó Gogáin et al. (2016) found that certain rhizodont genera were more common in marine facies (*Archichthys, Strepsodus*) while others (*Rhizodus*) were more numerous in brackish tidal estuary facies. This is supported by the presence of *Rhizodus in* Late Mississippian oxbow lake facies (Greb et al., 2015). Actinopterygian fish were the most common freshwater fish in the Carboniferous and Permian (Gray, 1988). Late Devonian-Early Carboniferous eurypterids are mostly restricted to brackish or freshwater environments (Braddy, 2001; Lamsdell and Braddy, 2010; Lamsdell et al., 2019) and were not tolerant of hypersalinity (Vrazo et al., 2016). *Modiolus* and *Naiadites* bivalves are typical of brackish to freshwater deposits in the Mississippian (Ballèvre and Lardeux, 2005; Bennison, 1960; Trueman and Weir, 1946), and of freshwater-brackish deposits in the Pennsylvanian (Eagar and Weir, 1971; Rogers, 1965). Restricted faunas, assemblages of *Serpula*, *Modiolus* and ostracods, are typical of Mississippian dolostones (Ramsbottom, 1973).

695

696 5.2.4. Hypersaline

697 A hypersaline-tolerant fauna has not been recognised from facies 5 dolostones. Today, however,
698 ostracods live in the dolomitic hypersaline lakes of the Coorong region, Western Australia, in salinities
699 ranging from 1 to 195‰ (De Deckker, 1983; De Deckker and Geddes, 1980). Some species are adapted to
700 hypersaline conditions, for example *Australocypris rectangularis* only occurs in salinities over 50‰. Further
701 analysis of ostracod-bearing facies 5 dolostones is required to determine if a salinity-tolerant fauna is
702 present.

703 In summary, the fauna and ichnofauna of the Ballagan Formation dolostones represent a mixture of
704 autochthonous fauna living within brackish lakes (fish, ostracods, bivalves) and allochthonous fauna derived
705 from marine incursions (*Spirorbis*, *Serpula,* gastropods, brachiopods, robust bivalves, ichnofossil trace-
706 makers). Plant material and eurypterid cuticle were derived from the nearby floodplain environment. The
707 taphonomy of the Ballagan Formation dolostones indicates that, apart from ichnofossil trace-makers, most
708 of the marine animals, with the exception of some serpulids, did not survive in the lacustrine environment.

709

710 ***5.3.*** *Palaeosalinity interpretation - isotopes*

711 The $\delta^{18}O$ of the dolostones will have been primarily controlled by palaeosalinity, waxing and waning
712 between fresh, brackish and marine environments. The presence of eogenetic dolomite in facies 1 and some
713 other samples shows that diagenetic fluids may have also had an influence on dolostone $\delta^{18}O$ composition.
714 We do not have data on the stable isotopic composition of a freshwater dolomite as an end member to
715 compare. However, comparisons can be made to other Mississippian datasets (Figure 12). The $\delta^{18}O$ data
716 from facies 2-5 dolostones are within the same range as data from Mississippian ferroan dolomites
717 associated with palaeosols (Barnett et al., 2012). Some facies 1 samples plot towards the range of calcite

cements (although there will be a fractionation difference of several per mil) analysed by Kearsey et al. (2016) and calcretes (Barnett et al., 2012), perhaps indicating a different formation mechanism.

Typical marine Mississippian dolomite will have $\delta^{18}O$ of around +4‰ (based on the difference in fractionation compared to marine calcite, Barnett et al., 2012) while freshwater dolomite will have lower $\delta^{18}O$. All the dolostones here have lower $\delta^{18}O$ than the marine dolomite value of Barnett et al. (2012), which may indicate a mixed input from marine, brackish, or fresher water. Evidence from palaeosols and overlying sandy siltstone cohesive debris flow deposits show that seasonal flooding events with high rainfall were common, adding freshwater to floodplain lakes (Bennett et al., 2016; Kearsey et al., 2016). An increase in the temperature of the dolomite-precipitating solution produces dolomite with lower $\delta^{18}O$ (Vasconcelos et al., 2005). Given the palaeoequatorial position temperature was likely elevated in shallow floodplain lakes, but evaporation is also important and this would result in higher $\delta^{18}O$ values. The analysis of only one facies 5 sample precludes further interpretation.

The dolostones from this study have $\delta^{13}C$ values lower than Mississippian marine dolomite with $\delta^{13}C$ of +2‰ (Barnett et al., 2012). The $\delta^{13}C$ data sit within the range of those recorded from dolomitic lake sediments of the Coorong, Australia (Wacey et al., 2007) where there has been degradation of terrestrial (and possibly some marine) organic matter by sulphate-reducing bacteria suggesting a marginal environment with freshwater incursion bringing terrestrial material. Andrews et al. (1991) proposed that dolostone $\delta^{13}C$ values are principally a combined result of bicarbonate ions originating from iron reduction and the methanogenesis of organic matter. Iron reduction would produce bicarbonate ions that were isotopically light ($\delta^{13}C$ of −23‰), while methanogenesis produced bicarbonate that was isotopically heavy ($\delta^{13}C$ of 0‰). Andrews et al. (1991) also discussed the role of methane oxidation, but typical very light signatures ($\delta^{13}C$ of −60‰) means that this was likely minimal. The equilibration of floodplain lakes with atmospheric CO_2 would also have changed the carbon isotope value of dissolved inorganic carbon in surface waters. Experimental models show that evaporation results in dissolved inorganic carbon with higher $\delta^{13}C$ values (Abongwa and Atekwana, 2013).

6. Discussion

6.1. *Palaeoenvironments*

Extensive planar dolostone beds represent formation in large coastal lakes, whereas nodular and discontinuous beds are interpreted to represent variations in topography at the edge of lakes, lateral changes in dolostone morphology, or cementation around fossils in the near sub-surface. The lateral extent of the lakes is a few kilometres in size at maximum, as individual dolostone beds do not correlate between the Norham Core and Burnmouth which are 13 km apart. There was a high degree of environmental complexity, with coastal lakes occurring at the same time as rivers, swamps and vegetated floodplains. The depositional environment of each dolostone facies and their main fossil assemblages is detailed in Figure 13.

6.1.1. Closed saline lake

Facies 2 dolostones developed with the growth of dolomite crystals in mud-rich lake sediments below wave base. The presence of zoned dolomite crystals, with increasing Mg towards the rim shows that salinity increased over time, probably due to evaporation. Rare detrital quartz grains and silt in these dolostones were probably derived from runoff flood-waters generated across the floodplain during times of heavy rainfall. The homogeneous character of many of these beds indicates hydrologically closed lakes with a minimal clastic input from rivers. This facies does contain some marine fossils, but relatively low percentage of samples with bioturbation shows that the water conditions were inhospitable to marine life, and were perhaps too saline. The high incidence of brecciation indicates water bodies that were subject to evaporation and the substrate starting to dry out.

6.1.2. Closed and hypersaline lake

766 Some closed lakes became highly evaporitic and hypersaline, precipitating gypsum, with a
767 continuum from facies 2 to 5. Facies 5 dolostones primarily represent formation in closed saline lakes that
768 became increasingly hypersaline over time. Though a continental sabkha model was proposed by Scott
769 (1986) to explain the formation of evaporites in the Ballagan Formation, Millward et al (2018) argued that
770 most of the evaporites formed in coastal floodplain sabkhas, ephemeral brine pans and semi-permanent
771 hypersaline lakes or salinas. Though most modern coastal evaporite deposits occur in arid or semi-arid
772 climate zones, they can form in seasonally wet tropical biomes, for example in the Bahamas and Florida
773 (Ziegler et al., 2003) and coastal lagoons in Belize (Rejmankova et al., 1996).

774

775 6.1.3. Open saline lake

776 Facies 3 has the highest number of samples that exhibit bioturbation, but the lowest incidence of
777 brecciation. These characteristics, in combination with alternations of clastic and carbonate material, suggest
778 a hydrologically open saline lake with a fluvial connection. Marine waters would have inundated the lakes at
779 times of storm surge, bringing small animals such as polychaete worms and microconchid larvae. Conditions
780 remained stable enough for *Serpula* colonies to form and *Chondrites* and phycosiphoniform trace-makers to
781 establish themselves. In modern dolomite-precipitating saline lakes 'soupy' soft substrates are typical (De
782 Deckker and Last, 1988). *Chondrites* and *Phycosiphon* have been reported from soft, clay-rich substrates
783 (Taylor et al., 2003) where *Chondrites* is one of the first colonisers (Ming, 2004). Facies 3 and facies 4 form
784 a continuum in terms of proximal to marine (facies 4) and distal (facies 3) lake environments (Figure 13).

785 Why are limestone beds missing in these successions? In a depositional model for the Famennian of
786 Belgium, dolomite was inferred to have formed closest to land, in evaporitic lagoons or marshes, and ooidal
787 limestones formed in tidal flats and skeletal limestones in the inner shelf (Thorez et al., 2006). In the
788 Mississippian Slade Formation of Kentucky, ferroan dolomites are laterally associated with peritidal
789 limestones (Barnett et al., 2012). Rare ooids and microbial mats are identified within the Ballagan Formation
790 (in facies 4, and associated with evaporites; Millward et al., 2018, 2019), and in Tournaisian dolostones of

Eastern Canada (Belt et al., 1967). Whereas ooids do not always form under marine conditions, limestones are a characteristic of the partially contemporaneous Lyne Formation in the Northumberland Basin (Leeder, 1975a, b), implying that marine deposition was taking place to the south and west (Millward et al., 2019). The 'missing' marine limestones in the Tweed Basin indicate that most dolomite formed in floodplain lakes that did not have an open marine connection. Instead these lakes were inundated by marine waters by storm surges which may have travelled a long distance inland across a very low-lying floodplain.

6.1.4. Coastal marsh

While fully developed palaeosol horizons did not form within the dolostones, the presence of brecciation, roots, mottling and other post-depositional modifications requires an assessment of their potential to be palustrine carbonates: sediments deposited in freshwater lakes or marshes then subjected to sub-aerial processes. Most modern and Palaeozoic palustrine carbonates are composed of micritic calcite and contain an assemblage of charophytes, ostracods and molluscs (usually gastropods), with rare fish material (Alonso-Zarza, 2003; Freytet and Verrecchia, 2002; Montañez and Cecil, 2013; Platt and Wright, 1992; Tandon and Andrews, 2001). Palustrine ferroan dolostones associated with roots or palaeosols, have been identified from South Wales (Searl, 1988; Wright and Robinson, 1988), South West England (Wright et al., 1977; Vanstone, 1991), Belgium (Muchez and Viaene, 1987), Tennessee (Caudill et al., 1996) and Kentucky (Barnett et al., 2012). In Tennessee ferroan dolomicrite overlies a Vertisol and is thought to have formed by the sporadic inundation of the coastal plain by storm tides (Caudill et al., 1996). In the Upper Mississippian of Kentucky, the dolostones are interpreted to have formed in a brackish to schizohaline coastal marsh (Barnett et al., 2012). These deposits are similar to the dolostones of the Ballagan Formation because they: 1) occur in between palaeosol or fluvial facies; 2) form continuous sheets extending several hundred meters; 3) have a micritic or microspar texture, with zoned rhombs; 4) commonly exhibit a homogeneous structure, with *in situ* brecciation; 5) have $\delta^{13}C$ and $\delta^{18}O$ compositions that are within the same range as dolostones. Also similar are Mississippian dolostones of South-West England, which occur overlying palaeosols or limestones (they do not replace either), and comprise dolomicrite with an average

817 crystal size of 4 μm (Wright et al., 1997; Vanstone, 1991). These deposits are interpreted to have formed in
818 brackish to schizohaline coastal marshes or swamps, with iron sourced from soil horizons and provide a
819 good analogue for the rooted bulbous bedded dolostones of the Ballagan Formation. Clay-rich
820 microcrystalline dolostones, some containing roots and tree casts, also occur in the Tournaisian Horton Bluff
821 Formation of Nova Scotia, interpreted as lacustrine marshes (Martel and Gibling, 1991).

822 The observation that secondary pedogenic alteration affects facies 1-4 dolostones may indicate that
823 some of the lakes evolved to become vegetated marshes. However, only 8-9% of the Ballagan Formation
824 dolostones are secondarily altered by brecciation and pedogenesis. While the evidence of tree rooting
825 structures within the dolostones (Figure 7) may indicate salt-tolerant vegetation, further studies are needed
826 to elucidate if there is a link between Mississippian dolostones and emerging new plant communities such as
827 *Rhizophora mangle-like* wetlands or mangroves (Greb et al., 2006).

828 The common desiccation cracks in all facies in the Norham Core (including siltstone, sandstone,
829 dolostone, palaeosol) indicate that very dry conditions alternated with wetter periods characterised by likely
830 seasonally heavy rains (Bennett et al., 2016; Kearsey et al., 2016). The presence of roots, root disturbance
831 and rarer desiccation cracks indicate that fluctuations in water level briefly exposed the top of the
832 dolostones, which sometimes became vegetated. The mottling indicates re-mobilisation of iron which is
833 thought to be due to changes in Eh of groundwater caused by oscillation in the water table (Alonso-Zarza,
834 2003). While evaporation would have led to the development of brecciation, desiccation and evaporites
835 within the dolostones, there is no evidence for long-lived arid conditions. The Ballagan Formation does not
836 contain calcrete-bearing palaeosols such as those seen in the Tournaisian of Southern England (Wright,
837 1990) and the older latest Devonian Kinnesswood Formation of Scotland (Wright et al., 1993).

838 A good analogue from the geological record that contains the variation in carbonate lakes seen in the
839 Ballagan Formation is the Early Cretaceous, Leza Formation of the Cameros Basin, Northern Spain (Suarez-
840 Gonzalez et al., 2015). The formation contains a mosaic of carbonate and clastic coastal wetland
841 depositional environments, including freshwater, brackish, marginal-marine, evaporitic and tidal carbonate
842 water bodies. Tidal water bodies were near the shoreline and contained ooidal sediment, while all lakes had

variable clastic input due to their connection with alluvial fans. In the Leza Formation carbonate rocks dominate over clastic rocks in terms of total thickness, but the mosaic of different water bodies provides a useful conceptual analogue to the range of dolostone facies in the Ballagan Formation. Although there are examples of tropical, coastal wetlands with highly saline conditions today, for example in the Salum, Gambia and Casamance river estuaries of Senegal and The Gambia, in West Africa (Barusseau et al., 1985) they do not form significant evaporite deposits.

Iron was essential to the formation of the dolostones, but synsedimentary ferroan dolostones are relatively rare in the geological record. The Ballagan Formation dolostones and evaporites formed at a time when crustal extension opened-up the southern margin of Laurussia to marine waters from the Palaeotethys and Panthalassa oceans (Millward et al., 2018, 2019). Basaltic volcanism preceded deposition of Ballagan Formation sediments and relicts of the volcanic fields may well have been exposed during at least some of the Tournaisian. This is evidenced by the intercalation of beds of volcaniclastic sedimentary rocks within the Ballagan succession in the Spilmersford and East Linton boreholes (Davies et al., 1986), and at Oxroad Bay (Bateman and Scott, 1990). Remnants of Devonian andesite volcanoes (Browne et al., 2002) from the Ochil Volcanic Formation and several other units (that formed the Cheviot, Pentland, Ochil and Sidlaw hills) may also have stood above the coastal plain and supplied sediment to the system. Newly rifted basins at sites of crustal extension in the Mississippian host ferroan dolostones (Figure 1A). At these locations, the enhanced weathering of volcanic bed-rock due to the wet tropical climate may have provided the right conditions for ferroan dolomite formation within coastal lakes.

6.2. Temporal trends

The tropical climate of the Ballagan Formation is thought to have been fairly constant throughout the formation, with seasonal wet-dry cycles, and no periods of aridity (Bennett et al., 2016; Kearsey et al., 2016; Millward et al., 2018). Long-term changes in sedimentology over time represent changing palaeoenvironments on the coastal floodplain. In both sections studied, thicker dolostones at the base of the

succession (the lowest 80 m at Norham, and the lowest 200 m at Burnmouth), indicate that hypersaline lakes were long-lived. Abundant dolostone beds can be interpreted as a product of more intense strong storm surges, or a more proximal marine shoreline. Thick and more common facies 5 dolostones and evaporites in the lowermost 80 m of the Norham Core (Millward et al., 2018) indicate that hypersaline lakes, ephemeral brine pans or salinas were common in the early Tournaisian at this location. Dolostone abundance patterns correspond to the abundance of bioturbated horizons, especially those colonised by *Chondrites*, and to occurrences of beds containing marine fauna (Bennett et al., 2017). These horizons are of the highest concentration at the base of the Norham Core, but also occur at other intervals throughout both successions.

Where dolostones are uncommon and thinner in the middle and top of both sections, the thickness of palaeosol horizons increases, interpreted as a lowering of the floodplain water table over time (Kearsey et al., 2016). Vertisols show the strongest trend and show the greatest development at times of low dolostone deposition, with units over one metre thick forming in the top part of both sections. There is a strong association between Vertisols and overlying sandy siltstone beds (Kearsey et al., 2016), which overlie palaeosols and form as cohesive debris flows in seasonal meteoric flooding events (Bennett et al., 2016). In the Norham Core where the abundance of sandy siltstone beds is low there is a corresponding increase in dolostone abundance, for example in the lowest 80 metres of the section. Although there are these larger scale associations, there is also much small-scale variability; sandy siltstones, desiccation cracks, *in situ* brecciation of dolostones, gleyed Inceptisols, Inceptisols and Entisols are all fairly well distributed throughout the Norham Core.

In summary, there is a large-scale pattern of waning marine influence and drying of the floodplain over the Tournaisian. At the base of the formation, marine fauna and infauna are washed into the lakes during storms, but fully marine conditions never develop, instead evaporation produced thick dolostones and in some cases a range of evaporite forms. In the middle to top of the formation, a drier, forested floodplain emerges, with shorter-lived saline-hypersaline lakes. Despite this long-term trend, there are smaller-scale peaks in dolostone abundance, and marine fauna do appear in the upper parts of the Tournaisian too. A long-term drying of the environment is not evident at Tournaisian sites in the Midland Valley of Scotland or in

894 the Northumberland – Solway Basin, where dolostones and evaporites are present throughout the formation
895 (Millward et al., 2018, 2019). The range of dolostone facies, and palaeosol types observed, and the changing
896 deposition of the sandstones of fluvial facies association all contribute to the complex picture. These thick
897 fluvial sandstone units and their interactions with the overbank facies association is the subject of a future
898 study. This study provides more evidence to confirm the long-lived existence of a mosaic of coastal
899 floodplain palaeoenvironments in the Tournaisian of the Scottish Borders.

900

901 **6.3. Importance to terrestrialisation**

902 Were coastal lakes and marshes important to the terrestrialisation of tetrapods? The *Pederpes* specimen
903 from Dumbarton was discovered between two dolostone beds within a nodule described as a *'clayey*
904 *limestone nodule typical of a cementstone facies*' (Clack, 2002). Further examination of the sample by CEB
905 reveals its composition to be a cemented siltstone, categorised as a facies 1 dolostone nodule. But there is no
906 evidence of tetrapods having lived within dolostone-forming environments in the Ballagan Formation, or in
907 the contemporaneous Horton Bluff Formation of Nova Scotia (Anderson et al., 2015). It is surprising that
908 tetrapods are absent from dolostones given that many Carboniferous groups appear to have been euryhaline
909 (Ó Gogáin et al., 2016). Numerous new tetrapod species have been reported from siltstones, sandy siltstones
910 overlain by palaeosols, or conglomerate lags within the Ballagan Formation, indicating that they inhabited
911 vegetated floodplain land surfaces, lakes and rivers (Bennett et al., 2016; Clack et al., 2016). Perhaps the
912 dolomite-forming coastal lakes were too hostile an environment, with water that was too saline for these
913 Tournaisian tetrapods. While there is no direct link between tetrapod terrestrialisation and these coastal lakes
914 and marshes; these environments may have been vital for numerous groups of euryhaline animals.
915 Coastal lakes precipitating dolomite were extensive across the region (Millward et al., 2019), had a wide
916 salinity range, and were a repeated feature of the coastal plain environment. The fauna autochthonous to the
917 dolostone-forming lakes (fish, ostracods and bivalves) appear to have thrived after the Hangenberg Crisis.
918 Dipnoans, actinopterygians and chondrichthyans recovered and diversified quickly (Challands et al. 2019;
919 Friedman, 2015; Richards et al., 2018; Sallan and Coates 2010; Smithson et al., 2016), whereas ostracods

and bivalves radiated into first brackish (Williams et al., 2006), then freshwater far later in the Mississippian (Bennett, 2008; Gray, 1988). Many fish groups (Ó Gogáin et al., 2016) and invertebrates such as *Naiadites* (Falcon-Lang et al., 2006) found in the dolostones maintained a euryhaline capacity into the Pennsylvanian. The coastal lakes may have acted both as a habitat for euryhaline animals, and as a place for them to breed. Carpenter et al. (2014) suggested that the Ballagan Formation lakes acted as nurseries for juvenile fishes and sharks. The lakes could also have been a pathway into freshwater rivers or pools for anadromous fishes. There is no evidence of a permanent marine connection, like the lagoon, brackish embayments, or tidal estuary environments euryhaline fish inhabited in the Pennsylvanian Minto Formation (Ó Gogáin et al., 2016). Yet the presence of allochthonous marine faunas and dolostone ichnoassemblages demonstrate marine input, so how did vertebrates access these coastal lakes? None of the vertebrates are stenohaline, and similar vertebrate assemblages have been documented from Ballagan Formation floodplain temporary lakes (Otoo et al., 2019) and rivers (Clack et al., 2019). We speculate that when these environments were flooded by marine storm surges the osmoregulatory capacity of the fishes enabled them to thrive in the new lakes which became increasingly saline over time. While there are no major marine transgression surfaces, the presence of rare scolecodonts and orthocones in overbank facies indicates a low-lying coastal floodplain with an intermittent marine influence (Bennett et al., 2016, 2017). There may have been a connection to the more marine Northumberland-Solway Basin (Millward et al., 2019) or a nearby lagoon environment which is unclear at this time.

The association of bivalves, ostracods, rhizodonts and actinopterygians is common in dolostones, but also in overbank sandy siltstones of the Ballagan Formation (Bennett et al., 2016), pointing towards both a euryhaline salinity adaptation, and feeding behaviours. The rich detrital plant matter in freshwater-brackish floodplain lakes (Bennett et al., 2016) would have provided a food source for invertebrates at the base of the food chain. Freshwater ostracods that inhabit lakes are usually detritivores (De Deckker, 2002; Rennie and Jackson, 2005), and Mississippian non-marine ostracods are thought to have consumed detrital plant material (Bennett et al., 2012). Modern freshwater bivalves are both suspension and filter feeders that consume bacteria, algae, detrital plant matter, dissolved organic matter and zooplankton (Coma et al., 2001; Vaughn et al., 2008). Bivalves from the Ballagan Formation may have consumed particulate or detrital plant

947 and algal material. It is likely that actinopterygians consumed ostracods and juvenile bivalves, as has been
948 recorded in modern environments (Masdeu et al., 2011; Victor et al., 1979). The diet of rhizodonts is
949 unknown, but their large size and predatory-type dentition (Jeffery, 2006) means that actinopterygians may
950 have been a part of their diet. The coastal lake environment played a major role in the radiation of life from
951 marine to freshwaters, by forming large, long-lived floodplain lake and marsh habitats, with an intermittent
952 marine connection.

953

954 **7. Conclusions**

955 • Synsedimentary ferroan dolostones occur in Mississippian successions deposited within newly rifting
956 basins along the southern margin of Laurussia. The Tournaisian Ballagan Formation of the Scottish
957 Borders provides an exceptional record enabling a comprehensive study of ferroan dolostones
958 through most of the Tournaisian, at a time when new terrestrial environments and ecosystems were
959 established after an extinction event.
960 • From this record, five ferroan dolostone facies are identified in core and field section: cemented
961 siltstone and sandstone; homogeneous dolomicrite; mixed dolomite and siltstone; mixed calcite and
962 dolomite; dolomite with evaporite minerals. Facies 1 formed by the diagenetic cementation of
963 alluvial and floodplain siliciclastic sediments, whereas facies 2-5 represent synsedimentary dolomite
964 formation, or the eogenetic replacement of calcite by dolomite. There is a continuum between
965 homogeneous dolostones and those containing evaporite minerals.
966 • The temporal and spatial occurrence of Mississippian dolostones is related to their palaeogeographic
967 position along the southern rift basins of Laurussia with a connection to marine water, and also to the
968 equatorial seasonal climate. The marine water crucial to initiate dolomite formation resulted from
969 storm surges, which also transported marine fossils across the floodplain.
970 • Dolomite and evaporite-forming environments include closed saline lakes, many becoming
971 hypersaline, brine pans, sabkhas, and open saline lakes connected to fluvial systems. The distribution
972 of these dolostones throughout the Ballagan Formation indicates a more established marine

973 connection at the base of the formation, then a gradual drying of the floodplain through time. There
974 was a mosaic of co-existing floodplain, alluvial and saline-hypersaline lake environments with
975 frequent periods of pedogenesis and desiccation.
976 • The palaeontology (macrofauna, microfauna, ichnofauna) and isotope geochemistry of the dolostones
977 reveal variable salinity from brackish to hypersaline conditions. The lakes were a habitat for
978 dipnoans, rhizodonts, actinopterygians, acanthodians, several types of chondrichthyans, bivalves and
979 ostracods. Most marine animals washed-into the lakes appear not to have survived, with the
980 exception of some *Serpula* colonies and *Chondrites*-producing polychaetes.
981 • Although tetrapods did not appear to inhabit these saline lakes, their variable salinity and habitat they
982 represent may have been an important factor in the radiation of aquatic animals (chondrichthyans,
983 actinopterygians, sarcopterygians, bivalves, ostracods and gastropods) from marine to freshwater at
984 this time.

985

986 **Acknowledgments**

987 This study is a contribution to the TW:eed Project (Tetrapod World: early evolution and diversification), a
988 major research programme investigating the rebuilding of Carboniferous ecosystems following a mass
989 extinction at the end of the Devonian. This study was funded by NERC Consortium Grant '*The Mid-*
990 *Palaeozoic biotic crisis: setting the trajectory of tetrapod evolution*', led by the late Prof. Jenny Clack
991 (University Museum of Zoology, Cambridge) and involving the universities of Leicester (NE/J020729/1)
992 and Southampton (NE/J021091/1), the British Geological Survey (NE/J021067/1) and the National Museum
993 of Scotland. Jenny Clack took a great interest in all aspects of the TW:eed Project and is thanked for
994 comments on a draft of the manuscript. We thank Anne Brown and Colin MacFadyan at NatureScot and
995 Paul Bancks from Crown Estate Scotland for permission to collect from the foreshore at Burnmouth. The
996 Norham cores are archived in the National Geological Repository at BGS, Keyworth. The support of staff in
997 curation and facilitating access is acknowledged. The following TW:eed Project volunteers are thanks for
998 their assistance with fossil identification from dolostone beds: Catherine Caseman, Rachel Curtis, Daniel

999 Downs, Graham Liddiard, Jessica Mason, James Mawson and Kirsty Summers. We thank Mike Turner for
1000 allowing the use of dolostone isotope data from his PhD thesis. TIK, DM, MAEB, PJB and MJL publish
1001 with the permission of the Executive Director, British Geological Survey. Julian Andrews, Paul Wright and
1002 an anonymous reviewer are thanked for their insightful comments on this manuscript.

1003

1004 **References**

1005 Abongwa, P.T. and Atekwana, E.A. 2013. Assessing the temporal evolution of dissolved inorganic carbon in
1006 waters exposed to atmospheric CO2 (g): A laboratory approach. Journal of hydrology, 505, 250-265.

1007 Alonso-Zarza, A.M. 2003. Palaeoenvironmental significance of palustrine carbonates and calcretes in the
1008 geological record. Earth-Science Reviews, 60, 261-298.

1009 Anderson, J.S., Smithson, T., Mansky, C.F., Meyer, T. and Clack, J. 2015. A diverse tetrapod fauna at the
1010 base of 'Romer's Gap'. PLoS ONE, 10, 1-27, doi:10.1371/journal.pone.0125446.

1011 Anderton, R. 1985. Sedimentology of the Dinantian of Foulden, Berwickshire, Scotland. Transactions of the
1012 Royal Society of Edinburgh: Earth Sciences, 76, 7-12.

1013 Andrews, J.E. and Nabi, G. 1994. Lithostratigraphy of the Dinantian Inverclyde and Strathclyde Groups,
1014 Cockburnspath Outlier, East Lothian-North Berwickshire. Scottish Journal of Geology, 30, 105-119.

1015 Andrews, J.E. and Nabi, G. 1998. Palaeoclimatic significance of calcretes in the Dinantian of the
1016 Cockburnspath Outlier (East Lothian-North Berwickshire). Scottish Journal of Geology, 34, 153-164.

1017 Andrews, J.E., Turner, M.S., Nabi, G. and Spiro, B. 1991. The anatomy of an early Dinantian terraced
1018 floodplain: palaeo-environment and early diagenesis. Sedimentology, 38, 271-287.

1019 Armstrong, M., Paterson, I.B. and Browne, M.A. 1985. Geology of the Perth and Dundee district. Memoir
1020 of the British Geological Survey, Sheets 48W, 48E and 49, Scotland.

1021 Bahniuk, A., McKenzie, J.A., Perri, E., Bontognali, T.R., Vögeli, N., Rezende, C.E., Rangel, T.P. and
1022 Vasconcelos, C. 2015. Characterization of environmental conditions during microbial Mg-carbonate

precipitation and early diagenetic dolomite crust formation: Brejo do Espinho, Rio de Janeiro, Brazil, in: Bosence, D.W.J., Gibbons, K.A., Le Heron, D.P., Morgan, W.A., Pritchard, T. and Vining, B.A., eds., Microbial Carbonates in Space and Time: Implications for Global Exploration and Production. Geological Society, London, Special Publications, 418, 243-259.

Baker, P.A. and Kastner, M. 1981. Constraints on the formation of sedimentary dolomite. Science, 213, 214-216.

Ballèvre, M. and Lardeux, H. 2005. Signification paléoécologique et paléogéographique des bivalves du Carbonifère inférieur du bassin d'Ancenis (Massif armoricain). Comptes Rendues Paleovol, 4, 109-121.

Barnett, A.J., Wright, V.P. and Crowley, S.F. 2012. Recognition and significance of paludal dolomites: Late Mississippian, Kentucky, USA. International Association of Sedimentology Special Publications, 45, 477-500.

Barusseau, J.P., Diop, E.H.S. and Saos, J.L. 1985. Evidence of dynamics reversal in tropical estuaries, geomorphological and sedimentological consequences (Salum and Casamance Rivers, Senegal). Sedimentology, 32, 543-552.

Bateman, R.M. and Scott, A.C. 1990. A reappraisal of the Dinantian floras at Oxroad Bay, East Lothian, Scotland. 2. Volcanicity, palaeoenvironments and palaeoecology. Transactions of the Royal Society of Edinburgh: Earth Sciences, 81, 161-194.

Belt, E.S., Freshney, E.C. and Read, W.A. 1967. Sedimentology of Carboniferous dolostone facies, British Isles and Eastern Canada. The Journal of Geology, 75, 711-721.

Bennett, C. 2008. A review of the Carboniferous colonisation of non-marine environments by ostracods. Senckenbergiana Lethaea, 88, 37-46.

Bennett, C.E., Howard, A.S.H., Davies, S.J., Kearsey, T.I., Millward, D., Brand, P.J., Browne, M.A.E., Reeves, E.J. and Marshall, J.E.A. 2017. Ichnofauna record cryptic marine incursions onto a coastal

floodplain at a key early Mississippian tetrapod site. Palaeogeography, Palaeoclimatology, Palaeoecology, 468, 287-300.

Bennett, C.E., Kearsey, T.I., Davies, S.J., Millward, D. Clack, J.A., Smithson, T.R. and Marshall, J.E.A. 2016. Early Mississippian sandy siltstones preserve rare vertebrate fossils in seasonal flooding episodes. Sedimentology, 63, 1677-1700.

Bennett, C.E., Siveter, D.J., Davies, S.J., Williams, M., Wilkinson, I.P., Browne, M. and Miller, C.G. 2012. Ostracods from freshwater and brackish environments of the Carboniferous of the Midland Valley of Scotland: the early colonisation of terrestrial water bodies. Geological Magazine, 149, 366-396.

Bennison, G.M. 1960. Lower Carboniferous non-marine lamellibranchs from East Fife, Scotland. Palaeontology, 3, 137-152.

Beus, S.S. 1980. Devonian serpulid bioherms of Arizona. Journal of Paleontology, 54, 1125-1128.

Bhattacharya, B. and Bhattacharya, H.N. 2007. Implications of trace fossil assemblages from late Paleozoic glaciomarine Talchir Formation, Raniganj basin, India. Gondwana Research, 12, 509-524.

Bicknell, R.D. and Pates, S. 2019. Xiphosurid from the Tournaisian (Carboniferous) of Scotland confirms deep origin of Limuloidea. Scientific reports, 9, 1-13.

Bontognali, T.R.R., Vasconcerlos, C., Warthmann, R.J., Bernasconi, S.M., Dupraz, C., Strohmenger, C.J. and McKenzie, J.A. 2010. Dolomite formation within microbial mats in the coastal sabkha of Abu Dhabi (United Arab Emirates). Sedimentology, 57, 824-844.

Boomer, I., Horne, D.J. and Slipper, I.J. 2003. The use of ostracods in palaeoenvironmental studies, or what can you do with an ostracod shell. Paleontological Society Papers, 9, 153-179.

Braddy, S. J. 2001. Eurypterid palaeoecology: palaeobiological, ichnological and comparative evidence for a ‘mass-moult-mate’hypothesis.". Palaeogeography, Palaeoclimatology, Palaeoecology, 172, 115-132.

Braga, J.C. and López-López, J.R. 1989. Serpulid bioconstructions at the Triassic-Liassic boundary in southern Spain. Facies, 21, 1-10.

1071 Brand, P.J. 2018. A list of fossil specimens in the BGS biostratigraphy collections from the Ballagan
1072 Formation in Scotland and from the former Lower Border Group of the Northumberland-Solway
1073 Basin. British Geological Survey Internal Report IR/18/03.

1074 Bridge, J.S., Gordon, E.A. and Titus, R.C. 1986. Non-marine bivalves and associated burrows in the Catskill
1075 Magnafacies (Upper Devonian) of New York State. Palaeogeography, Palaeoclimatology,
1076 Palaeoecology, 55, 65-77.

1077 Browne, M.A.E. 1980. The Upper Devonian and Lower Carboniferous (Dinantian) of the Firth of Tay,
1078 Scotland. Institute of Geological Sciences Report, 80/9.

1079 Browne, M.A.E., Dean, M.T., Hall, I.H.S., McAdam, A.D., Monro, S.K. and Chisholm, J.I. 1999. A
1080 lithostratigraphical framework for the Carboniferous rocks of the Midland Valley of Scotland. British
1081 Geological Survey Research Report, RR/99/07.

1082 Browne, M.A.E., Smith, R.A. and Aitken, A.M. 2002. Stratigraphical framework for the Devonian (Old Red
1083 Sandstone) rocks of Scotland south of a line from Fort William to Aberdeen. British Geological
1084 Survey Research Report, RR/01/04.

1085 Buatois, L.A., Gingras, M.K., Maceachern, J., Mángano, M.G., Zonneveld, J.P., Pemberton, S.G., Netto,
1086 R.G. and Martin, A. 2005. Colonization of brackish-water systems through time: evidence from the
1087 trace-fossil record. Palaios, 20, 321-347.

1088 Burchette, T.P. and Riding, R. 1977. Attached vermiform gastropods in Carboniferous marginal marine
1089 stromatolites and biostromes. Lethaia, 10, 17-28.

1090 Burrow, C.J., Long, J.A. and Trinajstic, K. 2009. Disarticulated acanthodian and chondrichthyan remains
1091 from the upper Middle Devonian Aztec Siltstone, southern Victoria Land, Antarctica. Antarctic
1092 Science 21, 71-88.

1093 Carpenter, D.K., Falcon-Lang, H.J., Benton, M.J. and Nelson, W.J. 2011. Fishes and tetrapods in the Upper
1094 Pennsylvanian (Kasimovian) Cohn coal member of the Mattoon formation of Illinois, United States:
1095 systematics, paleoecology, and paleoenvironments. Palaios 26, 639-657.

Carpenter, D.K., Falcon-Lang, H.J., Benton, M.J, and Henderson, E. 2014. Carboniferous (Tournaisian) fish assemblages from the Isle of Bute, Scotland: systematics and palaeoecology. Palaeontology, 57, 1215-1240.

Carvalho, I.D.S., Fernandes, A.C.S., Andreis, R.R., Paciullo, F.V.P., Ribeiro, A. and Trouw, R.A., 2005. The ichnofossils of the Triassic Hope Bay Formation, Trinity Peninsula Group, Antarctic Peninsula. Ichnos, 12, 191-200.

Cater, J.M.L., Briggs, D.E.G. and Clarkson, E.N.K. 1989. Shrimp-bearing sedimentary successions in the Lower Carboniferous (Dinantian) Dolostone and Oil Shale groups of northern Britain. Transactions of the Royal Society of Edinburgh: Earth Sciences, 80, 5-15.

Caudill, M.R., Driese, S.G. and Mora, C.I. 1996. Preservation of a palaeovertisol and an estimate of late Mississippian palaeoprecipitation. Journal of Sedimentary Research, 66, 58-70.

Chagas, A.A.P., Webb, G.E., Burne, R.V. and Southam, G. 2016. Modern lacustrine microbialites: towards a synthesis of aqueous and carbonate geochemistry and mineralogy. Earth Science Reviews, 162, 338-363.

Challands, T.J., Smithson, T.R., Clack, J.A., Bennett, C.E., Marshall, J.E.A., Wallace-Johnson, S.M. and Hill, H. 2019. A lungfish survivor of the end-Devonian extinction and an Early Carboniferous dipnoan radiation. Journal of Systematic Palaeontology, 17, 1825-1846.

Chisholm, J.I. and Brand, P.J. 1994. Revision of the late Dinantian sequence in Edinburgh and West Lothian. Scottish Journal of Geology, 30, 97-104.

Clack, J.A. 2002. An early tetrapod from 'Romer's Gap'. Nature, 418, 72-76.

Clack, J.A., Porro, L.B. and Bennett, C.E. 2018. A *Crassigyrinus*-like jaw from the Tournaisian (Early Mississippian) of Scotland. Earth and Environmental Science Transactions of the Royal Society of Edinburgh, 108, 37-46.

Clack, J.A., Bennett, C.E., Carpenter, D., Davies, S.J., Fraser, N.C., Kearsey, T.I., Marshall, J.E.A., Millward, D., Otoo, B.K.A., Reeves, E.J., Ross, A.J., Ruta, M., Smithson, K.Z., Smithson, T.R. and

121 Walsh, S. 2016. Phylogenetic and environmental diversity revealed for Tournaisian tetrapods. Nature
122 Ecology and Evolution, 1, 1-11, doi:10.1038/s41559-016-0002.

123 Clack, J.A., Bennett, C.E., Davies, S.J., Scott, A.C., Sherwin, J.E. and Smithson, T.R. 2019. A Tournaisian
124 (earliest Carboniferous) conglomerate-preserved non-marine faunal assemblage and its environmental
125 and sedimentological context. PeerJ, 6, p.e5972.

126 Clayton, G. 1986. Late Tournaisian miospores from the Ballycultra Formation at Cultra, County Down,
127 Northern Ireland. Irish Journal of Earth Sciences, 8, 73-79.

128 Coma, R., Ribes, M., Gili, J.M. and Hughes, R.N. 2001. The ultimate opportunists: consumers of seston.
129 Marine Ecology Progress Series, 219, 305-308.

130 Cook, A.G., Blodgett, R.B. and Becker, R.T. 2003. Late Devonian gastropods from the Canning Basin,
131 Western Australia. Alcheringa, 27, 181-207.

132 Cope, J.C.W., Guion, P.D., Sevastopulo, G. D, and Swan, A.R.H. 1992. Carboniferous, in Cope, J.C.W.,
133 Ingham, J.K. and Rawson, P.F. eds, Atlas of palaeogeography and lithofacies. Geological Society of
134 London Memoir, 13, 67-86.

135 Coward, M.P. 1993. The effect of Late Caledonian and Variscan continental escape tectonics on basement
136 structure, Paleozoic basin kinematics and subsequent Mesozoic basin development in NW Europe.
137 Geological Society, London, Petroleum Geology Conference series, 4, 1095-1108.

138 Craig, H. 1957. Isotopic standards for carbon and oxygen & correction factors for mass spectrometric
139 analysis. Geochemica et Cocmochemica Acta, 12, 133-149.

140 Crasquin-Soleau, S., Vaslet, D. and Le Nindre, Y. 2006. Ostracods of the Permian-Triassic Khuff
141 Formation, Saudi Arabia: palaeoecology and palaeobiogeography. GeoArabia, 11, 55-76.

142 Cressler, W.L., Daeschler, E.B., Slingerland, R. and Peterson, D.A. 2010. Terrestrialization in the Late
143 Devonian: a palaeoecological overview of the Red Hill site, Pennsylvania, USA. Geological Society,
144 London, Special Publications, 339, 111-128.

145 Davies, A., McAdam, A.D. and Cameron, I.B. 1986. Geology of the Dunbar district: Memoir of the British
146 Geological Survey, Sheet 33E and part of 41(Scotland).

147 Davies, N.S. and Gibling, M.R. 2013. The sedimentary record of Carboniferous rivers: Continuing influence
148 of land plant evolution on alluvial processes and Palaeozoic ecosystems. Earth-Science Reviews, 120,
149 40-79.

150 De Deckker P. 2002. Ostracoda Paleoecology, The Ostracoda: Applications in Quaternary Research
151 Geophysical Monograph 131. American Geophysical Union.

152 De Deckker, P. 1983, Notes on the ecology and distribution of non-marine ostracods in Australia.
153 Hydrobiologia, 106, 223-234.

154 De Deckker, P. and Geddes, M.C. 1980. Seasonal fauna of ephemeral saline lakes near the Coorong Lagoon,
155 South Australia. Australian Journal of Marine and Freshwater Research, 31, 677-699.

156 De Deckker, P. and Last, W.M. 1988. Modern dolomite deposition in continental, saline lakes, western
157 Victoria, Australia. Geology, 16, 29-32.

158 Donnelly, J.P., Butler, J., Roll, S., Wengren, M. and Webb, T. 2004. A backbarrier overwash record of
159 intense storms from Brigantine, New Jersey. Marine Geology, 210, 107-121.

160 Downs, J.P. and Daeschler, E.B. 2001. Variation within a large sample of *Ageleodus pectinatus* teeth
161 (Chondrichthyes) from the Late Devonian of Pennsylvania, U.S.A. Journal of Vertebrate
162 Paleontology, 21, 811–814.

163 Eagar, H.M.C. and Weir, J. 1971. Some Spanish Upper Carboniferous non-marine bivalve faunas: A
164 preliminary statement with emphasis on facies in north-west Spain and in Britain. Trabajos de
165 geología, 3, 87-101.

166 Falcon-Lang, H.J. 1999. The early Carboniferous (Courceyan-Arundian) monsoonal climate of the British
167 Isles: evidence from growth rings in fossil woods. Geological Magazine, 136, 177-187.

168 Falcon-Lang, H.J. 2004. Early Mississippian lycopsid forests in a delta-plain setting at Norton, near Sussex,
169 New Brunswick, Canada. Journal of the Geological Society, 161, 969-981.

Falcon-Lang, H.J., Benton, M.J., Braddy, S.J. and Davies, S.J. 2006. The Pennsylvanian tropical biome reconstructed from the Joggins Formation of nova Scotia, Canada. Journal of the Geological Society, 163, 561-576.

Falcon-Lang, H.J., Pufahl, P.K., Bashforth, A.R., Gibling, M.R., Miller, R.F. and Minter, N.J. 2015a. A marine incursion in the Lower Pennsylvanian Tynemouth Creek Formation, Canada: implications for paleogeography, stratigraphy and paleoecology. Palaios, 30, 779-791.

Falcon-Lang, H.J., Minter, N.J., Bashforth, A.R., Gibling, M.R. and Miller, R.F. 2015b. Mid-Carboniferous diversification of continental ecosystems inferred from trace fossil suites in the Tynemouth Creek Formation of New Brunswick, Canada. Palaeogeography, Palaeoclimatology, Palaeoecology, 440, 142-160.

Ferrero, L., Obenat, S. and Zárate, Z. 2005. Mid-Holocene serpulid build-ups in an estuarine environment (Buenos Aires Province, Argentina). Palaeogeography, Palaeoclimatology, Palaeoecology, 222, 259-271.

Francis, E.H., Forsythe, I.H., Read, W.A. and Armstrong, M. 1970. The geology of the Stirling district. Memoir of the British Geological Survey, Sheet 39.

Freshney, E.C. 1961. The Dolostone Group of the west Midland Valley of Scotland. Ph.D. thesis, Glasgow University.

Freytet, P. and Verrecchia, E.P. 2002. Lacustrine and palustrine carbonate petrography: an overview. Journal of Paleolimnology, 27, 221-237.

Friedman, M. 2015. The early evolution of ray- finned fishes. Palaeontology, 58, 213-228.

Friedman, M. and Sallan, L.C. 2012. Five hundred million years of extinction and recovery: a Phanerozoic survey of large- scale diversity patterns in fishes. Palaeontology, 55, 707-742.

Garvey, J.M. and Turner, S. 2006. Vertebrate microremains from the presumed earliest Carboniferous of the Mansfield Basin, Victoria. Alcheringa, 30, 43-62.

Ghummed, M.A. 1982. Petrology and geochemistry of the carbonates, Ballagan Formation, N.W. Midland Valley, Scotland. Ph.D. thesis, University of Glasgow.

Gierlowski-Kordesch, E.H. and Cassle, C.F. 2015. The 'Spirorbis' Problem Revisited: Sedimentology and Biology of Microconchids in Marine-Nonmarine Transitions. Earth-Science Reviews, 148, 209-227.

Given, R.K. and Wilkinson, B.H. 1987. Dolomite abundance and stratigraphic age: constraints on rates and mechanisms of Phanerozoic dolostone formation. Journal of Sedimentary Petrology, 57, 1068-1078.

Goodbred, S.L. and Hine, A.C. 1995. Coastal storm deposition: Salt-marsh response to a severe extratropical storm, March 1993, west-central Florida. Geology, 23, 679-682.

Gray, J. 1988. Evolution of the freshwater ecosystem: the fossil record. Palaeogeography, Palaeoclimatology, Palaeoecology, 62, 1-214.

Greb, S.F., DiMichele, W.A. and Gastaldo, R.A. 2006. Evolution and importance of wetlands in earth history, in Greb, S.F. and DiMichele, W.A. eds. Wetlands through time. Geological Society of America Special Paper, 399, 1-40.

Greb, S.F., Storrs, G.W., Garcia, W.J. and Eble, C.F. 2016. Late Mississippian vertebrate palaeoecology and taphonomy, Buffalo Wallow Formation, western Kentucky, USA. Lethaia, 49, 199-218.

Gregg, J.M., Bish, D.L., Kaczmarek, S.E. and Machel, H.G. 2015. Mineralogy, nucleation and growth of dolomite in the laboratory and sedimentary environment: a review. Sedimentology, 62, 1749-1769.

Gregg, J.M., Shelton, K.L., Johnson, A.W., Somerville, I.D. and Wright, W.R. 2001. Dolomitization of the Waulsortian Limestone (Lower Carboniferous) in the Irish Midlands. Sedimentology, 48, 745-766.

Greig, D.C. 1988. Geology of the Eyemouth district: Memoir of the British Geological Survey, Sheet 34.

Gueriau, P., Charbonnier, S. and Clément, G. 2014a. First decapod crustaceans in a Late Devonian continental ecosystem. Palaeontology, 57, 1203-1213.

Gueriau, P., Charbonnier, S. and Clément, G. 2014b. Angustidontid crustaceans from the Late Devonian of Strud (Namur Province, Belgium): insights into the origin of Decapoda. Neues Jahrbuch für Geologie und Paläontologie-Abhandlungen, 273, 327-337.

Gueriau, P., Rabet, N. and Hat, E.D.T. 2018. The Strud crustacean fauna (Late Devonian, Belgium): updated review and palaeoecology of an early continental ecosystem. Earth and Environmental Science Transactions of the Royal Society of Edinburgh, 107, 79-90.

Hodnett, J.P.M. and Elliott, D.K. 2018. Carboniferous chondrichthyan assemblages from the Surprise Canyon and Watahomigi formations (latest Mississippian–Early Pennsylvanian) of the western Grand Canyon, Northern Arizona. Journal of Paleontology, 92, 1-33.

Ivanov, A. 1996. The Early Carboniferous chondrichthyans of the South Urals, Russia. Geological Society, London, Special Publications, 107, 417-425.

Jeffery, J.E. 2006. The Carboniferous fish genera *Strepsodus* and *Archichthys* (Sarcopterygii: Rhizodontida): clarifying 150 years of confusion. Palaeontology, 49, 113–132.

Johnson, G.D. and Thayer, D.W. 2009. Early Pennsylvanian xenacanth chondrichthyans from the Swisshelm Mountains, Arizona, USA. Acta Palaeontologica Polonica, 54, 649-669.

Jones, B. 2013. Microarchitecture of dolomite crystals as revealed by subtle variations in solubility: implications for dolomitization. Sedimentary Geology, 288, 66-80.

Kaiser, S.I., Aretz, M. and Becker, R.T. 2016. The global Hangenberg Crisis (Devonian-Carboniferous transition): review of a first-order mass extinction, in Becker, R.T., Königshof, P. and Brett, C.E., eds. Devonian Climate, Sea Level and Evolutionary Events. Geological Society, London, Special Publications, 423, 387-437.

Kammer, T.W. and Lake, A.M. 2001. Salinity ranges of Late Mississippian invertebrates of the central Appalachian Basin. Southeastern Geology, 40, 99-116.

Kearsey, T., Twitchett, R.J. and Newell, A.J. 2012. The origin and significance of pedogenic dolomite from the Upper Permian of the South Urals of Russia. Geological Magazine, 149, 291-307.

Kearsey, T., Bennett, C.E., Millward, D., Davies, S.J., Gowing, C.J.B., Kemp, S., Leng, M.J., Marshall, J.E.A. and Browne, M.A.E. 2016. The terrestrial landscapes of tetrapod evolution in earliest

Carboniferous seasonal wetlands of the Ballagan Formation in S.E. Scotland. Palaeogeography, Palaeoclimatology, Palaeoecology, 457, 52-69.

Knaust, D. 2013. The ichnogenus *Rhizocorallium*: classification, trace makers, palaeoenvironments and evolution. Earth-Science Reviews, 126, 1-47.

Lamsdell, J.C. 2016. Horseshoe crab phylogeny and independent colonizations of fresh water: ecological invasion as a driver for morphological innovation. Palaeontology, 59, 181-194.

Lamsdell, J.C. and Braddy, S.J. 2010. Cope's Rule and Romer's theory: patterns of diversity and gigantism in eurypterids and Palaeozoic vertebrates. Biology Letters, 6, 265-269.

Lamsdell, J.C., Lagebro, L., Edgecombe, G.D., Budd, G.E. and Gueriau, P. 2019. Stylonurine eurypterids from the Strud locality (Upper Devonian, Belgium): new insights into the ecology of freshwater sea scorpions. Geological Magazine, 156, 1708-1714.

Leeder, M.R. 1973. Lower Carboniferous Serpulid patch reefs, bioherms and biostromes. Nature, 242, 41-42.

Leeder, M.R. 1974. Lower Border Group (Tournaisian) fluvio-deltaic sedimentation and palaeogeography of the Northumberland Basin. Proceedings of the Yorkshire Geological Society, 40, 129-180.

Leeder, M. 1975a. Lower Border Group (Tournaisian) limestones from the Northumberland Basin. Scottish Journal of Geology, 11, 151-167.

Leeder, M. 1975b. Lower Border Group (Tournaisian) stromatolites from the Northumberland basin. Scottish Journal of Geology, 11, 207-226.

Liu, D., Xu, Y., Papineau, D., Yu, N., Fan, Q., Qiu, X. and Wang, H. 2019. Experimental evidence for abiotic formation of low-temperature proto-dolomite facilitated by clay minerals. Geochimica et Cosmochimica Acta, 247, 83-95.

Liu, K.B., McCloskey, T.A., Bianchette, T.A., Keller, G., Lam, N.S., Cable, J.E. and Arriola, J. 2014. Hurricane Isaac storm surge deposition in a coastal wetland along Lake Pontchartrain, southern Louisiana. Journal of Coastal Research, 70, 266-271.

Long, A.G. 1959. The fossil plants of Berwickshire – a review of past work. Part 2. Work mainly done in the present century. History of the Berwickshire Naturalists' Club, 35, 26-47.

Long, A.G. 1960. On the structure of *Samaropsis scotia* Calder (emended) and *Eurystoma angulare* gen. et sp. nov. petrified seeds from the Calciferous Sandstone Series of Berwickshire. Transactions of the Royal Society of Edinburgh, 64, 261-284.

Lumsden, G. I., Tulloch, W., Howells, M. F. and Davis, A. 1967. The geology of the neighbourhood of Langholm: Memoir of the British Geological Survey, Sheet 11.

MacGregor, A.G. 1960. Divisions of the Carboniferous on Geological Survey Scottish maps. Bulletin of the Geological Survey of Great Britain, 16, 127-30.

Maharjan, D., Jiang, G., Peng, Y. and Henry, R.A. 2018. Paired carbonate-organic carbon and nitrogen isotope variations in Lower Mississippian strata of the southern Great Basin, western United States. Palaeogeography, Palaeoclimatology, Palaeoecology, 490, 462-472.

Mángano, M.G. and Buatois, L.A. 2004. Ichnology of Carboniferous tide-influenced environments and tidal flat variability in the North American Midcontinent. Geological Society, London, Special Publications, 228, 157-178.

Marshall, J.E.A., Reeves, E.J., Bennett, C.E., Davies, S.J., Kearsey, T.I., Millward, D., Smithson, T.R. and Browne, M.A. 2019. Reinterpreting the age of the uppermost 'Old Red Sandstone' and Early Carboniferous in Scotland. Earth and Environmental Science Transactions of the Royal Society of Edinburgh, 109, 265-278.

Martel, A.T. and Gibling, M.R. 1991. Wave-dominated lacustrine facies and tectonically controlled cyclicity in the Lower Carboniferous Horton Bluff Formation, Nova Scotia, Canada, in: Anadón, P., Cabrera, L.I. and Kelts, K., eds. Lacustrine Facies Analysis. International Association of Sedimentologists Special Publication, 13, 223-243.

Masdeu, M., Mello, F.T.D., Loureiro, M. and Arim, M. 2011. Feeding habits and morphometry of *Iheringichthys labrosus* (Lütken, 1874) in the Uruguay River (Uruguay). Neotropical Ichthyology, 9, 657-664.

Mather, C.C., Nash, D.J., Dogramaci, S., Grierson, P.F. and Skrzypek, G. 2019. Geomorphic and hydrological controls on groundwater dolocrete formation in the semi- arid Hamersley Basin, northwest Australia. Earth Surface Processes and Landforms, 44, 2752-2770.

McHargue, T.R. and Price, R.C. 1982. Dolomite from clay in argillaceous or shale-associated marine carbonates. Journal of Sedimentary Research, 52, 873-886.

Millward, D., Davies, S.J., Brand, P.J., Browne, M.A.E., Bennett, C.E., Kearsey, T.I., Sherwin, J.R. and Marshall, J.E.A. 2019. Palaeogeography of tropical seasonal coastal wetlands in northern Britain during the early Mississippian Romer's Gap. Earth and Environmental Science Transactions of the Royal Society of Edinburgh, 109, 279-300.

Millward, D., Davies, S.J., Williamson, F., Curtis, R., Kearsey, T.I., Bennett, C.E., West, I.M., Marshall, J.E.A. and Browne, M.A.E. 2018. Early Mississippian evaporites of coastal tropical wetlands. Sedimentology, 65, 2278-2311.

Millward, D., Kearsey, T.I. and Browne, M.A.E. 2013. Norham West Mains Farm Borehole: operations report. British Geological Survey Internal Report IR/13/033.

Ming, G.Y. 2004. Facies characteristics and tiering distributions of Chondrites. Acta Palaeontologica Sinica, 1, 1-8.

Montañez , I.P. and Cecil, C.B. 2013. Paleoenvironmental clues archived in non-marine Pennsylvanian-lower Permian limestones of the Central Appalachian Basin, USA. International Journal of Coal Geology, 119, 41-55.

Moore, C.G., Saunders, G.R. and Harries, D.B. 1998. The status and ecology of reefs of *Serpula vermicularis* L. (Polychaeta: Serpulidae) in Scotland: Aquatic Conservation. Marine and Freshwater Ecosystems, 8, 645-656.

Muchez, P. and Viaene, W. 1987. Dolocretes from the Lower Carboniferous of the Campine-Brabant Basin, Belgium. Pedologie, 37, 187-202.

Narkiewicz, M., Grabowski, J., Narkiewicz, K., Niedźwiedzki, G., Retallack, G.J., Szrek, P. and De Vleeschouwer, D. 2015. Palaeoenvironments of the Eifelian dolomites with earliest tetrapod trackways (Holy Cross Mountains, Poland). Palaeogeography, Palaeoclimatology, Palaeoecology, 420, 173-192.

Ó Gogáin, A., Falcon- Lang, H.J., Carpenter, D.K., Miller, R.F., Benton, M.J., Pufahl, P.K., Ruta, M., Davies, T.G., Hinds, S.J. and Stimson, M.R. 2016. Fish and tetrapod communities across a marine to brackish salinity gradient in the Pennsylvanian (early Moscovian) Minto Formation of New Brunswick, Canada, and their palaeoecological and palaeogeographical implications. Palaeontology, 59, 689-724.

Olanipekun, B.J. and Azmy, K. 2017. In situ characterization of dolomite crystals: Evaluation of dolomitization process and its effect on zoning. Sedimentology, 64, 1708-1730.

Otoo, B.K., Clack, J.A., Smithson, T.R., Bennett, C.E., Kearsey, T.I. and Coates, M.I. 2019. A fish and tetrapod fauna from Romer's Gap preserved in Scottish Tournaisian floodplain deposits. Palaeontology, 62, 225-253.

Owada, M. 2007. Functional morphology and phylogeny of the rock-boring bivalves *Leiosolenus* and *Lithophaga* (Bivalvia: Mytilidae): a third functional clade. Marine Biology, 150, 853-860.

Palma, R.M. and Angeleri, M.P. 1992. Early cretaceous serpulid limestones: Chachao Formation, Neuquen basin, Argentina. Facies, 27, 175-178.

Park, L.E., Siewers, F.D., Metzger, T. and Sipahioglu, S. 2009. After the hurricane hits: recovery and response to large storm events in a saline lake, San Salvador Island, Bahamas. Quaternary International, 195, 98-105.

Petrash, D.A., Bialik, O.M., Bontognali, T.R., Vasconcelos, C., Roberts, J.A., McKenzie, J.A. and Konhauser, K.O. 2017. Microbially catalyzed dolomite formation: From near-surface to burial. Earth-Science Reviews, 171, 558-582.

Pilarczyk, J.E., Horton, B.P., Soria, J.L.A., Switzer, A.D., Siringan, F., Fritz, H.M., Khan, N.S., Ildefonso, S., Doctor, A.A. and Garcia, M.L. 2016. Micropaleontology of the 2013 Typhoon Haiyan overwash sediments from the Leyte Gulf, Philippines. Sedimentary Geology, 339, 104-114.

Platt, N.H. and Wright, V.P. 1992. Palustrine carbonates and the Florida Everglades: Towards an exposure index for the fresh-water environment. Journal of Sedimentary Petrology, 62, 1058-1071.

Plummer, P.S. and Gostin, V.A. 1981. Shrinkage cracks: desiccation or synaeresis. Journal of Sedimentary Petrology, 51, 1147-1156.

Rameil, N. 2008. Early diagenetic dolomitization and dedolomitization of Late Jurassic and earliest Cretaceous platform carbonates: a case study from the Jura Mountains (NW Switzerland, E France). Sedimentary Geology, 212, 70-85.

Ramsbottom, W.H.C. 1973. Transgressions and regressions in the Dinantian: a new synthesis of British Dinantian stratigraphy. Proceedings of the Yorkshire Geological Society, 39, 567-607.

Rejmankova, E., Pope, K.O., Post, R. and Maltby, E. 1996. Herbaceous wetlands of the Yucatan Peninsula: communities at extreme ends of environmental gradients. Internationale Revue der gesamten Hydrobiologie und Hydrographie, 81, 223-252.

Rennie, M.D. and Jackson, L.J. 2005. The influence of habitat complexity on littoral invertebrate distributions: patterns differ in shallow prairie lakes with and without fish. Canadian Journal of Fisheries and Aquatic Sciences, 62, 2088-2099.

Richards, K.R., Sherwin, J.E., Smithson, T.R., Bennion, R.F., Davies, S.J., Marshall, J.E.A. and Clack, J.A. 2018. Diverse and durophagous: early Carboniferous chondrichthyans from the Scottish Borders. Earth and Environmental Science Transactions of the Royal Society of Edinburgh, 108, 67-87.

Rogers, M.J. 1965. A revision of the species of nonmarine Bivalvia from the Upper Carboniferous of eastern North America. Journal of Paleontology, 663-686.

Ross, A.J., Edgecombe, G.D., Clark, N., Bennett, C.E., Carriò, V., Contreras-Izquierdo, R. and Crighton, B. 2018. A new terrestrial millipede (Myriapoda: Diplopoda) fauna of earliest Carboniferous

(Tournaisian) age from the Scottish Borders helps fill 'Romer's Gap'. Earth and Environmental Science Transactions of the Royal Society of Edinburgh, 108, 99-110.

Rygel, M.C., Gibling, M.R. and Calder, J.H. 2004. Vegetation- induced sedimentary structures from fossil forests in the Pennsylvanian Joggins Formation, Nova Scotia. Sedimentology, 51, 531-552.

Rygel, M.C., Calder, J.H., Gibling, M.R., Gingras, M.K. and Melrose, C.S.A. 2006. Tournaisian forested wetlands in the Horton Group of Atlantic Canada. Geological Society of America, Special Publication, 399, 103–126.

Sallan, L.C. and Coates, M.I. 2010. End-Devonian extinction and a bottleneck in the early evolution of modern jawed vertebrates. PNAS, 107, 10131-10135.

Sallan, L.C. and Coates, M.I., 2013. Styracopterid (Actinopterygii) ontogeny and the multiple origins of post-Hangenberg deep-bodied fishes. Zoological Journal of the Linnean Society, 169, 156-199.

Sallan, L.C. and Galimberti, A.K. 2015. Body-size reduction in vertebrates following the end-Devonian mass extinction. Science, 350, 812-815.

Sánchez-Román, M., Vasconcelos, C., Warthmann, R. Rivadeneyra, M. and McKenzie, J.A. 2009. Microbial dolomite precipitation under aerobic conditions: results from Brejo do Espinho Lagoon (Brazil) and culture experiments. Special Publication of the International Association of Sedimentologists, 41, 167-178.

Scotese, C.R. and McKerrow, W.S. 1990. Revised world maps and introduction. Geological Society of London Memoirs, 12, 1-21.

Scott, A.C., Galtier, J. and Clayton, G. 1984. Distribution of anatomically-preserved floras in the Lower Carboniferous in Western Europe. Transactions of the Royal Society of Edinburgh: Earth Sciences, 75, 311-340.

Scott, W.B. 1971. The sedimentology of the dolostone group in the Tweed basin: Burnmouth and the Merse of Berwick. Ph.D. thesis, Sunderland Polytechnic.

Scott, W.B. 1986. Nodular carbonates in the Lower Carboniferous, Dolostone Group of the Tweed Embayment, Berwickshire: evidence for a former sulphate evaporite facies. Scottish Journal of Geology, 22, 325-345.

Searl, A. 1988. Pedogenic dolomites from the Oolite Group (Lower Carboniferous), South Wales. Geological Journal, 23, 157-169.

Shinn, E.A., Lloyd, R.M. and Ginsburg, R.N. 1969. Anatomy of a modern carbonate tidal-flat, Andros Island, Bahamas. Journal of Sedimentary Research, 39, 1202-1228.

Sibley, D.F. and Gregg, J.M. 1987. Classification of dolomite rock textures. Journal of Sedimentary Petrology, 57, 967-975.

Singh, B.P., Srivastava, V.K. and Kanhaiya, S. 2019. Sedimentological and geochemical characteristics of the late middle Eocene dolostone succession, Kachchh, western India. Geological Journal, 54, 3840-3859.

Slaughter, M. and Hill, R.J. 1991. The influence of organic matter in organogenic dolomitization. Journal of Sedimentary Research, 61, 296-303.

Smithson, T.R., Richards, K.R. and Clack, J.A. 2016. Lungfish diversity in Romer's Gap: reaction to the end- Devonian extinction. Palaeontology, 59, 29-44.

Smithson, T.R., Wood, S.P., Marshall, J. E.A. and Clack, J.A. 2012. Earliest Carboniferous tetrapod and arthropod faunas from Scotland populate Romer's Gap. PNAS, 109, 4532-4537.

Somerville, I.D., Strogen, P., Mitchell, W.I., Somerville, H.A. and Higgs, K.T. 2001. Stratigraphy of Dinantian rocks in WB3 borehole, Co. Armagh. Irish Journal of Earth Sciences, 19, 51-78.

Stephenson, M.H., Williams, M., Leng, M.J. and Monaghan, A.A. 2004a. Aquatic plant microfossils of probable non-vascular origin from the Ballagan Formation (Lower Carboniferous), Midland Valley, Scotland. Proceedings of the Yorkshire Geological Society, 55, 145-158.

Stephenson, M.H., Williams, M., Monaghan, A.A., Arkley, S., Smith, R.A., Dean, M., Browne, M.A.E. and Leng, M. 2004b. Palynomorph and ostracod biostratigraphy of the Ballagan Formation, Midland

Valley of Scotland, and elucidation of intra-Dinantian unconformities. Proceedings of the Yorkshire Geological Society, 55, 131-143.

Suarez-Gonzalez, P., Quijada, I.E., Benito, M.I. and Mas, R. 2015. Sedimentology of ancient coastal wetlands: insights from a Cretaceous multifaceted depositional system. Journal of Sedimentary Research, 85, 95-117.

Suttner, T. and Lukeneder, A. 2003. Accumulations of Late Silurian serpulid tubes and their palaeoecological implications (Blumau-Formation; Burgenland; Austria). Annalen des Naturhistorischen Museums in Wien, 105A, 175-187.

Tandon, S.K. and Andrews, J.E. 2001. Lithofacies associations and stable isotopes of palustrine and calcrete carbonates: examples from an Indian Maastrichtian regolith. Sedimentology, 48, 339-355.

Taylor, A., Goldring, R. and Gowland, S. 2003. Analysis and application of ichnofabrics. Earth-Science Reviews, 60, 227-259.

Taylor, P.D. and Vinn, O. 2006. Convergent morphology in small spiral worm tubes ('Spirorbis') and its palaeoenvironmental implications. Journal of the Geological Society, 163, 225-228.

Thorez, J., Dreesen, R. and Streel, M. 2006. Famennian. Geologica Belgica, 9, 27-45.

Törő, B. and Pratt, B.R. 2015. Eocene Paleoseismic Record of the Green River Formation, Fossil Basin, Wyoming, USA: Implications of Synsedimentary Deformation Structures in Lacustrine Carbonate Mudstones. Journal of Sedimentary Research, 85, 855-884.

Trueman, A.E. and Weir, J. 1946. A monograph of British Carboniferous non-marine Lamellibranchs. Palaeontographical Society Monographs 99, pts I-IX.

Turner, M.S. 1991. Geochemistry and diagenesis of basal Carboniferous dolostones from southern Scotland. Ph.D. thesis, University of East Anglia.

Vanstone, S.D. 1991. Early Carboniferous (Mississippian) palaeosols from southwest Britain: influence of climatic change on soil development. Journal of Sedimentary Petrology, 61, 445-457.

Vasey, G.M. 1984. Westphalian macrofaunas in Nova Scotia: palaeoecology and correlation. Ph.D. thesis, University of Strathclyde.

Vasconcelos, C. and McKenzie, J.A. 1997. Microbial mediation of modern dolomite precipitation and diagenesis under anoxic conditions (Lagoa Vermelha, Rio de Janeiro, Brazil). Journal of Sedimentary Research, 67, 378-390.

Vasconcelos, C., McKenzie, J.A., Warthmann, R. and Bernasconi, S.M. 2005. Calibration of the δ18O paleothermometer for dolomite precipitated in microbial cultures and natural environments. Geology, 33, 317-320.

Vaughn, C.C., Nichols, S.J. and Spooner, D.E. 2008. Community and foodweb ecology of freshwater mussels. Journal of the North American Benthological Society, 27, 409-423.

Victor, R., Chan, G.L. and Fernando, C.H. 1979. Notes on the recovery of live ostracods from the gut of the white sucker (*Catostomus commersoni* Lacepede) 1808, (Pisces: Catostomidae). Canadian Journal of Zoology, 57, 1745-1747.

Vinn, O. and Mutvei, H. 2009. Calcareous tubeworms of the Phanerozoic. Estonian Journal of Earth Sciences, 58, 286-296.

Vrazo, M.B., Brett, C.E. and Ciurca, S.J. 2016. Buried or brined? Eurypterids and evaporites in the Silurian Appalachian basin. Palaeogeography, Palaeoclimatology, Palaeoecology, 444, 48-59.

Wacey, D., Wright, D.T. and Boyce, A.J. 2007. A stable isotope study of microbial dolomite formation in the Coorong Region, South Australia. Chemical Geology, 244, 155-174.

Wanas, H.A. and Sallam, E. 2016. Abiotically-formed, primary dolomite in the mid-Eocene lacustrine succession at Gebel El-Goza El-Hamra, NE Egypt: An approach to the role of smectitic clays. Sedimentary Geology, 343, 132-140.

Warren, J. 2000. Dolomite: occurrence, evolution and economically important associations. Earth-Science Reviews, 52, 1-81.

Warren, J.K. 2006. Evaporites: Sediments, Resources and Hydrocarbons. Springer-Verlag, Berlin-Heidelberg, 1035 pp.

Waters, C.N. and Davies, S.J. 2006. Carboniferous: extensional basins, advancing deltas and coal swamps, in Brenchley, P.J. and Rawson, P.F., eds, The geology of England and Wales. Geological Society of London, 173-223.

Williams, H.F.L. 2009. Stratigraphy, Sedimentology, and Microfossil Content of Hurricane Rita Storm Surge Deposits in Southwest Louisiana. Journal of Coastal Research, 25, 1041-1051.

Williams, M., Stephenson, M.H., Wilkinson, I.P., Leng, M.L. and Miller, C.G. 2005. Early Carboniferous (Late Tournaisian-Early Viséan) ostracods from the Ballagan Formation, central Scotland, UK. Journal of Micropalaeontology, 24, 77-94.

Williams, M., Leng, M.L., Stephenson, M.H., Andrews, J.E., Wilkinson, I.P., Siveter, D.J., Horne, D.J. and Vannier, J.M.C. 2006. Evidence that Early Carboniferous ostracods colonised coastal flood plain brackish water environments. Palaeogeography, Palaeoclimatology, Palaeoecology, 230, 299-318.

Wilson, M.A., Vinn, O. and Yancey, T.E. 2011. A new microconchid tubeworm from the Artinskian (Lower Permian) of central Texas, USA. Acta Palaeontologica Polonica, 56, 785-791.

Wilson, M.J., Bain, D.C. McHardy, W.J. and Berrow, M.L. 1972. Clay-mineral studies on some Carboniferous sediments in Scotland. Sedimentary Geology, 8, 137-150.

Wright, D.T. 1999. The role of sulphate-reducing bacteria and cyanobacteria in dolomite formation in distal ephemeral lakes of the Coorong region, South Australia. Sedimentary Geology, 126, 147-157.

Wright, D.T. and Wacey, D. 2004. Sedimentary dolomite: a reality check. Geological Society, London, Special Publications, 235, 65-74.

Wright, V.P. 1990. Equatorial aridity and climatic oscillations during the early Carboniferous, southern Britain. Journal of the Geological Society, 147, 359-363.

Wright, V.P. and Robinson, D. 1988. Early Carboniferous floodplain deposits from South Wales: a case study of the controls on palaeosol development. Journal of the Geological Society, 145, 847-857.

Wright, V.P., Turner, M.S., Andrews, J.E. and Spiro, B. 1993. Morphology and significance of super-mature calcretes from the Upper Old Red Sandstone of Scotland. Journal of the Geological Society, 150, 871-883.

Wright, V.P., Vanstone, S.D. and Marshall, J.D. 1997. Contrasting flooding histories of Mississippian carbonate platforms revealed by marine alteration effects in palaeosols. Sedimentology, 44, 825-842.

Yazdi, M. and Turner, S. 2000. Late Devonian and Carboniferous vertebrates from the Shishtu and Sardar formations of the Shotori Range, Iran. Records of the Western Australian Museum, Supplement 58, 223-240.

Yen, T.C. 1949. Review of Palaeozoic non-marine gastropods and a description of a new genus from the Carboniferous rocks of Scotland. Journal of Molluscan Studies, 27, 235-240.

Yoo, E.K. 1988. Early Carboniferous Mollusca from Gundy, Upper Hunter, New South Wales. Records of the Australian Museum, 40, 233-264.

Zatoń, M., Vinn, O. and Tomescu, A.M.F. 2012. Invasion of freshwater and variable marginal marine habitats by microconchid tubeworms – an evolutionary perspective. Geobios, 45, 603-610.

Ziegler, A.M., Eshel, G., Rees, P.M., Rothfus, T., Rowley, D. and Sunderlin, D. 2003. Tracing the tropics across land and sea: Permian to present. Lethaia, 36, 227-254.

Ziegler, P.A. 1989. Evolution of Laurussia, a study in late Palaeozoic plate tectonics. Dordrecht, The Netherlands, Kluwer academic publishers, 102 p.

Figure Captions

Figure 1. Palaeogeography and location maps. A. Location map of Scotland and northern England. The Ballagan Formation outcrop is within the Tweed Basin (this study), the Midland Valley of Scotland and the Northumberland-Solway Basin. The primary field site of Burnmouth and the location of the Norham Core at Norham are indicated. Maps modified from Smithson et al. (2012); a detailed location map of Burnmouth and the Norham Core is given in Bennett et al. (2017). B. Palaeogeography of Mississippian synsedimentary dolostones. Map is a reconstruction at 335 Ma (modified from Ziegler, 1989). Numbers 1-8 refer to

published occurrences of dolostone facies: 1: Kentucky, USA (Barnett et al., 2012) and Tennessee, USA (Caudill et al., 1996); 2-4: Eastern Canada; New Brunswick, Nova Scotia and western Newfoundland (Belt et al., 1967; Martel and Gibling, 1991); 5: Northern Ireland (Clayton, 1986); 6: South Wales (Wright and Robinson, 1988) and South-West England (Vanstone, 1991; Wright et al., 1997); 7: Scottish Borders, Northumberland and Midland Valley of Scotland (Andrews et al., 1991; Freshney, 1961; Ghummed, 1982; Scott, 1971, 1986; Turner, 1991, and this study); 8: Booischot borehole, Campine-Brabant basin of Belgium (Muchez and Viaene, 1987). Dolostones occur within newly rifting basins along the southern margin of Laurussia.

Figure 2. The 490-m thick Norham Core showing dolostones. The thickness of each dolostone bed is illustrated with horizontal blue lines and the number of beds per 10 metre rock thickness by a continuous black line. The number of beds per 10 metre thickness decreases on average from the base to the top of the formation and is highest in the basal 80 m of the core. Dolostones are rare within the sandstones of the fluvial facies association. Dolostone facies are: Facies 1: Cemented siltstone and sandstone; Facies 2: Homogeneous micrite; Facies 3: Mixed dolomite and siltstones; Facies 4: Mixed calcite-dolomite; Facies 5: Dolomite with evaporite minerals. Facies 5 is more common at the base of the formation, with other facies types randomly distributed. The detailed section shows an example of a typical facies 2-3 type dolostone dominated sequence from the middle of the Norham Core.

Figure 3. Burnmouth section showing dolostones. The thickness and abundance of dolostone beds decreases from the base to the top of the formation. Note that the Burnmouth sequence has fewer dolostone beds identified to a facies level, as only beds that were sampled were assigned to a facies (see Table S1). Detailed section A: Part of the Burnmouth succession with the most abundant dolostone beds, with numerous facies 4 beds exhibiting soft sediment deformation. Refer to Figure 2 for the Key.

Figure 4. Dolostone facies in the Norham Core. A: Facies 1, cemented sandstone and siltstone, interbedded units that are rooted and bioturbated, two dolostone nodules occur in a siltstone bioturbated by *Chondrites*, 230.8 m. B: Facies 2, homogeneous dolomicrite, the bed has a brecciated interior and the basal contact is diffuse into siltstone, 334.95 m. C: Facies 3, interbedded dolomite and siltstone, the middle bed has soft

sediment deformation, 331.1 m. D: Facies 3, interbedded dolomite and siltstone, both units are extensively brecciated, the dolostone hosts ostracods and *Serpula*, 227.1 m. E: Facies 4, a 5 cm thick calcite-rich bed (in the upper part of the photograph) containing abundant fossils (*Serpula*, large bivalves, ?*Schizodus*, *Naiadites*, ostracods, fish fragments and *Spirorbis*, not visible in photograph). Above and below the bed are siltstones bioturbated by *Chondrites*, 473.45 m. F: Facies 5, anhydrite nodules in a dolomite matrix, overlain by dolomite with compacted laminations, 493 m. Scale bars 25 mm.

Figure 5. Key features of dolostone facies in outcrop, thin section scan and photomicrograph. The schematic logs illustrate an average 50 cm thick succession of the facies in outcrop or in core. Facies 1: Thin section scan: cemented siltstone with bivalves and *Serpula*, Norham Core, 336.7 m. Photomicrograph (plane-polars): dolomite crystals cementing a matrix of siltstone and fossil fragments. Facies 2: Thin section scan: micritic homogeneous dolostone with desiccation cracks filled with silt-rich carbonate, Norham Core, 39.95 m. Photomicrograph (plane-polars): small dolomite crystals within a clay matrix. Facies 3: Thin section scan: Interbedded dolomite and finely laminated silt, Norham Core, 321.85 m. Photomicrograph (plane-polars): Boundary between silt and dolomite layers. Facies 4: Thin section scan: micritic calcite and dolomite in patches, oolitic bed, Burnmouth, 209.92 m. Photomicrograph (plane-polars): ooids with dolomite spar in their centre are in a matrix of micritic calcite. Facies 5: Thin section scan: Laminated siltstone with a dolomite nodule bearing large anhydrite crystals, Norham Core, 492.92 m. Photomicrograph (crossed-polars): anhydrite crystals in a dolomicrite matrix. Colours in schematic log: yellow = dolomite, white = siltstone or sandstone, orange = calcite, pink = evaporites. Scale bars: thin section: 5 mm; photomicrograph 100 μm. Symbols: a, anhydrite; b, bivalves; c, calcite ; d, dolomite; q, quartz; s, *Serpula*.

Figure 6. Electron backscatter SEM images of dolostone thin sections. A: Facies 1, sandstone matrix cemented with non-planar anhedral dolomite, Burnmouth, 178.85 m. B: Facies 2, planar euhedral dolomite rhombs in a clay matrix, the rhombs are zoned with calcium-rich centres. One euhedral pyrite crystal is present, Norham Core, 368.07 m. C: Facies 3, planar euhedral dolomite rhombs within a siltstone matrix, no zoning is present, Norham Core, 321.85 m. D: Facies 4, planar euhedral dolomite rhombs and micritic dolomite within a clay matrix, Burnmouth, 184.03 m. E: Facies 4, patches of dolomite and calcite with

abundant bivalve fossils. Pyrite occurs along the rim of fossils, as discrete euhedral crystals and in clusters of small framboids, Norham Core, 473.64 m, this bed is also shown in Figure 4E. F: Facies 4, calcitic ooid partially replaced by dolomite, with a pyrite rim. The ooid has zoned small euhedral dolomite crystals in the interior, and dolomite spar in the matrix, Burnmouth, 209.92 m. G: Facies 5, anhydrite crystals in a dolomicrite matrix, Norham Core, 492.92 m. H: Facies 5, planar euhedral dolomite rhombs within a clay matrix, crystals are zoned with magnesium-rich centres, Norham Core, 449.65 m. Scale bars 50 μm. Symbols: a, anhydrite; b, bivalve; c, calcite; cl, clay minerals; d, dolomite; f, feldspar; p, pyrite; q, quartz.

Figure 7. Secondary alteration and bulbous dolostones. A. The percentage of dolostone samples of each facies from the Norham Core and Burnmouth section, which are brecciated, desiccated or pedogenically modified. Each facies is numbered (1-5), and the circumference of each facies indicates the relative number of beds of each facies. The number of beds of each facies present in the Norham Core are: Facies 1: 52; Facies 2: 85; Facies 3: 95; Facies 4: 9; Facies 5: 38. And at Burnmouth: Facies 1: 48; Facies 2: 40; Facies 3: 58; Facies 4: 13; Facies 5: 6. Internal brecciation is much more common than desiccation cracks. B-D: Facies 2 dolostones with a bulbous top or base. B. Top surface of a dolostone bed with large pillow shaped bulbous dolostone, internally brecciated and rooted, Burnmouth, 128.1 m. C. Basal surface of a dolostone bed with tree trunk impressions and brecciation, Burnmouth, 379.55 m. D. Bulbous top surface of a dolostone bed with a lycopsid root impression, Burnmouth, 334.5 m. Scale bars 5 cm.

Figure 8. Fossil content and bioturbation. In A and C each facies is numbered (1-5), and the circumference of each facies indicates the relative number of beds of each facies as in Figure 7. A: The percentage of dolostone samples of each facies from the Norham Core and Burnmouth which contain fossils. B: Graphs showing the percentage of fossil occurrence per facies. The presence of each fossil group is counted and the percentage calculated, for example, 25% of facies 1 dolostones in the Norham Core contain plant fragments. Of significance are the more common robust bivalves (R. bivalve), *Spirorbis* and *Serpula* burrows within Facies 4 and some Facies 3 beds. Not illustrated are fragments of arthropod cuticle and gastropods, which occur in almost all facies in very low numbers. C: The percentage of dolostone samples of each facies from

the Norham Core and Burnmouth, which are bioturbated. Core samples have a higher bioturbation percentage per facies, primarily because bioturbation is more easily seen in the core.

Figure 9. Autochthonous and allochthonous *Serpula* within dolostones. Autochthonous *Serpula* colonies are present within the centre of dolostone beds, whereas allochthonous *Serpula* comprises centimetre thick horizons of broken tube fragments that are at random orientations. A: Autochthonous *Serpula* within a dolostone containing siltstone patches, Norham Core, 368.12 m. Ostracods, *Spirorbis*, bivalve fragments, roots and plant fragments were identified in the hand specimen of this bed. B: Autochthonous *Serpula* and ostracods in thin section, within a dolostone, from the Burnmouth field section, 181.83 m height. Thin section scan, *Serpula* tubes are outlined (b1) and shown in a detailed plane-polarised light image (b2). The tube wall is composed of microcrystalline calcite and the tubes are infilled with large sparry calcite crystals. C: Allochthonous *Serpula* within a dolostone that is brecciated, Norham Core, at 227.13 m. A coquina of broken *Serpula* tubes and ostracods fill in the cracks. Thin section scan, crack outline and *Serpula* fragments are outlined in (c). In both B and C *Serpula* tubes are infilled with calcite (white colour) and dolomite crystals (grey) or silt-bearing dolomicrite (brown). Scale: A: 25 mm, B-C: scale bar 5 mm, b2: scale bar 250 μm.

Figure 10. Microfossil assemblages. Percentage counts of total assemblage microfossil counts for one sample of each facies. Facies 1 (n = 6468 specimens), Facies 2 (n = 779), Facies 3 (n = 1231), Facies 4 (n = 1372), and Facies 5 (n = 1853). The full data table of counts for all size fractions and microfossils per gram is detailed in Table S3. Abbreviations: acanth., acanthodian; actin., actinopterygian; chond., chondrichthyan; indet., indeterminate; rhizo., rhizodont.

Figure 11. Plate of common dolostone microfossils. A: Actinopterygian lepidotrichia bone, facies 2. B: Hybodont scale with spines that are joined together into a star shape, dorsal oblique view, facies 2. C. Rhizodont tooth with striated ornament, facies 3. D. Actinopterygian scale, exterior surface with a transverse grooved ornament, facies 4. E: Actinopterygian tooth, recurved, facies 4. F. Fish bone (indeterminate), with layered, porous internal structure, facies 4. G. Rhizodont scale with pustular ornament, facies 4. H:

615 *Cavellina* ostracod mould, juvenile, carapace, left lateral view, facies 4. I: Plant fragment, facies 5. Scale
616 bars 250 μm.

617 Figure 12. Dolostone isotope results. Carbon and oxygen isotope results for each dolostone facies from this
618 study and Turner (1991). Dolostone samples from Turner (1991) were classed into the facies scheme of this
619 study based on sample descriptions given. The data are compared with published calcite and dolomite
620 Mississippian isotopic data from a range of settings (numbered 1 to 4) and is most similar to palaeosol-
621 associated ferroan dolomite of the Appalachian and Illinois basins, Kentucky, USA (Barnett et al., 2012).

622 Figure 13. Dolostone depositional environments. The general setting is a tropical, coastal, low-lying
623 floodplain. The location of each dolostone facies (F) is indicated, note that all form in the sub-surface. The
624 main fossils occurring in each facies are highlighted for facies 2-4, with *Spirorbis,* gastropods, *Serpula* and
625 robust bivalves or brachiopods washed into lakes from the shallow-marine environment during storms. Each
626 of these facies can be secondarily modified by rooting, brecciation and pedogenic processes, with the lake
627 environment drying out and evolving to either shallow hypersaline evaporitic pools or to vegetated, brackish
628 coastal marshes.

629 Table 1. Fossil salinity tolerance and taphonomy. Fossils groups present within dolostones are listed from
630 left to right in order of their abundance. Plants are excluded, and so are chondrichthyans, acanthodians,
631 dipnoans, eurypterids, and gastropods, whose taphonomy has not been assessed. The taphonomy is taken as
632 an average for that fossil group, for example 70% of *Serpula* are allochthonous. The salinity tolerance is
633 discussed in the text and is based on published interpretations for that group; Ichnofauna (Bhattacharya and
634 Bhattacharya, 2007; Buatois et al., 2005; Knaust, 2013); Actinopterygian and rhizodont (Carpenter et al., 2014;
635 Greb et al., 2015; Ó Gogáin et al., 2016); Ostracod (Bennett, 2008; Bennett et al., 2012; Williams et al.,
636 2005); Bivalve (*Modiolus*, *Naiadites*) (Ballèvre and Lardeux, 2005; Bennison, 1960; Trueman and Weir,
637 1946); *Schizodus* (Kammer and Lake, 2001); *Spirorbis* (Gierlowski-Kordesch and Cassle, 2015); *Serpula*
638 (Beus, 1980; Braga and López-López, 1989; Palma and Angeleri, 1992; Suttner and Lukeneder, 2003);
639 Brachiopod (Kammer and Lake, 2001). Abbreviations: Auto, autochthonous assemblages; Allo,
640 allochthonous assemblages; Euryh., euryhaline.

641